ROYAUME DU MAROC
Université Mohammed V - RABAT -
جامعة محمد الخامس – الرباط –
Faculté des sciences
كلية العلوم
CENTRE D'ÉTUDES DOCTORALES - SCIENCES ET TECHNOLOGIES

N° d'ordre :3930

THÈSE

en vue de l'obtention du : **DOCTORAT**

Centre de Recherche :
Structure de Recherche : Equipe de science de la matiere et du rayonnement.
Discipline : Physique
Spécialité : Information quantique et nouvelles technologies

Présentée et Soutenue le : *04 / 06 / 2024*

par

Mohamed Housni El Moubaraka Ben ADBOU CHAKOUR

Contribution à la proposition d'un modèle petit réfrigérateur autonome et l'étude d'une machine quantique Otto

Devant le JURY :

Adil **BELHAJ**	PES	Établissement,Université MohammedV, faculté des sciences, Rabat	Président
Mustafa **FAQIR**	PES	Établissement, Université Internaltionale de Rabat UIR	Examinateur/Rapporteur
Ossama El **ABOUTI**	PH	Établissement, Université Abdelmalik Essadi, Tetouant	Examinateur/Rapporteur
Ahmed **JELLAL**	PES	Établissement, Université Chouaib Doukkali, El Jadida	Examinateur
Vazquez Ramallo **ALFONSO**	PES	Université de Saint-Jacques-de Compostelle, Institut Galicien de Physique des Hautes Énergies, Espagne	Examinateur
Abdessamad **BELFAKIR**	PA	Université Polytechnique Mohamed VI	Invité
Abderrahim **El Allati**	PH	Établissement , Université Abdelmalik Essadi, Tetouant	Co-Directeur de thèse
Yassine **HASSOUNI**	PES	Établissement, Université Mohammed V, faculté des sciences, Rabat	Directeur de thèse

Année Universitaire : 2023 - 24

Dedication

First and foremost, I dedicate this work to my family. Without their unwavering support, I would not be where I am today. I owe immense gratitude to my parents, whose upbringing and constant encouragement provided the motivation I needed to complete my studies despite the challenges. I also want to express my heartfelt thanks to my big sister, Hadia, who has become a second mother to me over the years. To all my family members who have, in various ways, contributed to making my life as a student easier, I am deeply grateful.

Acknowledgment

First and foremost, I would like to express my profound gratitude to the faculty members of the ESMAR team for granting me the opportunity to pursue my Master's degree in Matter and Radiation, and subsequently, to enroll in the doctoral program. Their invaluable support and insightful guidance have been fundamental pillars throughout my thesis, enabling me to conduct my research under optimal conditions. I also wish to extend my sincere appreciation for their constant availability and continuous efforts to ensure my success in all my academic endeavors.

No words can truly convey the extent of my gratitude towards my supervisors. Professor Yassine Hassouni, whose efforts and advice over the past seven years have been of immense value and importance. During this period, he provided me with the opportunity to work under his direction, never sparing any effort or hesitating to go beyond what was necessary to offer me all the essential conditions for my intellectual and social growth.

I would also like to thank Professor Abderrahim El Allati, who taught me everything I know today about quantum thermodynamics. Over the years we spent together, he offered me much more than just academic training. He provided a sense of familial support and protection, making my learning experience as rewarding on a personal level as it was scientifically enriching. His dedication to pedagogical excellence and commitment to student progress have been a source of inspiration and motivation throughout my journey. It has been a privilege to work under his supervision and learn by his side.

I would also like to express my gratitude to Mr. Adil Belhaj, Professor of Higher Education at Mohammed V University in Rabat, for agreeing to chair my thesis jury. Please accept, Professor, the expression of my deepest respect and consideration.

I am deeply grateful to Professor Mustafa Faqir for generously agreeing to be a reviewer of my thesis. His commitment and expertise have been invaluable to the progression of this work.

I also want to thank Professor Ossama El Abouti for agreeing to be a reviewer of my thesis and significantly contributing to the improvement of my work.

I extend my recognition to Professor Ahmed Jellal for serving as an examiner. His valuable comments have greatly impacted the quality of my work.

Additionally, I thank Professor Vazquez Ramallo Alfonso for his contribution as an examiner of my thesis and for his various comments. Please accept my heartfelt thanks.

I warmly acknowledge Professor Abdessamad Belfakir for honoring my defense with his presence and for evaluating the quality of this work.

Résume

Dans cette thèse, nous nous concentrons sur l'étude de la présence et de l'impact des caractéristiques quantiques induites au cours de l'évolution des réfrigérateurs quantiques discrets ou autonomes sur leurs performances thermodynamiques. Notre étude intègre une analyse théorique de la rentabilité de ces machines, en amalgamant les propriétés quantiques avec les performances de réfrigération des appareils. À cette fin, nous introduisons en premier lieu un modèle de couplage de deux réfrigérateurs autonomes, dans lequel nous examinons la corrélation générée au niveau de leur interaction. Grâce à cette approche, nous observons leur degré de corrélation et analysons l'interaction entre ces corrélations et l'efficacité des appareils. Ensuite, nous nous concentrons sur un modèle de réfrigérateur fonctionnant par le biais des réservoirs hiérarchiques. Notre objectif est d'observer dans quelle mesure ce type de réservoir peut affecter la dynamique du système d'exploitation et de discerner les conséquences de cette influence. Grâce à ces deux approches, nous espérons obtenir une vision plus nuancée du comportement quantique et des performances des réfrigérateurs quantiques. En approfondissant la complexité des corrélations induites entre les composants du système et en étudiant les effets de différents environnements, nous souhaitons fournir davantage d'informations qui permettront d'améliorer notre compréhension actuelle de l'impact des propriétés quantiques sur les performances des réfrigérateurs quantiques.

Mots-clefs : : Machines autonomes ; Réfrigérateur quantique ; Propriétés quantiques ; Bains thermaux ; Système quantique ouvert.

Abstract

In this thesis, we investigate the presence and impact of quantum features induced during the operation of discrete or self-contained quantum refrigerators on their thermodynamic performance. Our investigation integrates a theoretical analysis of the cost-effectiveness of these machines by amalgamating quantum properties with their cooling performance. To this end, we first introduce a coupling model between two autonomous refrigerators, where we study the quantum correlation generated during their interaction. Thanks to this approach, we observe the degree of correlation between the two refrigerators and analyze the interplay between these correlations and the efficiency of the devices. Secondly, we consider a refrigerator model that operates through hierarchical reservoirs. Here, we aim to observe the extent to which this type of reservoir can influence the dynamics of the system and to discern the consequences of this influence. We hope to gain a more nuanced view of the quantum refrigerator's behavior and performance through these two approaches. By delving deeper into the complexity of the correlations induced between the components of the system, and by studying the effects of different environments, we aim to provide more information that will improve our current understanding of the impact of quantum properties on the performance of the quantum refrigerators.

Keywords : Autonomous machines ; Quantum refrigerator ; Quantum properties ; Thermal baths ; Open quantum system.

List of publication

- Abdou Chakour, M. H. B., Allati, A. E. Hassouni, Y. Entangled quantum refrigerator based on two anisotropic spin-1/2 Heisenberg XYZ chain with Dzyaloshinskii–Moriya interaction. Eur. Phys. J. D 75, 42 (2021).

- Abdou Chakour, M. H. B., El Allati, A. Hassouni, Y. Coupling of two autonomous quantum refrigerators : Collective and relative performances. Physics Letters A 451, 128410 (2022).

- Abdou Chakour, M. H. E. M. B., El Allati, A. Hassouni, Y. On the coupling of three-level quantum refrigerators in the weak coupling limit. J. Phys. B : At. Mol. Opt. Phys. (2024).

- El Allati, A., El Anouz, K., Ben Abdou Chakour, M. H. Al-Kuwari, S. Non-Markovian effects on the performance of a quantum Otto refrigerator. Physics Letters A 496, 129316 (2024).

Liste of figures

Table des matières

Introduction

The rapid development of quantum mechanics in recent decades has prompted significant reflection on the orientation of scientific research and the emergence of new technologies. Quantum mechanics has emerged as a broad and far-reaching field of scientific inquiry, attracting considerable attention due to its diverse expectations, applications and future prospects. These include the construction of quantum electronic systems such as quantum computers, where the primary promise lies in exploiting quantum properties to construct systems that outperform their classical counterparts in terms of performance [1–4]. This outlook entails a diverse array of resources, including thermal equipment, and necessitates a comprehensive examination of their design and operation. Of particular importance is the ability to combine the study of the energetic processes of these systems, their design, operation, and quantum behavior on a unified information platform to assess their potential accurately [5–7].

Within this vast array of interactions, quantum thermodynamics has emerged as a central area of research to address these challenges. Quantum thermodynamics is presented primarily as a discipline that bridges thermodynamic principles and quantum perspectives [8–12]. As such, it represents a research field that facilitates the integration of the quantum properties of infinitesimal dimensional systems into a broader and more complex framework of their thermodynamic behavior, with the aim of improving the fundamental comprehension of the operation and performance of quantum thermal devices. Even more as an interdisciplinary field, it focuses on three main areas. First, the development of quantum thermodynamic devices, where the concept of quantum thermal machines remains central. Secondly, the study of quantum thermal machines in the light of quantum information and, finally, the elucidation of the role of quantum properties from a thermodynamic viewpoint.

Before delving into the study of quantum thermal devices, it is important to understand their design and operating mechanisms. A conventional term for such a quantum system is the quantum thermal machine [13–15]. In a general framework, it represents any quantum system with a working system, typically a quantum composite system, operating between different thermal baths. Depending on the mode of operation of the working system, two categories can be distinguished : discrete machines, in which the system operates over specific periods during which the same thermodynamic tasks are performed [16–18], and continuous machines, in which the system operates continuously without interruption [19–24]. In both cases, investigations are usually restricted to physical processes similar to classical thermodynamic ones, such as work performed, average heat flow, and entropy production. However, a pertinent question remains : how can we incorporate real quantum steps into the machine operation, and, if possible, what benefits can we derive from doing so ?

From a theoretical point of view, the study of quantum properties in thermal devices follows two complementary directions. Recent efforts have focused on the design of novel systems to generate and enhance quantum properties in thermal devices, resulting in a plethora of proposals [25–27]. A number of these approaches explore methods for establishing quantum corre-

lations using thermal resources such as thermal bath temperatures and heat fluxes. Moreover, quantum correlations have been identified as crucial for the design of efficient thermal processes, with theoretical proposals involving refrigerators and quantum engines [28–30]. Recent studies have explored the connection between induced heat fluxes during machine operation and the resulting quantum properties, establishing well-founded performance bounds. Despite the impressive theoretical progress in this area, the practical implementation of these concepts remains relatively unexplored and warrants considerable attention [31–34].

To effectively address these expectations, it is crucial to take advantage of the theory of open quantum systems [35–38] . This theory provides a comprehensive framework for describing the evolution of systems of infinitesimal dimensions interacting with their environment. By exploiting the insights provided by open quantum systems theory, we can delve deeper into the dynamics of the quantum thermal machines and gain a better understanding of their conceptualization in the quantum thermodynamic field. Furthermore, the combination of this theory with the principles of quantum thermodynamics allows us to establish a holistic representation of the behavior of non-equilibrium thermal devices under both transient and steady-state conditions, from theoretical conceptualization to practical implementation.

In this thesis, we investigate the interplay between quantum effects arising during the operation of quantum refrigerators and their thermodynamic performance. We investigate the thermodynamic behavior of different quantum refrigerator models under the influence of quantum properties. In the following chapters, we present a variety of quantum refrigerator models and carry out in-depth analyses of their refrigeration performance in regimes where quantum properties exert a significant influence. These efforts enable us not only to grasp the operational subtleties of our devices in the presence of quantum effects, but also to conduct a comparative evaluation of their efficiency compared to the case where these properties turn out to be non-existent.

In Chapter 1, we present a comprehensive exploration of the various aspects of open quantum systems. These fundamental concepts serve as the cornerstone for the analysis of the evolution of the devices under study in the following chapters. We define the different stages and scenarios in which a local approach to the master equation accurately represents the transitions of an open quantum system from one quantum state to another. Our approach relies mainly on the use of a weak coupling limit to approximate the system dynamics by a local master equation. In addition, we explicitly address some crucial aspects of the system dynamics, providing a convenient framework for distinguishing the system dynamics in Markovian and non-Markovian regimes. Second, we delve into the interesting realm of quantum features observed in the evolution of the system, highlighting the central relevance of quantum correlations, which form the cornerstone of our study.

In Chapter 2, we present a general introduction to the fundamental concepts of quantum thermodynamics, starting with an exploration of the internal energy of a system of interest. We then examine the different forms of energy involved in the variation of internal energy during system operation. To further elucidate these principles, we incorporate illustrative examples drawn from the devices studied in this thesis. In addition, we highlight the criticality of these principles by demonstrating their adherence to the laws of thermodynamics through various formulations. In Chapter 3, we present a detailed description of the quantum refrigerator models used in our study, as well as their modes of operation. Our central insight concerns the conditions required for these devices to operate in the cooling regime.

In Chapter 4, our attention turns to the introduction of coupling models for autonomous quantum refrigerators. These refrigerators are connected via their cold qubits, allowing for a subtle exploration of their behavior in regimes characterized by distinct degrees of correlation in their interaction. For three-body refrigerator models, we adopt entanglement as the measure of correlation, while in the context of two-body models, we rely on the measure of quantum discord. We then perform a comprehensive comparative analysis of the performance of these coupled refrigerator models against their uncoupled counterparts with identical parameters. Through this comparative investigation, we aim to gain a deeper appreciation of the effect of inter-device coupling on the thermodynamic performance of quantum refrigerators, thereby advancing our understanding of these complex systems.

In Chapter 5, we move to a model involving a working system coupled to hierarchical environments, each consisting of a thermal bath and an auxiliary system. Here we delve into the system operation in both discrete and continuous models, meticulously studying its operation within a cooling regime. Furthermore, we conduct a thorough investigation of the efficiency of the devices, especially when the dynamics of the working system evolve within either a Markovian or a non-Markovian regime. Through these analyses, we intend to unravel the complex dynamics governing the thermodynamic behavior of the system with respect to hierarchical environments and to elucidate aspects related to system efficiency.

Finally, we mark the culmination of our efforts with a comprehensive conclusion in which we synthesize the key ideas gleaned from our various contributions. In a detailed summary, we highlight the significant observations and results obtained. In addition, we pave the way for future projects by outlining our aspirations and potential avenues for further exploration.

Chapitre 1

Open quantum system

A basic knowledge on the dynamical evolution of a thermal machine's working system is a fundamental prerequisite for delving into the thermodynamic concepts of quantum thermal machines. From a thermodynamic perspective, the working system plays a pivotal role in the various flows of thermodynamic quantities, including heat transfer, and serves as a primary element in the dynamic processes of the thermal machine. Furthermore, in a quantum theoretical viewpoint, the working system can be viewed as an open system interacting with different thermal baths. These baths contribute to dissipative effects in the evolution of the thermal machine, giving rise to a dynamic evolution that can also be influenced by an external control system. In this context, the theory of open quantum systems provides a comprehensive framework for analyzing such dynamic behavior, laying the foundation for the development of quantum thermal machines.

Nevertheless, finding an appropriate approach to describe the dynamical evolution of quantum thermal machines without violating the thermodynamics laws remains a formidable theoretical challenge due to their inherent complexity, although it has been successfully accomplished in some cases, such as harmonic oscillators or two-level systems coupled to reservoirs [39, 40]. In general, their formulation relies on a perturbative approach to inter-site coupling, which requires fine-tuning between the energy and interaction time scales of the device components. Two main approaches are considered in the literature to deal with this particular issue. The first approach involves local coupling, where the thermal baths are locally connected to the machine's subsystems. In contrast, the second approach adopts a global coupling scheme, where the thermal baths are connected to the degrees of freedom of the total machine. Given the conceptual differences between the two approaches, the criteria relating to the thermal machine to be considered when choosing one or another approach also differ. Whereas the local approach is more persistent when we consider weak coupling and resonance between all the coupling sites in the device, the global approach has been shown to be more dominant when converging to strong coupling [41–47].

In this chapter, we aim to provide a theoretical background for the quantum master equation in the local approach, while giving an insight into some future considerations on the validity of this equation and its relevance both for the description of the system state and thermodynamic quantities.

1.1 The system-reservoir approach

An open quantum system is defined as a system interacting with at least one environment, see Fig.1.1. This interaction can be either continuous and time-invariant, or subject to a control protocol. Naturally, the total system (open system plus environment) can be described by a

Hamiltonian operator H representing a generic multipartite open system connected to environments,

$$H = H_{\mathcal{S}} + H_{\mathcal{R}} + H_{\mathcal{SR}}, \tag{1.1}$$

where $H_{\mathcal{S}}$ is the Hamiltonian of the system, $H_{\mathcal{R}}$ the Hamiltonian of the environments, and $H_{\mathcal{SR}}$ represents the interaction between the system and the environments.

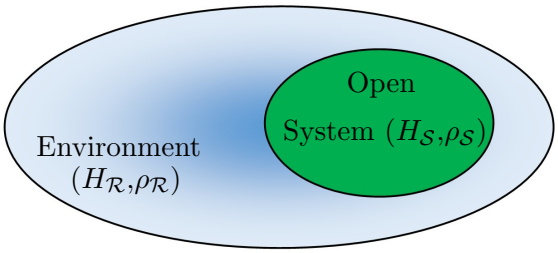

FIGURE 1.1 – Schematic representation of an open quantum system interacting with an environment.

Quantum systems that do not interact with any environment are defined as closed systems. This notion is even less conceivable in quantum mechanics since it is particularly difficult to isolate a system from any form of interaction with its environment. However, without loss of generality, we consider the total system, encompassing both the open system and its environment, as a closed system

1.1.1 Density operator

Quantum system states are generally described by wave functions or vector states $|\psi\rangle$, defined in a Hilbert space $\mathcal{H}$, which contain the maximum amount of information that can be stored in the system. However, in most cases, this representation is not sufficient to fully describe the state of the system, due to constraints on the information that can be gathered from the system. For example, consider a system prepared in a superposition of two states $|\psi_1\rangle$ and $|\psi_2\rangle$, with their respective probabilities p_1 and p_2. In the absence of prior information or measurements on the system, it is unlikely that the state of the system can be perfectly described by a vector state. This restriction arises from our incomplete knowledge of the system's information at all times, making it more plausible for the system to be in either of the two states. Consequently, we can state that the system exists in a set of states $\{|\psi_i\rangle\}$ with associated probabilities $\{p_i\}$, $i = 1, 2$.

More generally, suppose $i \geq 2$ with more than one pi different from 0. An alternative approach to represent the state of the system is defined by a density operator ρ in the form,

$$\rho = \sum_i p_i \left|\psi_i\right\rangle \left\langle\psi_i\right| . \tag{1.2}$$

The density operator ρ is usually called a density matrix, given its matrix representation on a specified basis. It follows from equation. (1.2) that any density operator must satisfy the following properties :

Hermiticity : The density operator ρ is Hermitian,

$$\rho^\dagger = \sum_i p_i^* (|\psi_i\rangle \langle\psi_i|)^\dagger = \sum_i p_i |\psi_i\rangle \langle\psi_i| = \rho. \tag{1.3}$$

Positive definite : For all vectors $|\phi\rangle \in \mathcal{H}$, the density operator ρ satisfies,

$$\langle\phi| \rho |\phi\rangle = \sum_i p_i |\langle\psi_i|\phi\rangle|^2 \geq 0. \tag{1.4}$$

Unit trace : The trace of the operator ρ on the states of the system is bounded,

$$\frac{1}{N^2} \leq Tr\left[\rho^2\right] \leq Tr\left[\rho\right] = \sum_i p_i Tr\left[|\psi_i\rangle \langle\psi_i|\right] = \sum_i p_i = 1, \tag{1.5}$$

where N is the dimension of the Hilbert space $\mathcal{H}$.

For a basic example of a density operator, consider the density matrix of a pure state, where $i = 1$ and $p_1 = 1$,

$$\rho = |\psi\rangle \langle\psi|, \tag{1.6}$$

being a projection operator on the state $|\psi\rangle$. It is straightforward to show the validity of the above conditions as long as the state $|\psi\rangle$ is normalized.

1.1.2 Partial trace

Consider a bipartite composite system described by a density state $\rho_{\mathcal{SR}}$. A common situation is encountered in open quantum system $\mathcal{S}$ interacting with its environment $\mathcal{R}$. The state of the total system is characterized by a density matrix $\rho_{\mathcal{SR}}$ in the Hilbert space

$$\mathcal{H}_{\mathcal{SR}} = \mathcal{H}_{\mathcal{S}} \otimes \mathcal{H}_{\mathcal{R}}, \tag{1.7}$$

with the subsystem Hilbert spaces

$$\begin{aligned} \mathcal{H}_{\mathcal{S}} &= span\{|\psi_i\rangle\}, \\ \mathcal{H}_{\mathcal{R}} &= span\{|\phi_j\rangle\}, \end{aligned} \tag{1.8}$$

where $i \in [0, N]$, N the dimension of the Hilbert space $\mathcal{H}_{\mathcal{S}}$, and $j \in [0, M]$, with M the dimension of the Hilbert space $\mathcal{H}_{\mathcal{R}}$.

The partial trace is a linear operator from the total Hilbert space $\mathcal{H}_{\mathcal{SR}}$ to the subsystem Hilbert spaces $\mathcal{H}_{\mathcal{S}}(\mathcal{H}_{\mathcal{R}})$, defined as :

$$Tr_{\mathcal{R}}\left[\rho_{\mathcal{SR}}\right] = \sum_j \langle\phi_j| \rho_{\mathcal{SR}} |\phi_j\rangle, \tag{1.9}$$

$$Tr_{S}\left[\rho_{\mathcal{SR}}\right] = \sum_i \langle\psi_i| \rho_{\mathcal{SR}} |\psi_i\rangle. \tag{1.10}$$

It follows from equations. (1.8) that the vector bases $\{|\psi_i\rangle\}$ and $\{|\phi_j\rangle\}$ act only on their respective Hilbert spaces . More specifically, the expression $\langle\phi_j| \rho_{\mathcal{SR}} |\phi_j\rangle$ is a partial element of the density matrix $\rho_{\mathcal{SR}}$ taken only from the reservoir, implying that the outcome $Tr_{\mathcal{R}}\left[\rho_{\mathcal{S}}\right]$ is an operator acting on $\mathcal{H}_{\mathcal{S}}$. Similarly, the expression $\langle\psi_i| \rho_{\mathcal{SR}} |\psi_i\rangle$ is a partial element of $\rho_{\mathcal{SR}}$ taken only in the system, and the result $Tr_{\mathcal{S}}\left[\rho_{\mathcal{SR}}\right]$ is also an operator acting on $\mathcal{H}_{\mathcal{R}}$.

The partial trace is extremely useful in the study of complex quantum systems in which we are interested in the information contained in one subsystem only. For instance, when our focus is on the properties of the system $\mathcal{S}$, it becomes evident that all its relevant information is effectively and completely described by the reduced state $Tr_{\mathcal{R}}[\rho_{\mathcal{SR}}]$. In a particular exemple, we can consider the case where the state of the reservoir and the state of the open system are completely separate and form a tensor product $\rho_{\mathcal{SR}} = \rho_S \otimes \rho_{\mathcal{R}}$. In such cases, it becomes feasible to determine the density operators of the individual subsystems through the application of the partial trace,

$$Tr_{\mathcal{R}}[\rho_{\mathcal{SR}}] = Tr_{\mathcal{R}}[\rho_S \otimes \rho_{\mathcal{R}}] = \sum_j \langle\phi_j| \rho_S \otimes \rho_{\mathcal{R}} |\phi_j\rangle = \sum_j \rho_S \otimes \langle\phi_j| \rho_{\mathcal{R}} |\phi_j\rangle = \rho_S, \quad (1.11)$$

$$Tr_S[\rho_{\mathcal{SR}}] = Tr_S[\rho_S \otimes \rho_{\mathcal{R}}] = \sum_i \langle\psi_i| \rho_S \otimes \rho_{\mathcal{R}} |\psi_i\rangle = \sum_s \rho_{\mathcal{R}} \otimes \langle\psi_i| \rho_S |\psi_i\rangle = \rho_{\mathcal{R}}. \quad (1.12)$$

These equations demonstrate how partial trace operations can effectively retrieve information about the individual subsystems, making it a powerful tool in the analysis of composite quantum systems.

1.1.3 Trace distance

Given two states of a quantum system $\rho^1_{\mathcal{S}}$ and $\rho^2_{\mathcal{S}}$, quantum mechanics has long been concerned with assessing the similarity between theses two states. A sophisticated approach to this challenge involves defining a suitable distance metric over the set of density operators. This distance metric can then be interpreted as a measure of the distinguishability between the quantum states. In the realm of quantum theory, the trace distance stands out as one of the most crucial and frequently employed measures for quantifying the the distinguishability of quantum states.

The trace distance between two density operators $\rho^1_{\mathcal{S}}$ and $\rho^2_{\mathcal{S}}$ is defined as

$$D(\rho^1_{\mathcal{S}}, \rho^2_{\mathcal{S}}) = \frac{1}{2} Tr|\rho^1_{\mathcal{S}} - \rho^2_{\mathcal{S}}|, \quad (1.13)$$

where $|A| = \sqrt{A^\dagger A}$ and the square root of a Hermitian operator $A^\dagger A$ with nonnegative eigenvalues a_i and eigenstates $|\psi_i\rangle$ is defined as

$$\sqrt{A^\dagger A} = \sum_i \sqrt{a_i} |\psi_i\rangle \langle\psi_i|. \quad (1.14)$$

When A is self-adjoint, the trace distance can be expressed as the sum of the absolute value of the eigenvalues a_i of A counting multiplicities

$$Tr|A| = \sum_i |a_i|. \quad (1.15)$$

The trace distance has several interesting mathematical and physical properties that make it a convenient distance measure within quantum information theory. Here are some of the properties satisfied by the trace distance as a general distance measure :

The trace distance between any pair of states is bounded,

$$0 \leq D(\rho^1_{\mathcal{S}}, \rho^2_{\mathcal{S}}) \leq 1, \quad (1.16)$$

with $D(\rho^1_{\mathcal{S}}, \rho^2_{\mathcal{S}}) = 0$ if and only if $\rho^1_{\mathcal{S}} = \rho^2_{\mathcal{S}}$ and $D(\rho^1_{\mathcal{S}}, \rho^2_{\mathcal{S}}) = 1$ if and only if $\rho^1_{\mathcal{S}}$ and $\rho^2_{\mathcal{S}}$ are orthogonal.

The trace distance is sub-additive with respect to tensor products of states,

$$D(\rho_{\mathcal{S}}^1 \otimes \rho_{\mathcal{S}}^3, \rho_{\mathcal{S}}^2 \otimes \rho_{\mathcal{S}}^4) \leq D(\rho_{\mathcal{S}}^1, \rho_{\mathcal{S}}^2) + D(\rho_{\mathcal{S}}^3, \rho_{\mathcal{S}}^4). \tag{1.17}$$

The trace distance is invariant under unitary transformations $\mathcal{U}$,

$$D(\mathcal{U}\rho_{\mathcal{S}}^1\mathcal{U}^\dagger, \mathcal{U}\rho_{\mathcal{S}}^2\mathcal{U}^\dagger) = D(\rho_{\mathcal{S}}^1, \rho_{\mathcal{S}}^2). \tag{1.18}$$

All trace preserving and completely positive maps $\mathcal{E}$ (see Sec.1.4.2), are contractible for the trace distance,

$$D(\mathcal{E}\rho_{\mathcal{S}}^1, \mathcal{E}\rho_{\mathcal{S}}^2) \leq D(\rho_{\mathcal{S}}^1, \rho_{\mathcal{S}}^2). \tag{1.19}$$

One can therefore state that a trace-preserving quantum dynamical map reduces or maintains the ability to distinguish any pair of quantum states. Hence, no quantum process that can be characterized by a family of dynamically trace-preserving and completely positive maps can increase the ability to distinguish a pair of system states from its initial value.

We will see later how these properties are commonly leveraged in quantum information theory, especially in the examination of the non-Markovianity of an open system and other quantum informations.

1.1.4 Weak coupling

Without specifying the form of interaction between the system and its environment, a more detailed configuration of the composite system's state implies that the density matrix of the total system can be expressed as :

$$\rho_{\mathcal{SR}} = \rho_{\mathcal{S}} \otimes \rho_{\mathcal{R}} + \rho_{int}, \tag{1.20}$$

where $\rho_{\mathcal{S}}$ and $\rho_{\mathcal{R}}$ are reduced density operators defined on the Hilbert space of the system $\mathcal{H}_{\mathcal{S}}$ and the Hilbert space of the reservoir $\mathcal{H}_{\mathcal{R}}$ respectively, and the entangled part ρ_{int} describes the correlations induced by the interaction between the subsystems.

Among various possible approaches and approximation schemes to model the state of the composite system comprising the open system and the reservoir, particular interest lies in the "weak coupling" approach. This approach assumes a weak interaction between the system and its environment. In this context, the contribution of the entangled term ρ_{int} to the state of the total system ρ is considered much smaller compared to the separate part $\rho_{\mathcal{S}} \otimes \rho_{\mathcal{R}}$. Consequently, the influence of ρ_{int} on the total system dynamics can be neglected, leading to the simplified form of the total system state :

$$\rho_{\mathcal{SR}} = \rho_{\mathcal{S}} \otimes \rho_{\mathcal{R}}. \tag{1.21}$$

Even though the assumption of weak coupling between the system and the reservoir is not imperative, it provides a rigorous mathematical procedure for deriving the master equations of an open quantum system, particularly in the Markov approximation.

1.2 Quantum entropy

Another fundamental concept of quantum information is the notion of entropy. Entropy was developed in the thermodynamics field and subsequently adopted in classical statistical mechanics and quantum statistics, as a measure of the degree of uncertainty in the state of a physical system [48–55]. A preliminary description of classical entropy was provided by Shannon in his mathematical interpretation of classical information, before being extended to the quantum domain through equivalent quantities.

1.2.1 Shannon Entropy

Consider a random variable X with a probability distribution $\{p(a_i)\}$, where $i = 1, ..d$, and $\sum_{i=1}^{d} p(a_i) = 1$. The Shannon entropy of X is defined as [56]

$$H(X) \equiv H(p(a_1), ..., p(a_d)) \equiv -\sum_{i=1}^{d} p(a_i) log(p(a_i)), \tag{1.22}$$

where we conventionally admit that $0log(0) = 0$. It is easy to observe that, in the case of a binary distribution ($d = 2$), the entropy of the probability distribution can be adapted to a single parameter given by :

$$H(p) = -plog(p) + (1-p)log(1-p), \tag{1.23}$$

where p is the probability of one of the outcomes.

When examining the same random variable X under two different probability distributions $\{p(a_i)\}$ and $\{q(a_i)\}$, the proximity of these distributions can be assessed through their relative entropy :

$$H(p(a_i)\|q(a_i)) = \sum_{i=1}^{d} p(a_i) log\left(\frac{p(a_i)}{q(q_i)}\right), \tag{1.24}$$

with $-p(a_i)log0 \equiv +\infty$, $\forall p(a_i) > 0$. Along the same lines, the information available from two different random variables, X and Y, associated with their joint distribution $p(a_i, b_j)$ is provided by the joint entropy defined in an obvious way,

$$H(X,Y) = -\sum_{i=1}^{d}\sum_{j=1}^{l} p(a_i, b_j) log(p(a_i, bj)). \tag{1.25}$$

To delve deeper,, let's assume we have prior knowledge about the value of Y given a pair of variables (X, Y). In this scenario, we quantify the information $H(Y)$ about the pair (X, Y). The residual uncertainty about the pair (X, Y) is then attributed to our lack of knowledge about X. As a result, the entropy of X under the condition that we know Y in advance is defined by the conditional entropy ;

$$H(X|Y) = H(X,Y) - H(Y). \tag{1.26}$$

The Shannon entropy H in the form of a function of random variables verifies the following properties :

> Subadditivity : $H(X,Y) \leq H(X) + H(Y)$ with equality if and only if X and Y are independent random variables.

Symmetry

$$H(X,Y) = H(Y,X) \tag{1.27}$$

$H(X) \leq H(X,Y)$, with equality if and only if Y is a function of X.

1.2.2 Von Neumann Entropy

The von Neumann entropy holds an important place in quantum statistical mechanics [57], particularly for characterizing the information inherent in a quantum state represented by a density operator ρ. It is defined as an extension of the Shannon entropy to the spectrum of a quantum state

$$S(\rho) \equiv -\rho log(\rho) \equiv -\sum_i a_i log(a_i), \tag{1.28}$$

where, in the second equality, a_i represents the eigenvalues of ρ, and the convention $0log0 = 0$ is adopted, as in the case of the Shannon entropy. The von Neumann entropy is always positive,subadditive and concave. The concavity property implies that for a set of density operator $\{\rho_i\}$ associated to a probability distribution $\{p_i\}$, with $\sum_i p_i = 1$, we have

$$\sum_i p_i S(\rho_i) \leq S(\sum_i p_i \rho_i). \tag{1.29}$$

Additionally, a quantum version of the relative entropy needs to be defined. Suppose ρ_1 and ρ_2 are density operators. The relative entropy of ρ_1 to ρ_2 is defined by

$$S(\rho_1 \| \rho_2) \equiv Tr(\rho_1 log \rho_1) - Tr(\rho_1 log \rho_2). \tag{1.30}$$

Relative entropy takes values from 0 to $+\infty$ relative to the assumption $-a_i log(0) = +\infty$, with $S(\rho_1 \| \rho_2) = 0$ if and only if $\rho_1 = \rho_2$. More specifically, it verifie the following conditions

The relative entropy is non symetrique

$$S(a \| b) \neq S(b \| a) \tag{1.31}$$

The relative entropy is invariant under unitary transformations,

$$S(\mathcal{U} a \mathcal{U}^\dagger \| \mathcal{U} a \mathcal{U}^\dagger) = S(a \| b). \tag{1.32}$$

1.3 Quantum Correlation

Quantum correlations serve as a crucial measure of the quantum characteristics inherent in a composite system comprising two or more elements [58–62]. They constitute a fundamental quantum signature for multipartite systems. Beyond their theoretical significance, quantum correlations and coherence hold substantial practical importance, as they are essential physical resources for various quantum information and computation processes. Despite the prolonged interest and investigation since the early days of quantum theory, these phenomena remain intriguing, leaving physicists with many unanswered questions.

Naturally, the states of a multipartite quantum system cannot be written as the tensor product of its subsystem states. States in this form are called separate states. Otherwise, the nature of the multipartite system implies a certain degree of shared information between the subsystems that do not allow a complete separation of their states. In this scenario, subsystems lose their individuality since a proportion of their physical properties are now partially embedded in correlations and therefore cannot be attributed to a single subsystem. Traditionally, this propertie has been a reference for characterizing quantum correlation in composite systems. However, it subsequently emerged that quantum correlation can be attributed to contexts that go beyond entanglement, whether stronger or weaker. Remarkably, quantum correlations can subsist even in separable states.

1.3.1 Quantum entanglement

Entanglement is a distinctive feature of non-separable quantum states, representing one of the most profound and insightful concepts illustrating the validity and limits of quantum mechanics [63–68]. With the advent of quantum information science, entanglement has attracted renewed interest as a valuable resource in quantum information processing. In particular, it is perceived as central to the implementation of various quantum protocols, including quantum teleportation, which can be achieved exclusively using entangled states.

The characterization and measurement of entanglement has for a long time been a complex, broad and dynamic area of research. Numerous methodologies for quantifying entanglement have been introduced, along with the formulation of essential criteria for its measurement. Multipartite systems, in particular, have witnessed significant progress and exploration, with several mechanisms devised to differentiate separable states from entangled ones, including the utilization of Schmid rank and von Neumann entropy.

Entanglement of bipartite system

The degree of separation and entanglement in a pure bipartite quantum state is used to assess the correlation present in the composite quantum system. Taking a pure bipartite state $|\psi_{\mathcal{S}_1\mathcal{S}_2}\rangle \in \mathcal{H}_{\mathcal{S}_1} \otimes \mathcal{H}_{\mathcal{S}_2}$, it can be asserted that $|\psi_{\mathcal{S}_1\mathcal{S}_2}\rangle$ is not entangled if and only if it can be written as a tensor product of pure states in the Hilbert spaces $\mathcal{H}_{S_1}(\mathcal{H}_{S_2})$ of its components

$$|\psi_{\mathcal{S}_1\mathcal{S}_2}\rangle = |\psi_{\mathcal{S}_1}\rangle \otimes |\psi_{\mathcal{S}_2}\rangle \tag{1.33}$$

where $|\psi_{\mathcal{S}_1}\rangle \in \mathcal{H}_{\mathcal{S}_1}$, and $|\psi_{\mathcal{S}_2}\rangle \in \mathcal{H}_{\mathcal{S}_2}$. The separability of state $|\psi_{\mathcal{S}_1\mathcal{S}_2}\rangle$ indicates that each subsystem can be characterized by its specific properties, accessible locally without affecting the state of the second subsystem.

A more elementary approach to determine the separability of pure states involves the Schmidt decomposition. For every pure bipartite state, the Schmidt decomposition posits the existence of two orthonormal bases for each subsystem such that :

$$|\psi_{\mathcal{S}_1\mathcal{S}_2}\rangle = \sum_{i}^{d} \sqrt{p_i}\, |\psi_{\mathcal{S}_1}\rangle_i \otimes |\psi_{\mathcal{S}_2}\rangle_i \tag{1.34}$$

where $\{|\psi_{\mathcal{S}_1}\rangle_i\}, \{|\psi_{\mathcal{S}_2}\rangle_i\}$ is an orthonormal basis pertaining to the local Hilbert space $\mathcal{H}_{\mathcal{S}_1}(\mathcal{H}_{\mathcal{S}_2})$ and $d \leq \min\{dim\left[\mathcal{H}_{\mathcal{S}_1}\right], dim\left[\mathcal{H}_{\mathcal{S}_2}\right]\}$. The coeficients p_i are are called Schmidt coefficients and satisfy $0 < p_i \leq 1$. It follows from the normalization of the totale state $|\psi_{\mathcal{S}_1\mathcal{S}_2}\rangle$ that $p_i \geq 0$ and $\sum_{i=1}^{d} p_i = 1$. Thus, a quantum state is considered to have a Schmidt rank of 1 if only one Schmidt coefficient is non-zero (and therefore equal to 1), which implies that the system

is separable. On the other hand, if the Schmidt rank is greater than 1 (i.e. if more than one Schmidt coefficient is non-zero), then the system is considered to be entangled.

Expanding from equation.(1.34), we can extend the concept of entanglement to the case of mixed states with the help of the Schmidt decomposition. In the broader context of the fundamental principles of the density operator formalism, we may define a state of a composite quantum system $\rho_{\mathcal{S}_1\mathcal{S}_2}$ as entangled if it cannot be expressed in the form :

$$\rho_{\mathcal{S}_1\mathcal{S}_2} = \sum_{i=1}^{d} p_i \rho^i_{\mathcal{S}_1} \otimes \rho^i_{\mathcal{S}_2} \tag{1.35}$$

where $p_i \geq 0$, $\rho^i_{\mathcal{S}_1} = |\psi_{\mathcal{S}_1}\rangle_i \langle\psi_{\mathcal{S}_1}|_i \in \mathcal{H}_{\mathcal{S}_1}$ and $\rho^i_{\mathcal{S}_2} = |\psi_{\mathcal{S}_2}\rangle_i \langle\psi_{\mathcal{S}_2}|_i \in \mathcal{H}_{\mathcal{S}_2}$. Notably, the reduced density operators $\rho_{\mathcal{S}_1}$ and $\rho_{\mathcal{S}_2}$ are obtained by taking the partial trace of the system state with respect to subsystem $\mathcal{S}_1$ or $\mathcal{S}_2$:

$$\rho_{\mathcal{S}_1} = Tr_{\mathcal{S}_2}\left[\rho_{\mathcal{S}_1\mathcal{S}_2}\right] = \sum_{i=1}^{d} p_i \rho^i_{\mathcal{S}_1}, \tag{1.36}$$

$$\rho_{\mathcal{S}_2} = Tr_{\mathcal{S}_1}\left[\rho_{\mathcal{S}_1\mathcal{S}_2}\right] = \sum_{i=1}^{d} p_i \rho^i_{\mathcal{S}_2}. \tag{1.37}$$

Considering the definition of separability in equation.(1.33) and the form of equation.(1.35), it can be asserted that the state $\rho_{\mathcal{S}_1\mathcal{S}_2}$ is separable if and only if there is a single non-zero value p_i . With this in mind, significant progress has been made to establish a measure of entanglement decay, and various indicators have been proposed. It has been agreed that a measure of entanglement E would eventually be conceivable if the following conditions are satisfied :

The degree of entanglement present in any separable state should be zero : $E(\rho_{\mathcal{S}_1\mathcal{S}_2}) = 0$ for all separable states.

The degree of entanglement present in any state should be invariant under local unitary operation

$$E(\rho_{\mathcal{S}_1\mathcal{S}_2}) = E(\mathcal{U}_1 \otimes \mathcal{U}_2 \rho_{\mathcal{S}_1\mathcal{S}_2} \mathcal{U}_1 \otimes \mathcal{U}_2) \tag{1.38}$$

The degree of entanglement present in two given pair of entangled states is additive

$$E(\rho_{\mathcal{S}_1\mathcal{S}_2} \otimes \sigma_{\mathcal{S}_1\mathcal{S}_2}) = E(\rho_{\mathcal{S}_1\mathcal{S}_2}) + E(\sigma_{\mathcal{S}_1\mathcal{S}_2}). \tag{1.39}$$

The degree of entanglement present in any given state must not increase under local operations and classical communication :

$$E(\rho_{\mathcal{S}_1\mathcal{S}_2}) \geq E(\sum_{i=1}^{d} p_i \mathcal{M}^i_{\mathcal{S}_2} \otimes \mathcal{M}^i_{\mathcal{S}_1} \rho_{\mathcal{S}_1\mathcal{S}_2} \mathcal{M}^i_{\mathcal{S}_2} \otimes \mathcal{M}^i_{\mathcal{S}_1}) \tag{1.40}$$

for any set of measurement operators $\mathcal{M}^i_{\mathcal{S}_1}$ and $\mathcal{M}^i_{\mathcal{S}_2}$ on subsystems $\mathcal{S}_1$ and $\mathcal{S}_2$ respectively. In this order, the only measure of entanglement that satisfies theses condition for a pure state, is the von Neumann entropy of reduced density matrices, defined as

$$\begin{aligned} E(|\psi_{\mathcal{S}_1\mathcal{S}_2}\rangle) &= S(\rho_{\mathcal{S}_1}) = S(\rho_{\mathcal{S}_2}) = -Tr\left[\rho_{\mathcal{S}_1} log(\rho_{\mathcal{S}_1})\right] \\ &= -Tr\left[\rho_{\mathcal{S}_2} log(\rho_{\mathcal{S}_2})\right] = \sum_i a_i log_2(a_i). \end{aligned} \tag{1.41}$$

where a_i are the eigenvalues of $\rho_{\mathcal{S}_1}(\rho_{\mathcal{S}_2})$. The entanglement measure E gives a number between 0 and 1, implying a product state and a maximally entangled state respectively.

Otherwise, the separability of a mixed state is particularly problematic to verify by any direct method. For this reason, certain types of entanglement measure have been proposed in the literature, incorporating new methods that are more suited to the properties of density operators. Separability often proves difficult to determine as soon as we move away from pure states, so a measurement of the density state mixture becomes an alternative way of quantifying entanglement in this case. This has led to the introduction of different measures of entanglement. The three main ones being the entanglement cost, the distillable entanglement and the entanglement of formation. Another favourite measure is the concurrence measure, originally defined for 2×2 systems, but later generalised to higher dimensions of Hilbert spaces. Wootters established an expression for quantifying the entanglement between a pair of two-level systems in any state by introducing a relevant measure termed concurrence. In the case of a pure state involving two qubits, the concurrence $\mathcal{C}$ is defined as :

$$C(|\psi_{\mathcal{S}_1\mathcal{S}_2}\rangle) = |\langle\psi_{\mathcal{S}_1\mathcal{S}_2}|\tilde{\psi}_{\mathcal{S}_1\mathcal{S}_2}\rangle|. \tag{1.42}$$

Here $|\tilde{\psi}\rangle_{\mathcal{S}_1\mathcal{S}_2} = \sigma_y^{\mathcal{S}_1} \otimes \sigma_y^{\mathcal{S}_2} |\psi^*\rangle_{\mathcal{S}_1\mathcal{S}_2}$ denotes the spin-flip operation applied to $|\psi_{\mathcal{S}_1\mathcal{S}_2}\rangle$, where σ_y represents the standard Pauli operator, and the symbol '*' signifies complex conjugation in the standard basis.

Let $\rho_{\mathcal{S}_1\mathcal{S}_2}$ be a density matrix of a bipartite system, we can introduce the the generale spin-flip density state

$$\tilde{\rho}_{\mathcal{S}_1\mathcal{S}_2} = (\sigma_y^{\mathcal{S}_1} \otimes \sigma_y^{\mathcal{S}_2})\rho^*_{\mathcal{S}_1\mathcal{S}_2}(\sigma_y^{\mathcal{S}_1} \otimes \sigma_y^{\mathcal{S}_2}) \tag{1.43}$$

where the complex conjugate is taken in the standard basis. A synthesis solution for the concurrence of an arbitrary mixed state of two qubits is given by

$$C(\rho_{\mathcal{S}_1\mathcal{S}_2}) = max\left(0, \sqrt{\lambda_1} - \sqrt{\lambda_2} - \sqrt{\lambda_3} - \sqrt{\lambda_4}\right) \tag{1.44}$$

where $\lambda_i, i = 1, 2, 3, 4$ are the eigenvalues in decreasing order of the product matrix $\rho_{\mathcal{S}_1\mathcal{S}_2}\tilde{\rho}_{\mathcal{S}_1\mathcal{S}_2}$. The eigenvalues λ_i are real and non-negative, and the concurrence value varies from 0 for a non-entangled state to 1 for a maximally entangled state. Consequently, C can be functionally represented as a physically realistic measure of entanglement for mixed states.

In the special case where the density matrix is given in the X-form :

$$\rho_{\mathcal{S}_1\mathcal{S}_2} = \begin{pmatrix} a & 0 & 0 & c \\ 0 & b & d & 0 \\ 0 & b^* & e & 0 \\ c^* & 0 & 0 & f \end{pmatrix}, \tag{1.45}$$

the diagonal elements a, b, e, f represent the populations of the system, while the off-diagonal elements c and d represent the coherent superpositions. The concurrence of the system in this form is described by the following relation [69–72] :

$$\mathcal{C} = 2\max\{0, |c| - \sqrt{be}, |d| - \sqrt{af}\}. \tag{1.46}$$

1.3.2 Quantum discord

The previous section taught that entanglement is potentially synonymous with quantum correlations for non-separated states. This statement is more persistent for pure states, where the measurement of entanglement is associated with the degrée of non-separability of the system state. A most recent advance was made by Ollivier, Zurek and Henderson [73], who evaluated that even for separable states, a quantum system can exhibit correlations that cannot be measured by a classical approximation. The existence of this type of quantum correlation, known as quantum discord, is essentially a manifestation of the impossibility of measuring one of the quantum states of the composite system without disturbing the other [74].

Quantum discord is the first fundamental measure intended to prove the occurrence of quantum correlations beyond entanglement. To grasp its significance, it is essential to hark back to classical information theory, where the Shannon entropy (1.22) quantifies the lack of volume of information stored in a probability distribution : the higher the Shannon entropy of a distribution, the less information we possess about the potential outcome of a random variable associated with that distribution. Moreover, we have seen that in classical information theory, when considering a pair of random variables, X and Y, with a joint probability distribution of obtaining outcomes $X = a$ and $Y = b$ denoted as $p(a, b)$, we can scrutinize the information of each random variable $X(Y)$ individually in terms of their entropy $H(X)(H(Y))$ tout comme leur joint information as well as their joint information $H(X, Y)$. Consequently, the correlation between X and Y is measured by the amount of additional information that is not local. This non-local information can be quantified by the mutual information,

$$\mathcal{I}(X, Y) = H(X) + H(Y) - H(X, Y), \tag{1.47}$$

where, $H(X, Y)$ is the joint entropie. With this definition, $\mathcal{I}$ can take the value 0 for independant variable. In addition, an equivalent formulation for the mutual information is given by :

$$\begin{aligned} \mathcal{J}(X, Y) &= H(X) - H(X|Y) && (1.48)\\ &= H(Y) - H(Y|X), && (1.49) \end{aligned}$$

where the conditional entropy $\mathcal{J}(X, Y)(\mathcal{J}(Y, X))$ quantifies the average uncertainty associated with $X(Y)$ given the value of $Y(X)$. The equality of $\mathcal{I}$ and $\mathcal{J}$ for classical random variables arises from Bayes' rule $p(a|b) = p(a, b)/p(b)$, which can be used to show that

$$H(X|Y) = H(X, Y) - H(Y), \tag{1.50}$$
$$H(Y|X) = H(X, Y) - H(X). \tag{1.51}$$

Refering to the Von Neuman entropy (1.28), we can generalise the expressions (1.50) to the quantum domain by extending the concept of a pair of random variables to a bipartite system with a density matrix $\rho_{\mathcal{S}_1\mathcal{S}_2}$, consisting of subsystems S_1 and S_2 with relative density operators $\rho_{\mathcal{S}_1}$ and $\rho_{\mathcal{S}_2}$. The quantum analogue of equation. (1.47) reads :

$$\mathcal{I}(\rho_{\mathcal{S}_1\mathcal{S}_2}) = S(\rho_{\mathcal{S}_1}) + S(\rho_{\mathcal{S}_2}) - S(\rho_{\mathcal{S}_1\mathcal{S}_2}) \tag{1.52}$$

with the Von Neumann entropy S. On the other hand, the generalisation of $\mathcal{J}(X, Y)$ is not entirely obvious, in the sense that a measure $\mathcal{M}$ on $\rho_{\mathcal{S}_1}$ induces a simultaneous shift in the entropy of $\rho_{\mathcal{S}_2}$. Thus, in the quantum case, the entropy $\mathcal{J}$ becomes dependent on the specified measure, and asymmetric in $\rho_{\mathcal{S}_1}$ and $\rho_{\mathcal{S}_2}$. Ollivier and Zurek proposed a generalization of $\mathcal{J}$ to the quantum theory using quantum measurements. For a bipartite quantum state $\rho_{\mathcal{S}_1\mathcal{S}_2}$, they defined the conditional entropy of $\rho_{\mathcal{S}_1}$ dependent on a measurement on $\rho_{\mathcal{S}_2}$,

$$S(\rho_{\mathcal{S}_1}|\{\Pi^k_{\mathcal{S}_2}\}) = \sum_k p_k S(\rho^k_{\mathcal{S}_1}) \tag{1.53}$$

where $\{\Pi^k_{\mathcal{S}_2}\}$ are measurement operators corresponding to a Von Neumann measure on the subsystem S_2. The probability p_k of getting the result $\rho^k_{\mathcal{S}_1}$ is of the form $p_k = Tr\left[\Pi^k_{\mathcal{S}_2}\rho_{\mathcal{S}_1\mathcal{S}_2}\Pi^k_{\mathcal{S}_2}\right]$ with its corresponding post-measurement state,

$$\rho^k_{\mathcal{S}_1} = \frac{Tr_{\mathcal{S}_2}\left[(\mathbb{1}_{\mathcal{S}_1} \otimes \Pi^k_{\mathcal{S}_2})\rho_{\mathcal{S}_1\mathcal{S}_2}(\mathbb{1}_{\mathcal{S}_1} \otimes \Pi^k_{\mathcal{S}_2})\right]}{p_k}. \tag{1.54}$$

Given the conditional entropy (1.54), the quantum version of equation. (1.48) is succinctly stated by

$$\mathcal{J}(\rho_{\mathcal{S}_1\mathcal{S}_2})_{\{\Pi^k_{\mathcal{S}_2}\}} = S(\rho_{\mathcal{S}_1}) - S(\rho_{\mathcal{S}_1}|\{\Pi^k_{\mathcal{S}_2}\}). \tag{1.55}$$

This version of the mutual information $\mathcal{J}$ relative to a quantum measurement does not, in general, coincide with the definition of the total mutual information in equation. (1.52), which represents the total quantity of correlations (both quantum and classical). An important aspect is that, unlike the classical case, this quantity is always less than the total mutual information before a measurement is made.

Since a quantum measurement on $\rho_{\mathcal{S}_2}$ leads to a perturbation on the quantum properties of the toal state $\rho_{\mathcal{S}_1\mathcal{S}_2}$, the decrease in the total correlation after measurement is associated with a loss of quantum correlation. A classical correlation measurement was therefore introduced by maximizing the mutual information in equation.(1.55) over all possible measurements. The idea is to quantify the classical correlations in the quantum states by maximizing $\mathcal{J}$ over all possible Von Neuman measurements on the subsystem $\rho_{\mathcal{S}_2}$:

$$\begin{aligned} \mathcal{C}(\rho_{\mathcal{S}_1\mathcal{S}_2}) &= \max_{\{\Pi^k_{\mathcal{S}_2}\}} (\mathcal{J}(\rho_{\mathcal{S}_1\mathcal{S}_2})_{\{\Pi^k_{\mathcal{S}_2}\}}) \\ &= S(\rho_{\mathcal{S}_1}) - \min_{\{\Pi^k_{\mathcal{S}_2}\}} \sum_k p_k S(\rho^k_{\mathcal{S}_1}) \end{aligned} \tag{1.56}$$

The quantum discord is defined as the difference of these two inequivalent expressions (quantum and classical versions) for the mutual information,

$$\mathcal{Q}(\rho_{\mathcal{S}_1\mathcal{S}_2}) = \mathcal{I}(\rho_{\mathcal{S}_1\mathcal{S}_2}) - \mathcal{C}(\rho_{\mathcal{S}_1\mathcal{S}_2}). \tag{1.57}$$

It should be noted that quantum discord is not symmetric so applying a measurement to the subsystem $\rho_{\mathcal{S}_1}$ rather than $\rho_{\mathcal{S}_2}$ will generally result in a different value of discord. This asymmetry indicates that the quantum discord quantifies the degree of quantum correlation with respect to the measured system. It is also important that quantum discord captures the quantum correlation of entangled states. However, while a measure of entanglement vanishes for separable states, quantum discord can be non-zero for these states. Although the theoretical description of quantum discord is clear, its calculation proves rather difficult due to the need to maximize all possible measurements on the system under consideration, as shown in equations.(1.56). Nevertheless, various procedures are introduced for the analytical expression of quantum discord in special cases, for example when the state of the system is in the form of a matrix X [75, 76].

1.4 Dynamique of an open quantum system

1.4.1 Liouville-von Neumann equation

First of all, we start our discussion of the equation governing the dynamics of an open system by considering the model of an open quantum system $\mathcal{S}$ interacting with an environment $\mathcal{R}$ introduced in the previous section. The Hamiltonian of the total system is therefore given in the form

$$H = H_{\mathcal{S}} + H_{\mathcal{R}} + H_{\mathcal{S}\mathcal{R}}, \tag{1.58}$$

with $H_{\mathcal{S}}$ is the Hamiltonian of the open systeme, $H_{\mathcal{R}}$ is the Hamiltonian of the bath and $H_{\mathcal{S}\mathcal{R}}$ is the system-bath interaction. Furthermore, we assign to the state of the total system a pure vector state $|\psi\rangle$ in a Hilbert space $\mathcal{H}$. Since the total system is closed, the time evolution of the state $|\psi\rangle$ can then be approximated according to the standards equation governing the evolution of a closed quantum system given by Schrödinger's equation

$$i\hbar \frac{d}{dt} |\psi(t)\rangle = H |\psi(t)\rangle , \tag{1.59}$$

with $\hbar$ being Planck's constant, which we will assume to be equal 1 for the rest of this work. The solution of the differential equation. (1.59), in the case of a time-independent Hamiltonian operator H, can be expressed as :

$$|\psi(t)\rangle = exp\left[-iH(t-t_0)\right]|\psi(0)\rangle\,, \tag{1.60}$$

where $|\psi(0)\rangle$ is the state of the system at an initial time point $t = 0$.

A general expression of equation. (1.60) is of the form of an unitary time-evolution operator $\mathcal{U}(t,0)$ which transforms the initial state $|\psi(0)\rangle$ to the state $|\psi(t)\rangle$,

$$|\psi(t)\rangle = \mathcal{U}(t,0)\,|\psi(0)\rangle\,, \tag{1.61}$$

with the time evolution operator $\mathcal{U}(t,0) = exp\left[-iH(t-0)\right]$. Of course, the particular structure of the evolution operator $\mathcal{U}(t,0)$ in terms of the Hamiltonian depends on the characteristics of the Hamiltonian itself. Once the Hamiltonian of the system is time dependent, the time evolution operator $\mathcal{U}(t,0)$ takes the form of an exponential integral,

$$\mathcal{U}(t,0) = T_{\leftarrow} exp\left(\int_0^t -iH(s)ds\right), \tag{1.62}$$

where $T_{\leftarrow}$ is the time-ordering operator. It is also clear that in both cases of the Hamiltonian operator, the unitary evolution operator verifies

$$\mathcal{U}(0,0) = \mathbb{1}. \tag{1.63}$$

A natural question that deserves attention from the above description is the dynamic evolution of the quantum system when its state at the initial time t_0 is given in the form of a mixed state,

$$\rho_{\mathcal{SR}}(0) = \sum_i p_i\,|\psi_i(0)\rangle\,\langle\psi_i(0)|\,. \tag{1.64}$$

According to the unitary evolution introduced in equation. (1.61), the time evolution of the density operator $\rho_{\mathcal{SR}}$ is then given by

$$\rho_{\mathcal{SR}}(t) = \sum_i p_i \mathcal{U}(t,0)\,|\psi(0)\rangle\,\langle\psi(0)|\,\mathcal{U}^\dagger(t,0), \tag{1.65}$$

being

$$\rho_{\mathcal{SR}}(t) = \mathcal{U}(t,0)\rho_{\mathcal{SR}}(0)\mathcal{U}^\dagger(t,0). \tag{1.66}$$

Equation. (1.66) gives the state of the total system at each instant t based on the total unitary evolution operator. As our focus is on the equation of motion for the open system, it becomes necessary to establish the expression for the derivative of the density operator $\rho_{\mathcal{S}}$. To achieve this, we will initiate the process by determining the expression for the derivative of the density operator $\rho_{\mathcal{SR}}$.

Given the above considerations, the equation of motion of the total density operator is obtained after a derivative of $\rho_{\mathcal{SR}}$ with respect to time,

$$\begin{aligned}\frac{d}{dt}\rho_{\mathcal{SR}}(t) &= \frac{d}{dt}\left(\mathcal{U}(t,0)\rho_{\mathcal{SR}}(0)\mathcal{U}^\dagger(t,0)\right)\\ &= -iH(t)\mathcal{U}(t,0)\rho_{\mathcal{SR}}(0)\mathcal{U}^\dagger(t,0) + i\mathcal{U}(t,0)\rho_{\mathcal{SR}}(0)\mathcal{U}^\dagger(t,0)H(t).\end{aligned} \tag{1.67}$$

Equation. (1.67) is commonly known as the Liouville von Neumann equation, and can be represented in simplified form

$$\frac{d}{dt}\rho_{\mathcal{SR}}(t) = -i\left[H(t), \rho_{\mathcal{SR}}(t)\right], \tag{1.68}$$

where the commutator $[A,B] = AB - BA$.

At this stage, we have established the equation of motion for the total system. Nevertheless, this does not correspond to our intention of finding the equation for the dynamics of the open system alone. It is therefore necessary to adjust equation. (1.68) in order to obtain an appropriate equation for the dynamics of the open system, , taking into account the influence of the interaction between the open system and the reservoir. To accomplish this, we will employ several conceptually different yet complementary approaches.

1.4.2 Quantum dynamical maps

In Equation. (1.66), the state of the total system $\rho_{\mathcal{SR}}$ is represented in terms of the unitary evolution operator of the total system. Naturally, it follows that by applying a partial trace over the environment, we can recover the open quantum system state at each instat t,

$$\rho_{\mathcal{S}}(t) = Tr_{\mathcal{R}}\left[\mathcal{U}(t,0)\rho_{\mathcal{SR}}(0)\mathcal{U}^{\dagger}(t,0)\right]. \tag{1.69}$$

One of the primary tasks stemming from this equation is to express the state of the open system $\rho_{\mathcal{S}}$ in terms of a dynamical map (Fig.5.2) acting on the space of density matrices $S(\mathcal{H}_{\mathcal{S}})$, connecting its initial state to its state at time t :

$$\begin{aligned} \mathcal{E}(t) \quad &: \quad S(\mathcal{H}_{\mathcal{S}}) \longrightarrow S(\mathcal{H}_{\mathcal{S}}) \\ &\qquad \rho_{\mathcal{S}}(0) \longrightarrow \rho_{\mathcal{S}}(t) = \mathcal{E}_t\rho_S(0), \qquad \forall t \geq 0, \end{aligned} \tag{1.70}$$

where, $\mathcal{E}_0 = \mathbb{1}$, is the identity map. The transformation mentioned above is generally crucial to derive, encompassing the entire future evolution of an open system. Its complexity arises not only from its dependence on the unitary evolution of the total system but also from the constraints on the states of the subsystems at the initial time. Particularly, when the initial state of the total system is correlated, constructing a map that accurately describes the transformation of the open system's state between two instants becomes challenging. However, as this situation falls outside the scope of our study, we will later consider the approximation that the initial state of the system can still be treated as separable.

Let us consider the state of the total system at time t_0 in an uncorrelated state $\rho_{\mathcal{SR}}(0) = \rho_{\mathcal{S}}(0) \otimes \rho_{\mathcal{R}}(0)$. The transformation changing the reduced system from time $t = 0$ to some later time $t > 0$ may be written in the form

$$\mathcal{E}_t\rho_S(0) = Tr_{\mathcal{R}}\left[\mathcal{U}(t,0)\rho_{\mathcal{S}}(0) \otimes \rho_{\mathcal{R}}(0)\mathcal{U}^{\dagger}(t,0)\right]. \tag{1.71}$$

The map $\mathcal{E}$ is also known as the universal dynamical map since it is independent of the state on which it acts [35] and describes any possible physical evolution for any abritrary initial state $\rho_{\mathcal{S}}(0)$. To ensure that the universal dynamical map $\mathcal{E}$ describes a physical process, transforming any density operators $\rho_{\mathcal{S}}(0)$ into a density operator $\rho_{\mathcal{S}}(t)$, $\mathcal{E}$ must satisfy the following conditions :

The map $\mathcal{E}$ is completely positive. That is, in addition to mapping a positive operator to a positive operator, when we extend the Hilbert space beyond the open system by including an additional system $\mathcal{S}_1$ that does not interact with the system $\mathcal{S}$ at any time, the map $\mathcal{E} \otimes I_{\mathcal{S}_1}$ acting on the total system maps a positive operator to a positive operator. If, in addition, we consider the trace preservation,

$$Tr\left[\mathcal{E}_t\rho_S(0)\right] = Tr\left[\rho_S(t)\right] = 1, \qquad t \geq 0, \tag{1.72}$$

then $\mathcal{E}$ is called a completely positive and trace preserving map.

The quantum map must be convex and linear. This means that, for any two density operators, $\rho_{\mathcal{S}_1}$ and $\rho_{\mathcal{S}_1}$ chosen randomly, we have

$$\mathcal{E}_t(p\rho_{\mathcal{S}_1} + (1-p)\rho_{\mathcal{S}_2}) \leq p\mathcal{E}_t(\rho_{\mathcal{S}_1}) + (1-p)\mathcal{E}_t(\rho_{\mathcal{S}_2}). \tag{1.73}$$

which must be valid for all $0 \leq p \leq 1$.

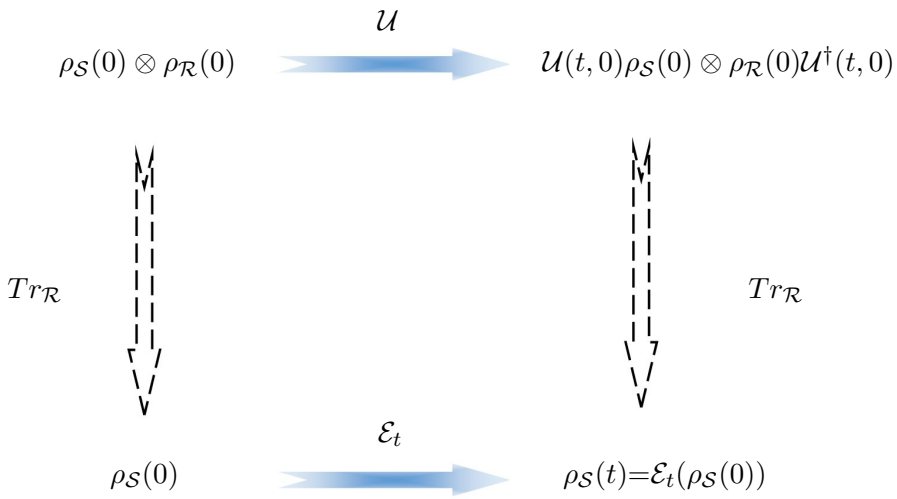

FIGURE 1.2 – Schematic representation of the two standard approaches that can be adopted to approximate the state of an open system at a given instant t from its initial state. In the first approach, the state of the system is derived from a partial trace $T_{\mathcal{R}}$ after a unitary evolution. In the second approach, the state of the system is obtained by mapping the initial state with a dynamic map $\mathcal{E}$.

An additional fundamental feature of quantum dynamical maps enunciated by Karl Kraus states that any completely positive and trace preserving dynamical map can be expressed by operators that act simply in the Hilbert space $H_{\mathcal{S}}$ of the open system. To derive this relation, we first require a spectral decomposition of the environment $\mathcal{R}$,

$$\rho_{\mathcal{R}} = \sum_i p_j \left|\phi_j\right\rangle \left\langle\phi_j\right|, \tag{1.74}$$

where $\{|\phi_j\rangle\}$ form a orthonormal basis in the Hilbert space $\mathcal{H}_{\mathcal{R}}$ and p_j are non-negative real coefficients satisfying $\sum_j p_j = 1$. The substitution of equation.(1.74) in equation.(1.71) provides

$$\begin{aligned} \rho_{\mathcal{S}}(t) &= Tr_{\mathcal{R}}\left[\mathcal{U}(t,0)\rho_{\mathcal{S}}(0) \otimes \rho_{\mathcal{R}}(0)\mathcal{U}^{\dagger}(t,0)\right] \\ &= \sum_j p_j Tr_{\mathcal{R}}\left[\mathcal{U}(t,0)\rho_{\mathcal{S}}(0) \otimes \left|\phi_j\right\rangle \left\langle\phi_j\right| \mathcal{U}^{\dagger}(t,0)\right] \\ &= \sum_{(j,i)} K_{(i,j)}(t,0)\rho_{\mathcal{S}}(0)K^{\dagger}_{(i,j)}(t,0), \end{aligned} \tag{1.75}$$

where $K_{(j,i)}(t,0) = \sqrt{p_j}\left\langle\phi_i\right|\mathcal{U}(t,0)\left|\phi_j\right\rangle$. Here, the set of operators $\{K_{(j,i)}$ are called Kraus operators [77, 78], mapping elements of the Hilbert space $\mathcal{H}_{\mathcal{S}}$ into the Hilbert space $\mathcal{H}_{\mathcal{S}}$ and satisfy the completeness relation

$$\sum_{j,i} K_{(j,i)}K^{\dagger}_{(j,i)} = \mathbb{1}. \tag{1.76}$$

Clearly, the operators $K_{(j,i)}(t,0)$ depend only on the total unitary evolution operator and the initial state of the subsystem $\mathcal{R}$. Kraus operators is not necessarily unique and may vary depending on the reservoir's orthonormal basis.

1.4.3 Lindblad master equation

The master equation known as Gorini-Kossakowski-Sudarshan-Lindblad equation, or often simply the Lindblad equation, is a valuable reference structure for deriving the master equation of a composite quantum system. It yields an effective equation of motion for a subsystem within a larger complex quantum system. In this section, our focus is on deriving the Lindblad's master equation, which governs the time evolution of an open quantum system.

Let's start by the transformation of a quantum operator from the Schrödinger picture to the interaction picture,

$$\tilde{O}(t) = \mathcal{U}_0^\dagger(t) O(t) \mathcal{U}_0(t), \tag{1.77}$$

where $\mathcal{U}_0(t)$ represents the unitary evolution operator of the total system, defined in the Schrödinger representation as :

$$\mathcal{U}_0(t) = e^{-i(H_\mathcal{S}+H_\mathcal{R})t}. \tag{1.78}$$

From equation. (1.24), one can directly obtain the Liouville-Von Neumann equation. (1.26) for the joint system in the interaction picture,

$$\begin{aligned} \frac{d}{dt}\tilde{\rho}_{\mathcal{SR}}(t) &= \frac{d}{dt}\left(\mathcal{U}_0^\dagger(t)\rho_{\mathcal{SR}}(t)\mathcal{U}_0(t)\right) \\ &= -i\mathcal{U}_0^\dagger(t)\left[H_{\mathcal{SR}}, \rho_{\mathcal{SR}}(t)\right]\mathcal{U}_0(t). \end{aligned} \tag{1.79}$$

This formal expansion follows from the commutation between the time evolution operator $\mathcal{U}_0(t)$ and the free Hamiltonian operator $H_0 = H_\mathcal{S} + H_\mathcal{R}$ and therefore provides the interaction picture of equation. (1.68)

$$\frac{d}{dt}\tilde{\rho}_{\mathcal{SR}}(t) = -i\left[\tilde{H}_{\mathcal{SR}}(t), \tilde{\rho}_{\mathcal{SR}}(t)\right]. \tag{1.80}$$

A particular solution is obtained by integrating each side of equation.(1.39) from $t = 0$ to t, which yields

$$\tilde{\rho}_{\mathcal{SR}}(t) = \tilde{\rho}_{\mathcal{SR}}(0) - i\int_0^t ds[\tilde{H}_{\mathcal{SR}}(s), \tilde{\rho}_{\mathcal{SR}}(s)]. \tag{1.81}$$

Upon inserting the expression for the density operator $\tilde{\rho}_{\mathcal{SR}}(t)$ into equation.(1.39), we obtain a description of the total state differential equation in the form

$$\begin{aligned} \frac{d}{dt}\tilde{\rho}_{\mathcal{SR}}(t) &= -i[\tilde{H}_{\mathcal{SR}}(t), \tilde{\rho}_{\mathcal{SR}}(0) - i\int_0^t ds[\tilde{H}_{\mathcal{SR}}(s), \tilde{\rho}_{\mathcal{SR}}(s)]] \\ &= -i[\tilde{H}_{\mathcal{SR}}(t), \tilde{\rho}_{\mathcal{SR}}(0)] - \int_0^t ds[\tilde{H}_{\mathcal{SR}}(t), [\tilde{H}_{\mathcal{SR}}(s), \tilde{\rho}_{\mathcal{SR}}(s)]]. \end{aligned} \tag{1.82}$$

In our main approach, we seek to find a local time equation for the density operator of the open system. For this purpose, a partial trace is applied to the degrees of freedom of the environment :

$$\frac{d}{dt}\tilde{\rho}_\mathcal{S}(t) = -iTr_\mathcal{R}[\tilde{H}_{\mathcal{SR}}(t), \tilde{\rho}_{\mathcal{SR}}(0)] - \int_0^t dsTr_\mathcal{R}[\tilde{H}_{\mathcal{SR}}(t), [\tilde{H}_{\mathcal{SR}}(s), \tilde{\rho}_{\mathcal{SR}}(s)]]. \tag{1.83}$$

The integral form of equation. (1.83) gives the state of the open system $\mathcal{S}$ at all times, albeit with a problematic computational complexity. Despite its applicability for any $t \geq t_0$, the behavior of the derivation $d\tilde{\rho}_\mathcal{S}/dt$ depends entirely on the information provided by the system since its initial state and throughout its history. This feature is typically associated with the Markovian nature of quantum system dynamics, presenting a cumulative computational problem to solve. To transform the master equation into a time-local equation, it is necessary to further approximate equation 1 by special approximations, in particular by eliminating the first term on the right-hand side of the equation.

α)Born approximation

The derivative $d\tilde{\rho}_{\mathcal{S}}/dt$ in equation.(1.42) involves an implicit dependence on the total system state $\tilde{\rho}_{\mathcal{SR}}(t)$, and is therefore not a closed time evolution equation for $\tilde{\rho}_{\mathcal{S}}(t)$. To address this issue, we introduce two hypotheses.
Firstly, we assume that at $t = 0$, the system and the environment are completely separate. In other words, there is no correlation between the system and the environment,

$$\tilde{\rho}_{\mathcal{SR}}(0) = \tilde{\rho}_{\mathcal{S}}(0) \otimes \tilde{\rho}_{\mathcal{R}}(0). \tag{1.84}$$

This approach seems obvious when the system and the environment have never interacted before $t = 0$, or when the correlation between the system and the environment needs a long time to be established after their first interactions. In a second case, we consider the contribution of the total system's correlations to be negligible. Of course, this does not imply an absence of interaction between the system and the reservoir, but it does suggest that the correlations generated from their interaction are marginal. In practical terms, this situation arises, for example, in cases where the environment is significantly larger than the open system, with a weak coupling between them. The interaction has little impact on the state of the environment, which remains largely unperturbed. Consequently, the state of the total system at any given time t can be approximated by a uncorrelated state in the form

$$\tilde{\rho}_{\mathcal{SR}}(t) = \tilde{\rho}_{\mathcal{S}}(t) \otimes \tilde{\rho}_{\mathcal{R}}, \quad \forall t \geq 0, \tag{1.85}$$

where $\tilde{\rho}_{\mathcal{R}} = \tilde{\rho}_{\mathcal{R}}(0)$ is the density operator for the environment at $t = 0$.

β) Interaction Hamiltonian form

A further premise is essential for obtaining an amenable master equation, assuming a specific form for the interaction Hamiltonian. A manifest structure of $H_{\mathcal{SR}}$ (in the Schrödinger representation) is of the form

$$H_{\mathcal{SR}} = \sum_i S_i \otimes E_i, \tag{1.86}$$

where E_i is an operator acting on the states of the environment and which verifies

$$\langle E_i \rangle_{\rho_{\mathcal{R}}} = Tr_{\mathcal{R}} \left(E_i \rho_{\mathcal{R}} \right) = 0. \tag{1.87}$$

Condition (1.87) is always manageable since, for systems where the interaction Hamiltonian takes the form (1.54) with $\langle E_i \rangle_{\rho_{\mathcal{R}}} \neq 0$, a transformation $H_{\mathcal{SR}} = \sum_i S_i \otimes (E_i - \langle E_i \rangle_{\rho_{\mathcal{R}}})$ in the Hamiltonian operator is realizable, which allows us to set the resolution $(E_i - \langle E_i \rangle_{\rho_{\mathcal{R}}}) = 0$. It should be noted that the relation (1.87) can be applied to the operator E_i in the interaction representation

$$\begin{aligned} \langle \tilde{E}_i(t) \rangle_{\tilde{\rho}_{\mathcal{R}}} &= Tr_{\mathcal{R}} \left(e^{iH_{\mathcal{R}}t} E_i \rho_{\mathcal{R}} e^{-iH_{\mathcal{R}}t} \right) \\ &= Tr_{\mathcal{R}} \left(E_i \rho \right) = 0. \end{aligned} \tag{1.88}$$

The system operators S_i are considered as eigenoperators of H_S acting on the open system states,

$$S_i(\omega) = \sum_{e_{l'} - e_l = \omega} \Pi_{e_l} S_i \Pi_{e_{l'}}. \tag{1.89}$$

Here, the sum is conducted along all energies e_l and $e_{l'}$ such that their difference remains fixed and is equal to ω for a fixed transition frequency ω. The operators

$$\Pi_{e_l} = |\psi\rangle \langle\psi|_l, \tag{1.90}$$

are projection operators on the discrete states of the system $\{|\psi\rangle\}$ with the eigenvalues of the energy $\{e_l\}$. From this decomposition, we can derive the following relations

$$\begin{aligned}
[H_{\mathcal{S}}, S_i(w)] &= \sum_{e_{l'}-e_l=\omega} H_{\mathcal{S}} |\psi\rangle \langle\psi|_l S_i |\psi\rangle \langle\psi|_{l,} - |\psi\rangle \langle\psi|_l S_i |\psi\rangle \langle\psi|_{l'} H_{\mathcal{S}} \\
&= \sum_{e_{l'}-e_l=\omega} e_l |\psi\rangle \langle\psi|_l S_i |\psi\rangle \langle\psi|_{l'} - e_{l'} |\psi\rangle \langle\psi|_l S_i |\psi\rangle \langle\psi|_{l'} \\
&= -\omega S_i(\omega), \qquad (1.91)
\end{aligned}$$

being

$$[H_{\mathcal{S}}, S_i(w)] = -\omega S_i(\omega). \qquad (1.92)$$

and taking the Hermitian conjugate :

$$[H_{\mathcal{S}}, S_i^\dagger(w)] = \omega S_i^\dagger(\omega). \qquad (1.93)$$

Looking back at the expression (1.83), we can clearly show that the first term of the master equation in the interaction pictur is such that,

$$Tr_{\mathcal{R}}[\tilde{H}_{\mathcal{SR}}, \tilde{\rho}_{\mathcal{S}}(0) \otimes \tilde{\rho}_{\mathcal{R}}] = \sum_i e^{-i\omega t}[S_i(\omega), \tilde{\rho}_{\mathcal{S}}(0)] \langle \tilde{E}_i(t)\rangle_{\tilde{\rho}_{\mathcal{R}}} = 0, \qquad (1.94)$$

where we are referring to the transformation $\tilde{S}_i = e^{-i\omega t} S_i$ of the operator S_i in the interaction picture.

Discarding the first term of equation. (1.83), we find a revised version of the master equation that is independent of the initial state of the system and constitutes a representation influenced by the cumulative historical events occurring from the initial time to time t. A reduced form of the master equation is then established by exploiting the cyclic property of the trace operator and the permutation between the Hamiltonian operator of the environment $\tilde{H}_{\mathcal{R}}$ and the density operator $\tilde{\rho}_{\mathcal{R}}$,

$$\begin{aligned}
\frac{d\tilde{\rho}_{\mathcal{S}}(t)}{dt} &= \sum_{i,j} \sum_{\omega,\omega'} e^{i(\omega'-\omega)t} \Gamma_{ij}(\omega) \left(S_j(\omega) \tilde{\rho}_{\mathcal{S}}(s) S_i^\dagger(\omega') - S_i^\dagger(\omega') S_j(\omega) \tilde{\rho}_{\mathcal{S}}(s) \right) \\
&\quad + e^{-i(\omega'-\omega)t} \Gamma_{ij}^* \left(S_i(\omega') \tilde{\rho}_{\mathcal{S}}(s) S_j^\dagger(\omega) - \tilde{\rho}_{\mathcal{S}}(s) S_j^\dagger(\omega) S_i(\omega') \right), \qquad (1.95)
\end{aligned}$$

where the correlation functions on the environment $\Gamma_{i,j}$ and their conjugates Γ_{ij}^* are such that

$$\Gamma_{ij}(\omega) = \int_0^t ds e^{-i\omega s} Tr_{\mathcal{R}}[E_i^\dagger(t) E_j(s) \hat{\rho}_{\mathcal{R}}], \qquad (1.96)$$

$$\Gamma_{ij}^*(\omega) = \int_0^t ds e^{i\omega s} Tr_{\mathcal{R}}[E_j^\dagger(s) E_i(t) \hat{\rho}_{\mathcal{R}}]. \qquad (1.97)$$

γ) Markov aproximation

At this stage, the master equation is not local in time, since the reduced density matrix still depends on the system's history. To overcome this problem, we use the Markov hypothesis for our system. Given that the dynamics of the system is influenced by its interaction with the reservoirs, we consider that the correlation of the latter occurs within a very short period of time. Then, memory effects do not play an important role in the system's evolution and, consequently, the evolution of the reduced density matrix depends only on its current state and not on its

history. These assertions can be summarized into a more fundamental concept, ensuring that the time scale of environmental correlation is significantly smaller than the time scale of interaction :

$$\tau_{\mathcal{R}} \ll \tau_{int}. \tag{1.98}$$

Here, $\tau_{\mathcal{R}}$ represents the correlation time scale, beyond which, $t \geq \tau_{\mathcal{R}}$, the state of the reservoir is practically independent of its initial correlations and $\tau_{\rm int}$ represents the interaction time scale characterizing the evolution of the density operator due to the effects of its interaction with the reservoir.

Moreover, an inescapable part of our derivation consists of substituting s by $t-s$ in equation. (1.64), without changing the nature of the equation. Since we consider the time evolution $t \gg \tau_{\mathcal{R}}$ and bath correlations vanish after a short time interval $t \in [0, \tau_{\mathcal{R}}]$, we may extend the upper limit of the integrals (1.96) to infinity. A fortiori, we can substitute $\rho_{\mathcal{S}}(t-s)$ by $\rho_{\mathcal{S}}(t)$, since the dynamics of $\rho_{\mathcal{S}}$ are much slower than the decay of Γ_{ij}, the short-memory effect of the correlation function ensures that $\rho_{\mathcal{S}}$ only keeps track of events at the precise moment of their occurrence. With this Markov approximation, equation. (1.95) becomes :

$$\begin{aligned}\frac{d\tilde{\rho}_{\mathcal{S}}(t)}{dt} = & \sum_{i,j}\sum_{\omega\omega'} e^{i(\omega'-\omega)t}(\omega)\left(S_j(\omega)\tilde{\rho}_{\mathcal{S}}(t)S_i^{\dagger}(\omega') - S_i^{\dagger}(\omega')S_j(\omega)\tilde{\rho}_{\mathcal{S}}(t)\right) \\ & + e^{-i(\omega'-\omega)t}\Gamma_{ij}^{*}\left(S_i(\omega')\tilde{\rho}_{\mathcal{S}}(t)S_j^{\dagger}(\omega) - \tilde{\rho}_{\mathcal{S}}(t)S_j^{\dagger}(\omega)S_i(\omega')\right)\end{aligned} \tag{1.99}$$

where the correlation functions,

$$\Gamma_{ij}(\omega) = \int_0^{\infty} ds e^{i\omega s} Tr_{\mathcal{R}}[E_i^{\dagger}(t)E_j(t-s)\hat{\rho}_{\mathcal{R}}], \tag{1.100}$$

$$\Gamma_{ij}^{*}(\omega) = \int_0^{\infty} ds e^{-i\omega s} Tr_{\mathcal{R}}[E_j^{\dagger}(t-s)E_i(t)\hat{\rho}_{\mathcal{R}}]. \tag{1.101}$$

Secular approximation

The exponential coefficients in the master equation are dependent on the difference between frequencies in the system. It's evident that these coefficients attain their maximum value when $\omega = \omega'$ and decrease as $|\omega - \omega'|$ increases. Given this evidence, contributions with very high $|\omega - \omega'|$ are likely to have a very negligible contribution to the dynamics of the open quantum system. Therefore, it would be appropriate to neglect them in favor of terms with $\omega = \omega'$. This approximation is commonly known as the rotating wave approximation and leads to a a master equation in the form :

$$\begin{aligned}\frac{d\tilde{\rho}_{\mathcal{S}}(t)}{dt} = & \sum_{i,j}\sum_{\omega}\{\Gamma_{i,j}(\omega)(\left(S_j(\omega)\tilde{\rho}_{\mathcal{S}}(t)S_i^{\dagger}(\omega) - S_i^{\dagger}(\omega)S_j(\omega)\tilde{\rho}_{\mathcal{S}}(t)\right) \\ & + \Gamma_{i,j}^{*}(\omega)\left(S_i(\omega)\tilde{\rho}_{\mathcal{S}}(t)S_j^{\dagger}(\omega) - \tilde{\rho}_{\mathcal{S}}(t)S_j^{\dagger}(\omega)S_i(\omega)\right),\end{aligned} \tag{1.102}$$

which represents the general form of the master equation in the Born-Markov approximation.

Finally, we derive a more explicit form of equation. (1.102), referred to the *standard form*, by decomposing the correlation functions,

$$\Gamma_{ij} = \frac{1}{2}\gamma_{ij}(\omega) + i\chi_{ij}(\omega), \tag{1.103}$$

where

$$\gamma_{ij}(\omega) = \Gamma_{ij}(\omega) + \Gamma_{ij}^{*}(\omega), \tag{1.104}$$

$$\chi_{ij}(\omega) = \frac{1}{2i}(\Gamma_{ij}(\omega) - \Gamma_{ij}^{*}(\omega)). \tag{1.105}$$

After rearrangement, we get the standard expression for the master equation, composed of a commutator term and a dissipation operator :

$$\frac{d\tilde{\rho}(t)}{dt} = -\frac{i}{\hbar}[\tilde{H}_{LS}, \tilde{\rho}_{\mathcal{S}}(t)] + \mathcal{L}_{\mathcal{R}}(\tilde{\rho}(t)), \tag{1.106}$$

where we define the Hamiltonian operator

$$\tilde{H}_{LS} = \sum_{ij}\sum_{\omega} \hbar\chi_{ij}(\omega) S_i^{\dagger}(\omega) S_j(\omega), \tag{1.107}$$

called the *Lamb shift Hamiltonian*. The second term is a super operator which describes the dissipations effects of the thermal baths on the system

$$\mathcal{L}_{\mathcal{R}}(\tilde{\rho}(t)) = \sum_{ij}\sum_{\omega} \gamma_{ij}(\omega) \left(S_j(\omega)\tilde{\rho}_{\mathcal{S}}(t) S_i^{\dagger}(\omega) - \frac{1}{2}\{S_i^{\dagger}(\omega) S_j(\omega), \tilde{\rho}_{\mathcal{S}}(t)\} \right). \tag{1.108}$$

1.4.4 Back to the Schrödinger representation

Now we can resort to the correspondence (1.77) to get a description of the standard equation on the Schrödinger representation. From the relation between the density operator of the system $\rho_{\mathcal{S}}$ on the Schrödinger representation and its interaction representation $\tilde{\rho}_{\mathcal{S}}(t)$ introduced in the section 1.4.3,

$$\tilde{\rho}_{\mathcal{S}}(t) = e^{iH_{\mathcal{S}}t} \rho_{\mathcal{S}}(t) e^{-iH_{\mathcal{S}}t}, \tag{1.109}$$

we introduce a time derivative to the both sides :

$$\frac{d\tilde{\rho}_{\mathcal{S}}(t)}{dt} = ie^{iH_{\mathcal{S}}t}[H_{\mathcal{S}}, \rho_{\mathcal{S}}(t)]e^{-iH_{\mathcal{S}}t} + e^{-iH_{\mathcal{S}}t}\frac{d\rho_{\mathcal{S}}t}{dt}e^{iH_{\mathcal{S}}t}. \tag{1.110}$$

At this stage, we can substitute the derivative $d\tilde{\rho}_S(t)/dt$ by its expression defined in the Markov equation (1.75),

$$e^{iH_{\mathcal{S}}t}\frac{d\rho_{\mathcal{S}}(t)}{dt}e^{-iH_{\mathcal{S}}t} = -ie^{iH_{\mathcal{S}}t}[H_{\mathcal{S}}, \rho_{\mathcal{S}}(t)]e^{-iH_{\mathcal{S}}t} - i[H_{LS}, \rho_{\mathcal{S}}(t)] + \mathcal{L}_{\mathcal{R}}(\rho(t)). \tag{1.111}$$

Finally, it's enough to multiply the right-hand side of each member of the previous equation by $e^{-iH_{\mathcal{S}}(t)}$ and the left-hand side of each member by $e^{iH_{\mathcal{S}}(t)}$ to obtain the master equation of the system in Schrödinger's representation.

$$\frac{d\rho_{\mathcal{S}}(t)}{dt} = -i[H_{\mathcal{S}} + H_{LS}, \rho_{\mathcal{S}}(t)] + \mathcal{L}_{\mathcal{R}}(\rho(t)). \tag{1.112}$$

In the absence of dissipation operators, this equation differs from the Von-Neumann equation due to the presence of the Lamb-Shift term on the Hamiltonian operator which generally introduces a renormalization depending on the frequency of the system. However, for the purposes of our study, we will neglect this renormalization term since it manifests as a simple perturbation parameter in the Hamiltonian and does not play a pivotal role in our investigation.

1.5 Relaxation of a two-level system in a bosonic environment

Let's consider a bipartite system composed of a two-level $\{|0\rangle, |1\rangle\}$ system $\mathcal{S}$ and a bosonic environment as reservoir $\mathcal{R}$. The Hamiltonian operator of the system is defined on the Schrödinger representation by

$$H_{\mathcal{S}} = \frac{\omega}{2}\sigma_z, \tag{1.113}$$

where ω represents the system frequency and σ_z the Pauli matrix defined on the system standard basis by

$$\sigma_z = \begin{pmatrix} 1 & 0 \\ 0 & -1 \end{pmatrix}. \tag{1.114}$$

The Pauli matrix σ_z is related to the operator σ and its adjoint operator $\sigma^\dagger$ through a commutation relation

$$\sigma_z = [\sigma, \sigma^\dagger] = |1\rangle\langle 1| - |0\rangle\langle 0|. \tag{1.115}$$

Here we have introduced two system transition operators :

The excitation operator of the system, from its ground state $|0\rangle$ to its excited state $|1\rangle$,

$$\sigma = |0\rangle\langle 1| = \begin{pmatrix} 0 & 0 \\ 1 & 0 \end{pmatrix}. \tag{1.116}$$

The relaxation operator from its excited state $|1\rangle$ to its ground state $|0\rangle$,

$$\sigma^\dagger = |1\rangle\langle 0| = \begin{pmatrix} 0 & 1 \\ 0 & 0 \end{pmatrix}. \tag{1.117}$$

Note that the system transition operators represent the eigenoperators of the Hamiltonian $H_{\mathcal{S}}$,

$$[H_{\mathcal{S}}, \sigma] = -\omega\sigma, \tag{1.118}$$

$$[H_{\mathcal{S}}, \sigma^\dagger] = \omega\sigma^\dagger. \tag{1.119}$$

We assume the environment to be an infinite collection of uncorrelated bosonic modes (harmonic oscillators) spanning a continuous frequency spectrum. The Hamiltonian operator of the environment in the Schrödinger representation is thus expressed as a sum of all the modes in the environment,

$$H_{\mathcal{R}} = \sum_k \Omega_k b_k^\dagger b_k. \tag{1.120}$$

The operators $b_k^\dagger$ and b_k are respectively the creation operator and the annihilation operator for a mode k of the environment and verify the commutation relation.

$$[b_k, b_{k'}^\dagger] = \mathbb{1}\delta_{k,k'}, \tag{1.121}$$

where $\delta_{kk'}$ is the Kronecker delta symbol, which is equal to 1 if $k = k'$ and 0 otherwise.

The interaction between the system and a mode k of the environment is defined through the Jayne-Cumming Hamiltonian operator

$$H_{\mathcal{SR}_k} = g_k(\sigma^\dagger b_k + \sigma b_k^\dagger), \tag{1.122}$$

where g_k is the coupling strength between the system and the mode k of the environment. Expression (1.122) refers to the various potential exchanges between the system and the environment. Its derivation is based on the dipole approximation and is consistent with the principle of energy conservation for the total system. The products $\sigma^\dagger b_k$ and $\sigma b_k^\dagger$ correspond respectively to an excitation of the system by annihilation of a mode k of the environment and to a gain of energy of a mode k of the environment through the relaxation of the system.

The transformation introduced in equation. (1.77) allows us to derive the interaction representation of the Hamiltonian operator. (1.122) as follows :

$$\begin{aligned}\tilde{H}_{\mathcal{SR}_k} &= e^{i(H_{\mathcal{S}}+H_{\mathcal{R}})t} H_{\mathcal{SR}} e^{-i(H_{\mathcal{S}}+H_{\mathcal{R}})t} \\ &= g_k(\sigma^\dagger b_k e^{-i(\Omega_k-\omega)t} + \sigma b_k^\dagger e^{i(\Omega_k-\omega)t}),\end{aligned} \tag{1.123}$$

resulting in the general form of the interaction Hamiltonian operator that characterizes the interaction between the system and the reservoir :

$$\tilde{H}_{\mathcal{SR}} = \sum_k g_k(\sigma b_k^\dagger e^{-i(\omega-\Omega_k)t} + \sigma^\dagger b_k e^{i(\omega-\Omega_k)t}). \tag{1.124}$$

1.5.1 Master equation

There are several ways of deriving the Markovian master equation for our open system, but all of them have their validity regime. The natural extension of the approaches presented here is to use the general formulation of equation.(1.67) with a secular approximation. This approach allows us to retain only the mean of the slowly rotating terms in the master equation. Thus, the equation of motion of the open system in the interaction picture takes the following form :

$$\begin{aligned}\frac{d\tilde{\rho}_{\mathcal{S}}(t)}{dt} &= \Gamma_1(\sigma\tilde{\rho}_{\mathcal{S}}(t)\sigma^\dagger - \sigma^\dagger\sigma\tilde{\rho}_{\mathcal{S}}(t)) + \Gamma_2(\sigma^\dagger\tilde{\rho}_{\mathcal{S}}(t)\sigma - \sigma\sigma^\dagger\tilde{\rho}_{\mathcal{S}}(t)) + \Gamma_3 2\sigma\tilde{\rho}_{\mathcal{S}}(t)\sigma \\ &+ \Gamma_1^*(\sigma\tilde{\rho}_{\mathcal{S}}(t)\sigma^\dagger - \tilde{\rho}_{\mathcal{S}}(t\sigma^\dagger\sigma)) + \Gamma_2^*(\sigma^\dagger\tilde{\rho}_{\mathcal{S}}(t)\sigma - \tilde{\rho}_{\mathcal{S}}(t)\sigma\sigma^\dagger) + \Gamma_3^* 2\sigma^\dagger\tilde{\rho}_{\mathcal{S}}(t)\sigma^\dagger,\end{aligned} \tag{1.125}$$

with the coefficients $\Gamma_i, i = 1, 2, 3$ defined by the bath correlation functions,

$$\begin{aligned}\Gamma_1 &= \int_0^t ds \sum_k g_k^2 e^{i(\omega-\Omega_k)(t-s)}(N_{\Omega_k}+1), \\ \Gamma_2 &= \int_0^t ds \sum_k g_k^2 e^{-i(\omega-\Omega_k)(t-s)} N_{\Omega_k}, \\ \Gamma_3 &= \int_0^t ds \sum_k g_k^2 e^{-i(\omega-\Omega_k)(t-s)} M_{\Omega_k}^*,\end{aligned} \tag{1.126}$$

and the mean boson occupation number of the reservoir operators,

$$N_{\Omega_k} = Tr_{\mathcal{R}}[b_k b_k^\dagger \rho_{\mathcal{R}}] \qquad and \qquad M_{\Omega_k} = Tr_{\mathcal{R}}[b_k^2 \rho_{\mathcal{R}}]. \tag{1.127}$$

1.5.2 Continuous limit

The integral forms in equation.(1.126) do not necessarily simplify the master equation, as they rely on the accumulation of a fixed number of distinct modes of the environment. For convenience, let's explore an alternative approach by transforming this discrete summation into an integral over a continuous range of environmental modes. To underpin this approximation, we introduce the spectral density of the environment in a continuous limit,

$$J(\omega) = \sum_k g_k^2 \delta(\omega - \Omega_k), \tag{1.128}$$

which characterizes the number of reservoir modes, of frequency Ω_k, interacting with the system under the action of an interaction force g_k. The symbol δ in the previous equation designates the Kronecker delta notation shifted to ω, which is 1 for $\Omega_k = \omega$ and 0 otherwise. Expression (1.128) allows us to replace the sum over the previous coefficients Γ_i by an integral. In addition, we need to fix the form of the environment state, in order to calculate the expressions N_{Ω_k} and M_{Ω_k}. For convenience, let's consider that the state of the environment is initially in thermal

equilibrium and that it is also invariant during the process (Born-approximation). In this case, the expression of the reservoir density operator $\rho_{\mathcal{R}}$ at each instant is described by the Gibbs state

$$\rho_{\mathcal{R}} = \frac{e^{-\beta H_{\mathcal{R}}}}{Z_{\mathcal{R}}} \tag{1.129}$$

where the partition function $Z_{\mathcal{R}}$ is evaluated by using the action of the Hamiltonian operator $H_{\mathcal{R}}$ on the energy eigenstates of the environment,

$$Z_{\mathcal{R}} = Tr_{\mathcal{R}}(e^{-\beta H_{\mathcal{R}}}) = \frac{1}{1 - e^{-\beta \sum_k \Omega_k}}. \tag{1.130}$$

In what follows, it is convenient to introduce the following partition of the coefficients Γ_i in the continuous limit, , while considering the Markovian approximation,

$$\begin{aligned} \Gamma_1 &= \int_0^\infty d\Omega \int_0^\infty ds e^{-i(\omega-\Omega)s} J(\Omega)(N_\Omega + 1) \\ &= \pi J(\omega)(N_\omega + 1) - iP \int_0^\infty d\Omega J(\Omega) \frac{N_\Omega + 1}{\omega - \Omega}, \end{aligned} \tag{1.131}$$

where P is the principal Cauchy value. A similar expression for Γ_2 is obtained by replacing $N_\Omega + 1$ by N_Ω,

$$\Gamma_2 = \pi J(\omega) N_\omega + iP \int_0^\infty d\Omega J(\Omega) \frac{N_\Omega}{\omega - \Omega}, \tag{1.132}$$

It becomes apparent that when we reintegrate the coefficients Γ_i in equation.(1.125), their real parts combine to constitute a dissipation operator. In fact, setting $\gamma_0 = 2\pi J(\omega)$, the dissipation operator adopts the following form,

$$\mathcal{L}_{\mathcal{R}}(\tilde{\rho}(t)) = \gamma_0(N_\omega + 1)(\sigma \tilde{\rho}(t) \sigma^\dagger - \frac{1}{2}\{\sigma^\dagger \sigma, \tilde{\rho}(t)\}) + \gamma_0 N_\omega (\sigma^\dagger \tilde{\rho}(t) \sigma - \frac{1}{2}\{\sigma \sigma^\dagger, \tilde{\rho}(t)\}). \tag{1.133}$$

The imaginary integral parts in the coefficients γ_i form the usually called Lamb-Shift Hamiltonian part,

$$-i[\tilde{H}_{LS}, \tilde{\rho}_{\mathcal{S}}(t)] \tag{1.134}$$

where the Lamb-Shift Hamiltonian is given by

$$H_{LS} = iP \int_0^\infty d\Omega J(\Omega) \frac{2N_\Omega + 1}{\omega - \Omega} [\sigma^\dagger \sigma, \tilde{\rho}_{\mathcal{S}}(t)]. \tag{1.135}$$

We find the Markov master equation for a qubit interacting with a bosonic reservoir

$$\frac{d\tilde{\rho}_{\mathcal{S}}(t)}{dt} = -i[\hat{H}_{LS}, \tilde{\rho}_{\mathcal{S}}(t)] + \mathcal{L}_{\mathcal{R}}(\tilde{\rho}(t)). \tag{1.136}$$

The Markov equation (1.132) is characterised by the damping coefficient γ_0, which depends on the spectral density of the reservoir modes that are at the same frequency ω as the qubit and on the mean of the number operator $\langle N \rangle_{\rho_E}$.

1.6 Markovian and Non-Markovian Dynamics

1.6.1 Markovian dynamics

So far, we have sketched the dynamics of open quantum systems mainly through a Markovian approach, where the historical background of the system does not explicitly affect its dynamics at any time t. This has been achieved by making various assumptions about the nature of the system and the reservoir, as well as their interaction. Here we propose a further review of markovianity in the dynamics of open quantum systems, based on the dynamical map approach. Importantly, this approach involves a significantly detailed insight into the evolution of the total system and allows us to establish the essential conditions for the dynamics of the system to be Markovian or non-Markovian, without necessarily specifying the system parameters in detail .

Let us suppose that we can prepare the state of the total system at the initial time $t = 0$ as an uncorrelated product state,

$$\rho_{\mathcal{SR}}(0) = \rho_{\mathcal{S}}(0) \otimes \rho_{\mathcal{R}}(0), \tag{1.137}$$

where $\rho_{\mathcal{S}}(0)$ is the initial state of the open system $\mathcal{S}$ and $\rho_{\mathcal{R}}(0)$ represents the state of the environment. The transformation governing the evolution of the open system from the initial time $t = 0$ to a subsequent time $t \geq 0$ is defined in equation. (1.70) by :

$$\begin{aligned} \mathcal{E}_t \quad &: \quad S(\mathcal{H}_{\mathcal{S}}) \longrightarrow S(\mathcal{H}_{\mathcal{S}}) \\ &\quad\quad \rho_{\mathcal{S}}(0) \longrightarrow \rho_{\mathcal{S}}(t) = \mathcal{E}_t \rho_S(0). \end{aligned} \tag{1.138}$$

In other hand, consider again an intermediate instant $t^{'}$ such that $0 < t^{'} < t$. A crucial aspect of the dynamical maps $\mathcal{E}_t$ is their continuity over time. Indeed, one might expect that the evolution between $t = 0$ and $t > 0$ could be expressed as the composition of dynamycal maps

$$\mathcal{E}_t = \mathcal{E}^{'}\mathcal{E}^{''}, \tag{1.139}$$

where $\mathcal{E}^{'}$ and $\mathcal{E}^{''}$ denote the concatenation of two dynamical maps. Here, $\mathcal{E}^{'}$ describes the evolution of the open system from the initial time $t = 0$ to $t^{'}$, and $\mathcal{E}^{''}$ describes the evolution of the open system from $t^{'}$ to t. Given the decomposition of the dynamical maps, $\mathcal{E}_t = \mathcal{E}'\mathcal{E}''$, it is plausible to represent the evolution of the open system $\mathcal{S}$ from $t = 0$ to any subsequent time $t^{'}$ by means of a dynamical map,

$$\mathcal{E}_t^{'}(\rho_{\mathcal{S}}(0)) = Tr_{\mathcal{R}}\left[\mathcal{U}(t^{'},0)\rho_{\mathcal{S}}(0) \otimes \rho_{\mathcal{R}}(0)\mathcal{U}^{\dagger}(t^{'},0)\right]. \tag{1.140}$$

where the above form is obtained by assuming that the system state is initially uncorrelated. Now let us see whether the same operation can be repeated for the operator $\mathcal{E}^{''}$:

$$\mathcal{E}_t^{''}(\rho_{\mathcal{S}}(t^{'})) = Tr_{\mathcal{R}}\left[\mathcal{U}(t,t^{'})\rho_{\mathcal{SR}}(t^{'})\mathcal{U}^{\dagger}(t,t^{'})\right]. \tag{1.141}$$

Without additional conditions on the total system evolution parameters, the state of system $\rho_{\mathcal{SR}}$ at an instant $t^{'}$ may contain correlations induced by its dynamic evolution and therefore cannot be written as a product of two distinct states. Consequently, it is not always obvious to express the operator $\mathcal{E}^{''}$ as a dynamical map, which maps the state of the open system from $t^{'}$ to t.

It is clear from the above considerations that the dynamical map $\mathcal{E}$ is not necessarily continuous in time, as it cannot generally be divided into multiple maps, except in a process where the dynamical effects generated in the open system due to the interaction with its environment can be considered as uncorrelated from one infinitesimal instant to the next. At each time interval, the state of the total system is therefore separated and the dynamic maps can take the form :

$$\mathcal{E}_t = \mathcal{E}'\mathcal{E}''. \tag{1.142}$$

Such a definition gives us a mathematical perception of Markov dynamicsas a time evolution process described by a dynamic evolution operator satisfying the composition law.

Markovian processes play an important role in physics and are relatively easy to model analytically [35, 77–82]. One of their key features is that all the information that determines the future of a process depends on the states of the entities involved in the process at the instant in question, and not on their historical background. In the context of open quantum systems, the Markovian approach is built upon certain assumptions that constrain the type and nature of interactions between the system and its environment. The most common hypotheses is the non-memory effect, where the environment is not expected to store any information about the system for a given period, despite their interaction. This hypothesis is essentially the one that is widely used to characterize non-Markovian dynamics, making a Markovian process so easy to deal with, as it ensures that the entire hierarchy of correlations induced in the system dynamics can be attributed to an instantaneous perturbation that survives in a short period.

1.6.2 Non-Markovian Dynamics

Even though Markov master equations have proven to be invaluable for describing many situations in quantum physics, there has been a growing interest in non-Markovian processes recently. This is primarily due to the realization that many quantum models do not necessarily satisfy the conditions required for a Markovian approximation. In terms of dynamics, a new line of research aimed to describe the non-Markovian dynamics of open quantum systems using different approaches has been initiated for special purposes, such as a strong coupling between the system and the reservoir, or even based on engineering reservoirs.

The development of effective methods for dealing with non-Markovian dynamics is currently a complexe topic of much discussion in the research community. One reason for this complexity is that algebraic approaches, such as the deviations of a given dynamic map from its total divisibility, are laboriously seen to be difficult to exploit so potentially manipulable evolutionary approaches seem desirable. Recently, attention has turned to the formal evaluation of the various dimensions in which non-Markovianity is manifested, to characterize the phenomenology of non-Markovian dynamics in open systems using appropriate tools. For example, Breuer et al. proposed to quantify non-Markovian effects by examining the feedback induced on the system under study by its memory-keeping environment. Other approaches have been considered and measures suggested, inspired by the use of other interesting frameworks such as the quantum fisher information.

Breuer et al. proposed a measure of non-Markovianity based on memory effects in the dynamics of open systems by optimizing the behavior of the trace distance under completely positive and trace preserving maps [83–87]. They consider the contraction property of universal dynamic maps for trace distance (see equation. (1.19)). Since Markov dynamic is governed by universal dynamic maps, the trace distance must be monotonic and decreasing with time,

$$D(\rho^1_{\mathcal{S}}(t), \rho^2_{\mathcal{S}}(t)) \leq D(\rho^1_{\mathcal{S}}(0), \rho^2_{\mathcal{S}}(0)). \tag{1.143}$$

This proposition naturally leads to the following definition : a quantum process described by a set of quantum dynamical maps is considered Markovian if the trace distance between all pairs of initial states decreases monotonically for all times $t > 0$. Conversely, a quantum process is labeled non-Markovian if there exists a pair of initial states for which the trace distance fails to

monotonically decrease ; in other words, it begins to increase after a certain time. Such instances signify a flow of information from the environment to the open system, indicating the presence of memory effects. Information from the open system is temporarily stored in the environment and later reintroduced to influence the system.

Based on the above definition of non-Markovian dynamics, we are prompted to highlight the key problem arising from the non-specification of the initial pair of system states. The requirement that finding at least one pair of states satisfying condition (1.143) is sufficient to justify the non-Markovianity of the system dynamics imposes a rudimentary difficulty. To overcome this, we introduce the following measure

$$\mathcal{N}(\mathcal{E}) = \max_{\rho_{\mathcal{S}}^{1,2}(0)} \int_{\sigma>0} dt\sigma(t, \rho_{\mathcal{S}}^{1,2}(0)), \tag{1.144}$$

where $\mathcal{E}$ is the dynamical map under consideration, $\rho_{\mathcal{S}}^1$ and $\rho_{\mathcal{S}}^2$ are two initial states of the system, and we have introduced the rate of change of the trace distance

$$\sigma(t, \rho_{\mathcal{S}}^{1,2}(0)) = \frac{d}{dt} D(\rho_{\mathcal{S}}^1(t), \rho_{\mathcal{S}}^2(t)). \tag{1.145}$$

In Equation (1.144), the time integral spans all intervals where $\sigma > 0$, indicating instances where the trace distance increases with time. The maximum is computed over all pairs of initial states $\rho_{\mathcal{S}}$ within the open system's state space $S(\mathcal{H}_{\mathcal{S}})$. Consequently, $\mathcal{N}$ is a positive function of the family of dynamical maps $\mathcal{E}$, serving as a measure of the maximum total flow of information from the environment back to the open system. By design, $\mathcal{N} = 0$ precisely when the process exhibits Markovian behavior. Simplifying the maximization over all pairs of quantum states in Equation (1.144) is facilitated by leveraging several key properties of $\mathcal{N}$ and the convex structure inherent in the set of quantum states.

1.7 Summary

In this chapter, we have summarised the key notions of the theory of open quantum systems which will be exploited in the remainder of this thesis. The evolution of an open quantum system in contact with a reservoir is described employing a Markov approximation. Additionally, we have introduced key definitions related to principles of quantum mechanics, including quantum correlation, which will prove instrumental in the subsequent discussions and analyses presented in our work.

Initially, we established the notion of a composite system consisting of an open quantum system interacting with an environment. Considering the composite system as closed, the derivation of the dynamics of the total system follows naturally from the equation of motion of the system vector state. We then used the various approximations exploitable through a weak coupling limit estimation to derive a local master equation for the open system. In simple terms, the master equation derived in this chapter is Markovian and local in time and space. So that, when considering the open system as a complex entity, the dissipations induced by each thermal bath have a direct impact only on the local subsystem to which it is connected.

We have also proposed a description of quantum correlations in an open quantum system. Although this is an appropriate overview, it highlights the different manifestations of quantum correlations in several forms. By construction, we have proposed two reference measures for quantifying correlations in a two-body quantum system. Although these approaches can be applied to the same range of pure systems, they exhibit several points of divergence. One notable

distinction lies in the complete dependence of the discord measure on local measures. Additionally, it is worthwhile to consider the applicability of the discord measure in scenarios involving separated states, where entanglement is entirely absent.

Finally, have outlined a set of perspectives to contextualize non-Markovianity in the evolution of open systems. In achieving this, we leveraged the inherent properties of dynamical evolution without imposing any specific boundary conditions on the system's properties. The characterization of Markovianity was accomplished through the analysis of the separability of dynamic maps. Then, moving towards a more realistic description, we delved into the concept of system state discernability. This approach enables the examination of memory effects by comparing the distinguishability of two dynamic states, providing a means to quantify a measure of non-Markovianity.

Chapitre 2

Concepts of Quantum thermodynamics

The development of thermodynamics at the nanoscale requires a solid basis of theory and experimental foundation, which has given rise to some interesting questions over the years. A significant challenge lies in the development of theoretical frameworks that reconcile the dynamical evolution of many-body systems with the operation of thermodynamic devices at the infinitesimal scale. In this context, a plethora of research has been carried out to provide further insight into these issues [88–96]. A priori, the main goal is the quantum description of thermodynamic quantities such as work, heat, entropy, and the different factors governing the production of such quantities in small systems, where quantum mechanics inevitably comes into play [97–102]. It follows from this approach that taking the quantum mechanics as an exhaustive theory, gives rise to a complex and broad theoretical field in which one can describe the thermodynamic processes and study how the thermodynamic laws emerge from a quantum system. This theoretical approach, open to microscopic domains, is usually extended to quantum thermal, giving us a clearer understanding of the physics of thermodynamic devices. More importantly, it also allows us to clarify the physical perception of thermal machines and identify which operations can or cannot be carried out when quantum properties exert their impact [103–109].

In the following, we present a few details of the theoretical resources on the formalism of quantum thermodynamics. In section 2.1 and 3.1, we present the basic theory governing the operation of thermodynamic devices, including the description of thermodynamic quantities and the laws of thermodynamics. In sections 2.3, we introduce the notions of discrete and continuous quantum machines, and discuss some examples that will be useful in the remainder of this thesis. In section 2.4, we discuss the interaction between entropy production and the operation of quantum thermal machines.

2.1 Basic thermodynamic concepts

The emergence of quantum thermodynamics is closely associated with the quantum approximation of various quantities and fundamental principles observed in thermodynamic processes. This advancement has been significantly propelled by progress in statistical mechanics, facilitating the transition from macroscopic principles to microscopic systems. Despite the paradigms in this field, the cornerstone of quantum thermodynamics remains the definition and interpretation of the concepts governing thermodynamic phenomena such as heat, work and entropy production. These basic concepts serve as the foundation upon which the framework of quantum thermodynamics is built, guiding researchers in understanding and modeling complex thermodynamic processes at the quantum level.

The central element in the development of quantum thermodynamics is the concept of quantum thermal machines, which has proved to be very useful in addressing various problems relating to the extension of classical thermodynamic concepts to the quantum case [110–114]. Quantum thermal machines offer straightforward configurations for studying thermodynamics at a fundamental level, laying the groundwork for understanding the quantum mechanics of thermodynamic devices [115–117] . They also represent a close insight into the interplay between quantum information and the principles of thermodynamics. In essence, the term quantum thermal machine includes any physical device comprising a working system, which is naturally a composite quantum system coupled to different thermal baths, whether or not under external control. This broad definition encompasses a wide range of systems and scenarios, offering a versatile platform for exploring the quantum aspects of thermal processes [118–120].

2.1.1 Internal energy and the first law of thermodynamics

Given a quantum system $\mathcal{S}$ with $H_{\mathcal{S}}(t)$ and $\rho_{\mathcal{S}}(t)$ its Hamiltonian and density operator, respectively, at time t. The internal energy of the system is defined as the average energy of all processes (forward process, backward process) that can be carried out in the system :

$$U(t) = Tr\left[\rho_{\mathcal{S}}(t)H_{\mathcal{S}}(t)\right]. \tag{2.1}$$

In other words, when the system changes in a time interval $t \in [0, \tau]$, the Hamiltonian and the state of the system evolve from a time $t = 0$ to a time $t = \tau$. The average change in the internal energy of the system is given by :

$$\Delta U = U_\tau - U_0 = Tr\left[\rho_{\mathcal{S}}(\tau)H_{\mathcal{S}}(\tau)\right] - Tr\left[\rho_{\mathcal{S}}(0)H_{\mathcal{S}}(0)\right], \tag{2.2}$$

meaning that the variation of a system's internal energy depends only on the information present in its initial and final conditions. Using the time derivative of the internal energy, Eq.(2.2) can be expressed as an integral in the form :

$$\begin{aligned}
\Delta U &= U_\tau - U_0 = \int_0^\tau dU(t)/dt \\
&= \int_0^\tau d\{Tr\left[\rho_{\mathcal{S}}(t)H_{\mathcal{S}}(t)\right]\}/dt \\
&= \int_0^\tau \{Tr\left[\frac{d\rho_{\mathcal{S}}(t)}{dt}H_{\mathcal{S}}(t)\right] + Tr\left[\rho_{\mathcal{S}}(t)\frac{dH_{\mathcal{S}}(t)}{dt}\right]\}.
\end{aligned} \tag{2.3}$$

In the above equation, we can see how the change in the system's internal energy gives rise to an energy contribution, which depends on the change in the system's Hamiltonian operator, and another quantity, which depends on the change in the system's state. Notably, the variation of the density operator $\rho_{\mathcal{S}}(t)$ and the Hamiltonian operator $H_{\mathcal{S}}(t)$ of a system in a thermodynamic process is typically attributed to a contribution from the heat exchanged between the internal system and its environment and a contribution from the work performed by a control protocol, respectively. Thus, the change in mean energy ΔU can be represented as a sum of the mean average heat Q and the quantum work performed on the system W :

$$\begin{aligned}
Q &= \int_0^\tau \delta Q = \int_0^\tau Tr\left[\frac{d\rho_{\mathcal{S}}(t)}{dt}H_{\mathcal{S}}(t)\right]dt, \\
W &= -\int_0^\tau \delta W = \int_0^\tau Tr\left[\rho_{\mathcal{S}}(t)\frac{dH_{\mathcal{S}}(t)}{dt}\right]dt.
\end{aligned} \tag{2.4}$$

Here, we recover the assertion of the first law of thermodynamics, which relates to the conservation of energy, and states that the sum of the average heat and work performed on the system constitutes its average energy change,

$$\Delta U = Q - W. \tag{2.5}$$

Clearly, for a cyclic process in which the system returns to its initial conditions at the end of the process,

$$\rho_{\mathcal{S}}(\tau) = \rho_{\mathcal{S}}(0) \quad \text{and} \quad H_{\mathcal{S}}(\tau) = H_{\mathcal{S}}(0), \tag{2.6}$$

the work and heat consumed during the process are related, following definition (2.2), by the relation :

$$Q_{cyc} = W_{cyc}. \tag{2.7}$$

Moreover, in contrast to the variation in internal energy, which is dependent solely on information about the initial and final states of the system, heat and work both depend on the trajectory taken by the system. Precisely how the quantum dynamics of the system evolve over time. Therefore, for an infinitesimal process, relation (2.5) can be written as follows :

$$dU = \delta Q - \delta W, \tag{2.8}$$

with the symbol δ to specify that heat and work are (in general) not exactly differentiable and do not correspond to observables, while mean average energy does.

2.1.2 Thermodynamic Processes

A central feature in thermal machine operation is the allocation of device processes. Basically, three types of processes can be distinguished, depending on the nature and quality of exchanges between the system and its environment :

Isothermal process : In this case, the temperature of the system remains constant throughout the process, although energy and matter may be exchanged between the system and its surroundings.

Isochoric process : The system can exchange energy with its environment, but not matter. In the classical case, for P-V systems, an isochoric process takes place at constant volume.

Adiabatic process : In this case, the process takes place without any exchange of average heat or matter between the system and the environment, and only the work performed by a control protocol contributes to the dynamics of the system.

Another approach to specifying thermodynamic processes is based on the evolution of the system. In this respect, thermodynamic processes can be divided into two categories :

Reversible process : When the system evolves under the action of an external control protocol, while remaining in quasi-equilibrium with its environment. In this case, it is possible to perform the opposite process, moving both the system and its environment from their final states to their respective initial states by reversing the protocol.

Irreversible process : Otherwise, when the state of the system deviates from its equilibrium state in the dynamics governing its evolution over time, it is not adequate to restore the states of the system and its environment, and the process is considered irreversible. In an irreversible process, it is possible to restore the initial state of the system by applying a reverse protocol. However, this generates a perturbation in the state of the environment.

2.1.3 Second law of thermodynamics

The second law of thermodynamics states the type of energy exchanged in the course of a thermodynamic operation, including the direction of the energy flow distribution : *when no work is done on the system, heat never flows spontaneously from a cold bath to a hot bath.* A preliminary formalization was originally proposed by Clausius [121, 122] in his research after the basic observations made by Sadi Carnot. The latter introduced the second law of thermodynamics for the first time as a condition for the maximum extraction of work from a heat engine operating between a temperature difference, i.e., two heat reservoirs at different temperatures [123, 124]. More precisely, when all operations performed by the thermal machine are reversible and on the assumption that no heat is lost, the operation of a cyclic machine can reach a maximum efficiency limited by the Carnot efficiency, which is a property of the machine,

$$\eta_c = 1 - \frac{T_{cold}}{T_{hot}}. \tag{2.9}$$

Later, in 1865, Rudolf Clausius advanced a new perception to study the thermodynamics of a system interacting with multiple thermal baths. Among other things, he stated that in a cyclic process, the variation in the quantity of heat during all reversible steps of the process can be described in a similar manner to the variation in the internal energy of a system :

$$\oint \frac{\delta Q_{rev}}{T} = 0. \tag{2.10}$$

Eq. (2.10) gives an idea about how the integral of the variation $\delta Q/dt$ in a reversible process joining two states $\rho_{\mathcal{S}}(\tau)$ and $\rho_{\mathcal{S}}(0)$, depends only on the states $\rho_{\mathcal{S}}(\tau)$ and $\rho_{\mathcal{S}}(0)$ and is independent of any trajectory followed by the system. Based on this perception, Clausius introduced the thermodynamic entropy as a function of the system's initial and final states,

$$\Delta S_{th} = \int_0^\tau \frac{\delta Q_{rev}}{T}, \tag{2.11}$$

where

$$\Delta S_{th} = S_\tau - S_0 \tag{2.12}$$

is the change in system entropy between time $t = 0$ and time τ and δQ_{rev} is the heat consumed by the system during the reversible process. However, a thermodynamic process does not necessarily follow a reversible path and, in this case, a certain amount of heat is dissipated throughout the process. The previous relations are generalized by the Clausius inequality :

$$\Delta S_{th} \geq \int_0^\tau \frac{\delta Q_{rev}}{T}. \tag{2.13}$$

Looking further afield, advancements in the study of quantum thermodynamics have revealed the possibility of deriving universal relations that can replace the traditional second law of thermodynamics. The second law of thermodynamics can take several forms. Notably, if we consider the system of interest as an open quantum system, the second law of thermodynamics can generally be expressed as

$$\Delta S_{th} = \Delta_i S_{th} + \Delta_e S_{th} \geq 0, \tag{2.14}$$

where the term $\Delta_e S_{th}$ corresponds to the entropy changes in the system due to energy and matter exchanges with the surroundings, and $\Delta_i S_{th}$ is the entropy change in the system due to irreversible processes within the system. This formulation emphasizes that the total entropy change of the system, which includes contributions from both internal irreversible processes and exchanges with the environment, must be non-negative.

2.2 Classical Otto machine

Before looking at the various quantum thermal schemes, let's revisit the Otto quantum thermal machine theory, one of the pioneering works in the field of thermal machines. The Otto cycle is a sequence of four successive strokes, including two adiabatic processes and two thermalization processes, which combine to form a cyclic operation. The classical Otto cycle was initially introduced around 1876 by the German engineer Nikolaus A. Otto to illustrate a four-stroke reciprocating internal combustion engine [125]. It consists of a piston-cylinder unit in which combustion of the air-fuel mixture is triggered by a spark plug as illustrated in Figure.2.1. This classical framework serves as a foundation for understanding the principles underlying thermal machines and provides valuable insights into the operation and efficiency of such systems.

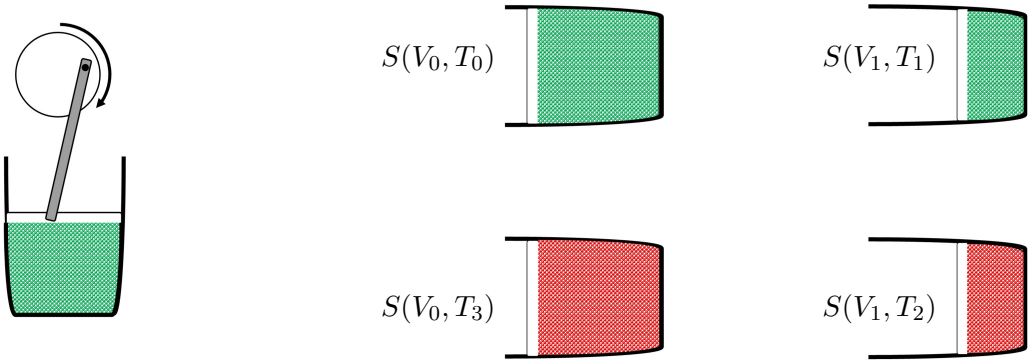

FIGURE 2.1 – Schematic representation of a four-stroke internal combustion Otto cycle. The left image depicts the device, comprising a piston-cylinder assembly. On the right are the four thermodynamic states characterized by the variation in volume and temperature $S(V, T)$ of the working system.

The engine operates between four thermodynamic states characterized by the variation of the volume and temperature $S(V, T)$ of the working system :

First isentropic process : An isentropic compression, where the working fluid is compressed adiabatically at constant entropy. The characteristics of the working system change accordingly from $S(V_0, T_0)$ to $S(V_1, T_1)$.

Second isochoric process : The working system is heated at a constant volume until reaching a temperature T_2. The piston is now allowed to equilibrate thermally with a hot thermal bath, while maintaining a constant volume. Only the temperature of the working system changes during this process so that the system passes from $S(V_1, T_1)$ to $S(V_1, T_2)$.

Third isentropic expansion : The working system is isolated from the hot bath and expanded adiabatically. In this process, the volume of the piston is restored to its initial value. The characteristics of the working system change accordingly from $S(V_1, T_2)$ to $S(V_0, T_3)$

Fourth isochore process : The system is cooled back to its initial state in an isochore process. At the end of this process, the working system is restored to its initial volume and temperature. The system then recovers its primary characteristics through the transition from $S(V_0, T_3)$ to $S(V_0, T_0)$.

2.2.1 Thermodynamic quantities

In the context of the Otto cycle, where no work is done in the two isochoric strokes, the heat exchanges in these processes are given by :

$$Q_h = MC_V(T_2 - T_1), \tag{2.15}$$

$$Q_c = MC_V(T_3 - T_0), \tag{2.16}$$

where Q_h represents the heat supplied to the piston during the heating operation, and Q_c is the heat released during the refreshing operation. The constant M is the mass of the working system and C_V is the specific heat capacity at constant volume. Once the device is configured to function in the engine regime, the efficiency η of the Otto cycle is defined as the ratio between the work performed and the heat supplied by the hot bath :

$$\eta = \frac{W_{cycle}}{Q_h} = 1 - \frac{Q_c}{Q_h} \tag{2.17}$$

$$= 1 - \frac{T_3 - T_0}{T_2 - T_1}. \tag{2.18}$$

Alternatively, the machine can be converted to a refrigeration regime by changing the sequence of operations on the strokes. The coefficient of performance is then defined by :

$$COP = \frac{Q_c}{W_{cycle}}. \tag{2.19}$$

It is quite straightforward to simplify the above expressions for an ideal gas, assuming that the first and third processes are isentropic and that the working system obeys the equation of state $TV^{\gamma^{-1}} = const$,

$$T_3 V_0^{\gamma^{-1}} = T_2 V_1^{\gamma^{-1}} \tag{2.20}$$

$$T_0 V_0^{\gamma^{-1}} = T_1 V_1^{\gamma^{-1}}. \tag{2.21}$$

where

$$\gamma = \frac{C_P}{C_V}, \tag{2.22}$$

is the specific-heat ratio of the heat capacities at constant pressure C_p and constant volume C_V. Consequently, the previous equations yield the relation

$$(T_3 - T_0)V_0^{\gamma^{-1}} = (T_2 - T_1)V_1^{\gamma^{-1}}. \tag{2.23}$$

From these correspondences, we can simplify the expressions for efficiency and coefficient of performance for an ideal gas,

$$\eta = 1 - \left(\frac{V_1}{V_0}\right)^{\gamma^{-1}} \tag{2.24}$$

and

$$COP = \frac{1}{\left(\frac{V_1}{V_0}\right)^{\gamma^{-1}} - 1}, \tag{2.25}$$

with the compression ratio V_1/V_0.

2.2.2 Maximum efficiency in the Otto cycle

In finite-time thermodynamic processes, the working system undergoes partial thermalization for a limited duration. The piston is detached from the heat bath before complete thermalization occurs, and the adiabatic stroke commences. In the classical Otto cycle, however, thermalization is complete in both isochoric processes, which in principle requires a very long duration

As previously indicated, a primary goal in machine engineering is to create machines with optimal performance. In pursuit of this objective, comprehensive investigations into cyclic Otto machines have revealed an upper efficiency limit within the thermodynamic framework. This limit applies to Otto machines operating between two thermal baths at different temperatures :

$$\eta_O = 1 - \sqrt{\frac{T_1}{T_0}}. \tag{2.26}$$

The efficiency η_O depends mainly on the temperatures of the thermal baths, where T_0 and T_1 are respectively the temperatures of the hot and cold baths. It was introduced by Yvon and Novikov in a particular model of nuclear machine with complete thermalization [126, 127], then generalized by Curzon and Ahlborn in situations independent of the model considered. However, in the general perspective of any heat engine, the maximum efficiency achievable reads

$$\eta_C = 1 - \frac{T_1}{T_0} \tag{2.27}$$

which is the Carnot efficiency representing the maximum efficiency attainable by any heat engine operating between two heat reservoirs.

2.3 Quantum thermal Machine

Addressing the fundamental questions of quantum thermodynamics requires an extensive theoretical framework associated with an appropriate experimental design. In recent years, considerable progress has been made in the development of quantum thermal machines. These advances have provided a basic tool for researchers to highlight the fundamental principles of thermodynamics in the quantum framework and predict microscopic thermodynamic applications in terms of quantum intrigue. The concept of a quantum thermal machine refers to any physical system designed to perform thermodynamic tasks such as the conversion of one form of energy into another or heat transfer using the heat flow between different thermal reservoirs. This transfer is achieved by means of a working system, which is essentially a quantum system, acting as a transport agent between two or more heat baths.

Since Carnot's pioneering work on the classical model of thermal machines, it wasn't until 1956 that Scovil and Dubois proposed the quantum equivalence of a three-level heat engine with a Carnot heat engine [123]. The basic concept behind Scovil's proposition is based on the conversion of population inversion into output power in the form of radiation, Figure.2.2. A reservoir at high temperature induces transitions between the ground state and the most excited state. A low-temperature reservoir couples the ground state and the intermediate state. The amplifier operates by coupling the transition between the intermediate and most excited levels to a radiation field, generating an output frequency. Such a machine is likely to operate as a heat engine with an efficiency close to Carnot efficiency, and its operation can be reversed to provide a refrigerator, which can also achieve maximum efficiency [21, 128, 129]. Following this pioneering work, substantial work has been conducted in this area. Various suggestions have been put forward concerning the concept of quantum thermal machines and the way in which thermodynamic processes, and even the laws of thermodynamics, can be defined in the

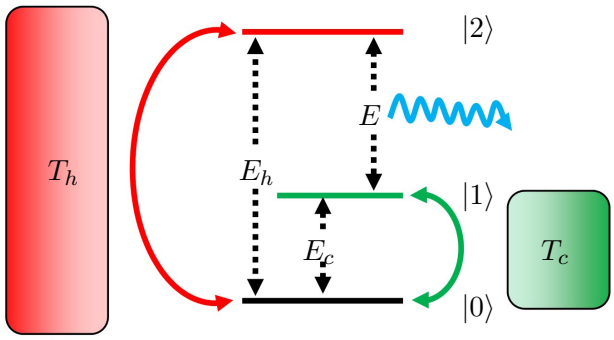

FIGURE 2.2 – Schematic representation of the three-level quantum thermal machine. The working system is a three-level system with energy levels $|0\rangle$, $|1\rangle$ and $|2\rangle$ and populations n_1, n_2 and n_3, respectively. A hot bath with temperature T_h induces transitions between energy levels $|0\rangle$ and $|2\rangle$, while a cold bath with temperature T_c induces transitions between $|0\rangle$ and $|1\rangle$. Work is performed by an external field in resonance with the energy gap $E = E_h - E_c$.

microscopic context of quantum mechanics. From a dynamical point of view, quantum thermal machines can be classified into two categories : discrete thermal machines and continuous one. For the first category, the machine operates through different segments of time during which a particular operation takes place, for example, thermalization or work extraction with the support of an external agent. For the second one, the devices operate without any interruption until reaching a steady state.

The thermal machine described above is based on a one-body model with an external agent. However, recent studies on quantum thermal machines have provided a wealth of information on their different structures and possible modeling. A plethora of models have since received important contributions in the area of many-body systems [130–134] . These conceptions generally contrast in the approaches used to describe working systems, thermal baths, and in particular, their various couplings. Recent proposals including models of thermal machines based on a small number of quantum systems as the working system, have proved to be promising models with the possibility of implementation [135–137].

Upon taking these different configurations, the Hamiltonian of the total machine, defined by the joint system and all interaction units, can be formally written as follows :

$$H = H_{\mathcal{S}} + H_{\mathcal{R}} + H_{\mathcal{SR}}, \tag{2.28}$$

where $H_{\mathcal{S}}$ is the system Hamiltonian, $H_{\mathcal{R}} = \sum_i H_{\mathcal{R}_i}$ is the baths Hamiltonian and

$$H_{SR} = \sum_i H_{SR_i}, \tag{2.29}$$

is the system-baths interaction. The average energy of the global system (internal system plus environment) following the Hamiltonian (2.28) is given by :

$$\langle H \rangle = \langle H_{\mathcal{S}} \rangle + \langle H_{\mathcal{R}} \rangle + \langle H_{\mathcal{SR}} \rangle, \tag{2.30}$$

where

$$\langle A \rangle = Tr\left[A\rho(t)\right], \tag{2.31}$$

is the trace over the density operator of the total machine.

The first and second terms in Eq. (2.30) can clearly be associated with the variations in energy of the internal system and environments. However, some confusion arises as to the attribution of the composite system interaction energy term $\langle H_{\mathcal{SR}} \rangle$. A particular solution emerges when we adopt the weak coupling limit, in which the interaction part of the Hamiltonian takes the form

$$H_{SR} = \sum_i \alpha_i V_{SR_i}, \tag{2.32}$$

with α_i is extremely small compared to the values of the energy gaps of the system components. In such a case, the average $\langle H_{\mathcal{SR}} \rangle$ results in very small and negligible values compared with the other quantities which can be neglected. An approximation of Eq. (2.30) takes the form :

$$\langle H \rangle \simeq \langle H_{\mathcal{S}} \rangle + \langle H_{\mathcal{R}} \rangle. \tag{2.33}$$

Building upon the Markovian dynamics of the open system (1.112), we are able to separate the variation in the internal energy of the system, $d\langle H_{\mathcal{S}} \rangle / dt$, into two contributions. One is associated with a change induced by the exchange with its environment, and the other with a change in its Hamiltonian,

$$\frac{d}{dt}\langle H_{\mathcal{S}} \rangle = \langle \frac{\partial H_{\mathcal{S}}}{\partial t} \rangle + \sum_i \langle \mathcal{L}_{\mathcal{R}_i} H_{\mathcal{S}} \rangle. \tag{2.34}$$

Based on the definition of work and heat in a thermodynamic process defined in equation. (2.4), we can recover the expression of the average heat exchanged between the working system and a thermal bath R_i by :

$$\dot{Q}_i = Tr\left[H_{\mathcal{S}} \mathcal{L}_{R_i}(\rho_{\mathcal{S}}(t))\right], \tag{2.35}$$

and the average work performed throughout the process by,

$$\dot{W} = \langle \frac{\partial H_{\mathcal{S}}}{\partial t} \rangle. \tag{2.36}$$

Consequently, the derivative form of the first law reads :

$$\dot{U}_{\mathcal{S}} = \sum_i \dot{Q}_i + \dot{W}. \tag{2.37}$$

It's important to note that, according to the principle of thermodynamics, we adhere to the basic idea that an average of thermodynamic quantities, heat $\dot{Q}$ or work $\dot{W}$, is injected in to the working system when $\dot{Q}(\dot{W}) > 0$ and, conversely, extracted from the system when $\dot{Q}(\dot{W}) < 0$. The efficiency of the machine when operating as an engine is given by the ratio between the average work performed on the system over the hot bath thermal current

$$\eta_e = \frac{W}{Q_h}. \tag{2.38}$$

Similarly, the coefficient of performance (COP) of a refrigerator can be evaluated by taking the ratio between the heat flow from the cold bath over the average work

$$COP = \frac{Q_c}{W}. \tag{2.39}$$

2.3.1 Discrete quantum thermal machine

As previously stated, the purpose of a quantum thermal machine is to achieve thermodynamic operations through the transfer of heat between reservoirs at different temperatures and by means of a working system. When the working system performs a prescribed thermal operation over different strokes, the machine is classified as a discrete machine. Various models, generally similar to the Carnot or Otto models, can be proposed on the basis of this principle.

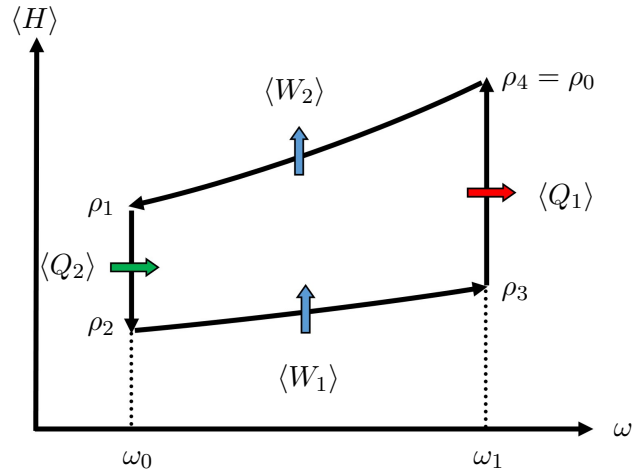

FIGURE 2.3 – Energy-frequency diagram of a four-stroke quantum refrigerator. The thermodynamic cycle consists of two adiabatic processes and two isochoric processes. In both isochoric processes, the refrigerator absorbs heat from the cold reservoir $\langle Q_2 \rangle$ or transfers heat $\langle Q_1 \rangle$ to the hot reservoir. During the two adiabatic processes, the quantum refrigerator performed a total work of $\langle W_1 \rangle + \langle W_2 \rangle$ to pump the heat absorbed from the cold reservoir $\langle Q_2 \rangle$ to the hot reservoir in heat $\langle Q1 \rangle$.

The potential transformations in the evolution dynamics of a four-stroke thermal machine's working system are categorized into two processes. This division aids in a clear analysis of the variation in internal energy and facilitates the thermodynamic examination of the devices. In the first scenario, two different unitary transformations $\mathcal{U}$ are applied to move the system from its initial condition (ρ_i, H_i) to a final condition (ρ_f, H_f) through the impact of a unitary evolution induced by the action of an external agent. In an Otto cycle, these two processes are associated with the two isothermal processes. The external agent acts on the Hamiltonian to bring the system from its initial conditions to its final conditions. Nonetheless, the populations of the system's state energy levels remain unchanged, as they are isolated from thermal baths throughout the process. No heat is exchanged during the process, and the change in the internal energy of the working system is associated with the work done by external forces :

$$W := U_f - U_i = Tr\left[\rho_i(\mathcal{U}^\dagger H_f \mathcal{U} - H_i)\right]. \tag{2.40}$$

Secondly, the system remains in contact with one of the thermal baths during two separate thermalization processes. Heat is exchanged between the system and the bath without any modification of the system's Hamiltonian operator $H_i = H_f$. The working system thus passes from initial conditions (ρ_i, H_i) to final conditions (ρ_f, H_f). These processes refer to the two isothermal processes, which do not involve any work. The variation in internal energy is then associated with the heat exchanged between the system and the environment :

$$Q = U_f - U_i = Tr\left[H_i(\rho_f - \rho_i)\right]. \tag{2.41}$$

Until now, there was no indication about how the Hamiltonian operator H or the final state was generated. Usually, the transformation operations are dependent on either linear or non-linear functions, in terms of the working system's frequency and the stroke's duration. Regarding thermalization, there are two discernible scenarios : full thermalization, where the system passes from one Gibbs state to another, and partial thermalization, where the process halts before the system attains a steady state. As a result, the system's ultimate state depends on the dynamic evolution that its interactions with the environment foster. In this instance, the thermodynamic quantities rely not only on the parameters of the system but are also impacted by the system's dynamic evolution.

By way of illustration, let us consider the four-stroke Otto quantum refrigerator, as depicted in the Fig.2.3. In the course of the refrigerator's operation, the working system undergoes a four-stage cycle, consisting of two adiabatic processes and two isothermal processes, during which it may or may not be coupled with the heat reservoirs. The refrigerant starts the cycle in the hot Gibbs state $\rho_0 = e^{-\beta_h H_0}/Z_h$, where $\beta_h = 1/kT_h$ is the hot inverse temperature, H_0 is the initial Hamiltonian of the working system, and $Z_h = Tr\left[e^{-\beta_h H_0}\right]$ is the associated partition function.

Stage 1 : The system is detached from the hot bath and undergoes an adiabatic process. A compression is performed on the refrigerant frequency, such as ω_0 is decreased to ω_1 leading to an output of power while the energy level populations remain constant. As there is no heat flow, the work done during this stroke is therefore the change in energy in the system :

$$W_1 = U_1 - U_0 = Tr\left[\rho_0(\mathcal{U}_1^\dagger H_1 \mathcal{U}_1 - H_0)\right]. \tag{2.42}$$

with state $\rho_1 = \mathcal{U}_1 \rho_0 \mathcal{U}_1^\dagger$ at the end of the process.

Stage 2 : The system is coupled to the cold bath at the inverse temperature β_c and starts an interaction process. During this stroke, the Hamiltonian of the working system is kept fixed at H_1 for the duration of the interaction. Nevertheless, the energy levels of the working system are allowed to change thanks to the heat absorbed from the cold bath moving the state of the system from ρ_1 to a state ρ_2,

$$Q_c = U_2 - U_1 = Tr\left[(\rho_2 - \rho_1)H_1\right]. \tag{2.43}$$

Stage 3 : The system is detached from the cold bath and the frequency is increased from ω_1 back to its initial value ω_0 by means of adiabatic expansion due to the work done on the system :

$$W_2 = U_3 - U_2 = Tr\left[\rho_2(\mathcal{U}_2^\dagger H_0 \mathcal{U}_2 - H_1)\right]. \tag{2.44}$$

whith the system's state $\rho_3 = \mathcal{U}_2 \rho_2 \mathcal{U}_2^\dagger$ at the end of the process.

Stage 4 : In order to close the cycle, this last phase consists of a complete thermalization of the refrigerant with the hot reservoir at the inverse temperature β_h. During this process, the Hamiltonian is held fixed at H_2, while the population of the working system is allowed to change as heat flows through the system :

$$Q_h = U_4 - U_3 = Tr\left[(\rho_0 - \rho_3)H_2\right]. \tag{2.45}$$

The total work performed along the cycle is then given by

$$W = W_1 + W_2. \tag{2.46}$$

The coefficient of performance of the refrigerator is rewritten by

$$COP = \frac{Q_c}{W}. \tag{2.47}$$

For the special case, when the working system consists of a multi-level system, the Hamiltonian of the system is given by :

$$H_s = \sum_n E_n \left|n\right\rangle \left\langle n\right|. \tag{2.48}$$

where $|n\rangle$ is the n-th eigen state of the system and E_n is its corresponding energy with $E_0 = 0$ the energy of the ground state $|0\rangle$. Without loss of generality, we consider here the scenario where each thermalization is complete and, at the end of each thermalization, the system reaches a steady state with the thermal bath. At the end of the step, the state of the system is in the form

$$\rho_S^{ss} = \sum_n P_n \left|n\right\rangle \left\langle n\right|, \tag{2.49}$$

whith

$$P_n = \exp\left[-\beta E_n / k_B\right] / Z, \tag{2.50}$$

is the probability of occupation of each state $|n\rangle$,

$$Z = \sum_n \exp\left[-\beta E_n / k_B\right] \tag{2.51}$$

is the partition function of the system, β is the inverse temperature and k_B is the Boltzmann's constant. Hence, a variation in internal energy can be expressed as

$$dU = \sum_n \Big(dP_n E_n + P_n dE_n \Big). \tag{2.52}$$

The expression for the heat exchanged with a thermal bath is derived from the previous descriptions of heat and work along a thermodynamic process :

$$\bar{d}Q = \sum_n P_n dE_n, \tag{2.53}$$

as well as the work that is performed along a stroke

$$\bar{d}W = \sum_n dP_n E_n. \tag{2.54}$$

where $\bar{d}$ reflects the fact that Q and W are not completely differentiable. A fundamental requirement for the system to function as a refrigerator is positive work dissipation, relative to the heat absorbed by the system from the cold bath.

2.3.2 Continuous quantum thermal machine

In this section, we introduce the second category of quantum thermal machines, known as continuous quantum thermal machines. These machines, in contrast to the previously described model, are distinguished by an ongoing interaction between the reservoirs and the working system. The device generates a continuous flow of energy between the thermal baths through the working system, which is kept in constant contact with the thermal baths at different temperatures. Continuous thermal machines are further classified into two categories depending on the device's configuration. The continuous driven machines, where the working system is subject to an external power source and autonomous ones, where the device operates without any external intervention.

α) Three-level quantum thermal Machine

The thermodynamic future of the three-level quantum thermal machine described in Fig.2.2 has been the subject of much discussion over time, leading to proposals for its physical implementation. Geva and Kosloff were pioneers in investigating three-level amplifiers within the framework of finite-time thermodynamics. They played a pivotal role in formulating numerous propositions aimed at optimizing the thermodynamic performance of these machines, considering various control parameters such as the frequency and amplitude of the external agent or the coupling constants between the elements of the device. Subsequently, some new ideas have emerged to further strengthen the concepts of quantum thermodynamics, with various proposals falling into two main categories. Firstly, there is a focus on studying thermodynamic principles like work, thermal heat, and entropy at the level of infinitesimal processes. Secondly, an exploration of how quantum properties contribute to the operation and production of thermal machines. Both of these aspects form the core of the field's exploration and development of the thermodynamics of quantum thermal machines.

The free Hamiltonian of the working system is given by

$$H_{\mathcal{S}} = E_c \left|1\right\rangle \left\langle 1\right| + E_h \left|2\right\rangle \left\langle 2\right|, \tag{2.55}$$

where we consider the energy of the ground state $E_0 = 0$. When the device operates until reaching a steady state, the population Eq.(2.50) of each level is derived from equation.(2.50) by :

$$P_0 = 1/Z, \quad P_1 = e^{-\beta_c E_c}/Z, \quad P_2 = e^{-\beta_h E_h}/Z, \tag{2.56}$$

where Z is the partition function, E_μ the energy eigenvalue of the i-th level, and β_μ the inverse temperature of the thermal bath coupled with the level transition. The ratios between the populations at the system levels are then given by

$$\frac{P_1}{P_0} = e^{-\beta_c(E_c - E_0)} = e^{-\beta_c E_c}, \tag{2.57}$$

$$\frac{P_2}{P_0} = e^{-\beta_h(E_h - E_0)} = e^{-\beta_h E_h}. \tag{2.58}$$

With these settings, the machine operates as an engine under the conditions of positive amplification gain or population inversion defined by

$$P_2 - P_1 \geq 0 \rightarrow \frac{E_c}{E_h} \geq \frac{T_c}{T_h}. \tag{2.59}$$

In the inverse process, the gain is negative and the system absorbs the heat flux from the cold bath to the hot bath, using energy provided by an external agent,

$$P_2 - P_1 \leq 0 \rightarrow \frac{E_c}{E_h} \leq \frac{T_c}{T_h}, \tag{2.60}$$

and the machine operates like a refrigerator.

β) Many-body quantum thermal machine

An alternative concept to the previous model is the many-body quantum thermal machine, which is more suitable for the thermodynamic analysis of a certain range of quantum processes. Here, the working system consists of interacting quantum systems coupled to different thermal baths. The most appropriate approaches for investigating these devices may differ depending on their configuration, including whether all the coupling sites are in resonance or not, with weak or strong coupling limits. The observations made in these different cases show considerable differences and confirm the need for in-depth reflection on the approach to be adopted.

The most fundamental example of many-body quantum devices is the two-body quantum thermal machines. The machine consists of two interacting qubits coupled to their respective thermal baths at different temperatures, T_h and T_c with $T_h > T_c$, as shown in Fig.2.4.

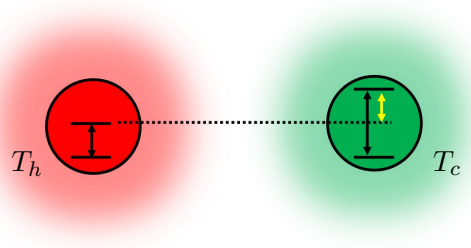

FIGURE 2.4 – Sketch of a two-body quantum thermal machine. The two interacting bodies are respectively coupled to two independent thermal baths at different temperatures. In the absence of external input, heat is transferred from the hot bath at temperature T_h to the colder bath at temperature T_c. However, the system can be controlled by an external agent to reverse the process.

The hamiltonian of the total machine is given by

$$H = H_{\mathcal{S}} + H_{\mathcal{R}} + H_{\mathcal{SR}}, \tag{2.61}$$

where $H_{\mathcal{S}} = H_0 + H_{int}$ is the Hamiltonian of the two qubits comprising the free energy of the two qubits and the interaction part

$$H_0 = \sum_{\mu=c,h} \epsilon_\mu A_\mu^\dagger A_\mu, \tag{2.62}$$

$$H_{int} = g(A_c^\dagger A_h + A_c A_h^\dagger). \tag{2.63}$$

where A_μ is an operator in the Hilbert space of the system $\mathcal{S}_\mu$, e_μ is an energy gap and g is the coupling constant. In the following description, we consider the case where the Hamiltonian is time-independent and only an external energy input affects the operation of the machine. Furthermore, other research has taken into account certain scenarios in which a control protocol drives the operational system, revealing notable effects on the machine's performance. The Hamiltonian $H_{\mathcal{R}} = \sum_{\mu=c,h} H_{\mathcal{R}_\mu}$ of the two baths is considered in the form :

$$H_{\mathcal{R}_\mu} = \sum_k \omega_{\mu,k} B_{\mu,k}^\dagger B_{\mu,k}. \tag{2.64}$$

with $B_{\mu,k}$ are defined in the Hilbert space of the thermal bath $\mathcal{R}_\mu$. Finally, the interaction between the qubits and the baths characterizes an exchange of excitation between the system and the bath, depending on the timescales considered, which does not necessarily require energy conservation,

$$H_{\mathcal{SR}} = \sum_{\mu=c,h} \sum_k \lambda_{\mu,k}(A_\mu^\dagger B_{\mu,k} + A_\mu B_{\mu,k}^\dagger). \tag{2.65}$$

A more tractable approach for the master equation governing the dynamics of many-body problems is the local master equation. (1.112), in which incoherent thermal baths create and eliminate excitations at the boundaries components of the system,

$$\dot{\rho}_{\mathcal{S}} = -i\,[H_{\mathcal{S}}, \rho_{\mathcal{S}}] + \sum_\mu \mathcal{L}_{R_\mu}(\rho_{\mathcal{S}}). \tag{2.66}$$

Once the coupling between the device's components is resonant, a flow of heat from the hot bath to the cold bath must be generated until the system reaches a steady state at a constant temperature T_{eff}. In accordance with the definition in Eq. (2.35), the amount of heat exchanged with a thermal bath can be expressed as,

$$\dot{Q}_\mu = Tr\left[H_s\left(\gamma^\mu_\downarrow(A_\mu\rho_S A^\dagger_\mu - \frac{1}{2}(A^\dagger_\mu A_\mu\rho_S + \rho A^\dagger_\mu A_\mu)) + \gamma^\mu_\uparrow(A^\dagger_\mu\rho_S A_\mu - \frac{1}{2}(A_\mu A^\dagger_\mu\rho_S + \rho_S A_\mu A^\dagger_\mu))\right)\right], \tag{2.67}$$

and the net heat current

$$\mathcal{J} = \dot{Q}_h + \dot{Q}_c. \tag{2.68}$$

However, in the case of a non-fully resonant interaction between the system's units, external work is inherently required to complete the thermodynamic operations of the device. This required work (work cost) can be deduced from the first law of thermodynamics by :

$$\dot{W} = \frac{d}{dt}\langle H_S\rangle - \sum_\mu \dot{Q}_\mu. \tag{2.69}$$

For the machine to operate at engine speed, heat must flow from the hot bath to the cold bath through the working system. In doing so, the system must produce a certain amount of power. Simply put, the machine's output has to satisfy the following conditions :

$$\dot{W} < 0, \quad \dot{Q}_h > 0 \quad \dot{Q}_c < 0. \tag{2.70}$$

In a refrigeration regime, the system must consume an energy input that allows heat flow from the cold bath to the hot bath through the system. That is

$$\dot{W} > 0, \quad \dot{Q}_h < 0 \quad \dot{Q}_c > 0. \tag{2.71}$$

Despite these differences, the study of heat transport in quantum many-body systems has seen impressive and promising progress over the past two decades. Representative examples include heat transport in atomic, molecular junctions, nanostructures and condensed matter systems. The observation of quantum effects on thermal conductance and thermal rectifiers is an essential tool for improving thermal management in electronic structures.

2.3.3 Self-contained quantum thermal machine

A particular form of quantum thermal machine has recently emerged. These are self-contained quantum thermal machines, designed to operate without any external intervention or driven control. In this type of machine, the device is configured to perform without any work cost until reaching a steady state. In the general framework, a self-contained quantum machine consists of a small number of quantum systems as a working system, including quantum qubits, harmonic oscillators, quantum dots, and multilevel systems, interacting with thermal reservoirs at different temperatures. The key idea behind this concept is that, in parallel with the temperature difference between the thermal baths, the coupling between the elements of the working system must be resonant, such that energy conservation occurs at all possible transitions and the heat transfer is carried out without any input cost. The first law of thermodynamics can be reformulated in this instance as follows :

$$\dot{U} = \sum_i \dot{Q}_i, \tag{2.72}$$

where $\dot{Q}_i$ is the amount of heat exchanged with a thermal bath $\mathcal{R}_i$ and under steady-state conditions, we obtain

$$\sum_i \dot{Q}_i = 0. \tag{2.73}$$

To further clarify the operation of a self-contained thermal machine, let's consider a two-qubit machine similar to the one depicted in Fig.2.4. Each qubit is coupled to a thermal bath at different inverse temperatures, β_1, β_2. The working system can thus be viewed as a composite system of four energy levels, including the ground state $|0\rangle_1 |0\rangle_2$, the most excited level $|1\rangle_1 |1\rangle_2$ and two intermediate levels $|1\rangle_1 |0\rangle_2$ and $|0\rangle_1 |1\rangle_2$ with $0, E_1 + E_2$, E_1 and E_2 their respective eigenenergy values. Note that in this precise regard, we consider $E_2 > E_1$. From this configuration, we can extract a two-level system, engineered from any two-dimensional Hilbert subspace of the composite system, which will be called the machine's virtual qubit. It is characterized by its virtual energy E_v and its virtual temperature T_V, which are in general different from the temperatures of the two thermal baths.

For the convenience of the self-contained quantum thermal machine conception, we rely on the virtual qubit composed of the two intermediate levels

$$|0\rangle_V = |1\rangle_1 |0\rangle_2 \quad \text{and} \quad |1\rangle_V = |0\rangle_1 |1\rangle_2 , \tag{2.74}$$

with virtual energy and virtual inverse temperature

$$E_V = E_2 - E_1 \quad and \quad \beta_V = \frac{1}{E_V} \ln\left(\frac{P_0^V}{P_1^V}\right). \tag{2.75}$$

Here P_0^V and P_1^V are the populations of the ground and excited states of the virtual qubits. In formal consideration, each qubit is assumed to be in thermal equilibrium with its respective reservoir. Then the ratio between the ground state and excited state populations is given by

$$\frac{P_0^V}{P_1^V} = \frac{e^{-E_1/T_1}}{e^{-E_2/T_2}} = e^{-\beta_V E_V}, \tag{2.76}$$

where the inverse temperature of the virtual qubit is expressed in this case as a function of the temperatures and energies of the two machine components,

$$\beta_V = \frac{1}{E_V}\left(\frac{E_2}{T_2} - \frac{E_1}{T_1}\right). \tag{2.77}$$

Furthermore, given the fundamental and excited state populations of the virtual qubit, we consider the normalization of the virtual qubit ,

$$N_V = P_0^V + P_1^V. \tag{2.78}$$

The latter can be seen as a tool for distinguishing between a standard qubit and a virtual qubit. In contrast to the standard qubit, where the sum of the populations is equal to 1, the sum of populations for virtual qubits is generally different from 1, specifically :

$$N_V \leq 1. \tag{2.79}$$

An autonomous quantum thermal machine is achieved by coupling a third body, interacting with a thermal bath, to the virtual qubits via a three-body interaction Hamiltonian of the form

$$H_{int} = g(|0\rangle_1 |1\rangle_2 |0\rangle_3 \langle 1|_1 \langle 0|_2 \langle 1|_3 + |1\rangle_1 |0\rangle_2 |1\rangle_3 \langle 0|_1 \langle 1|_2 \langle 0|_3), \tag{2.80}$$

where g is the interaction constant. More importantly, for the machine to operate autonomously without any loss of information, this interaction must be resonant, i.e.

$$E_3 = E_V. \tag{2.81}$$

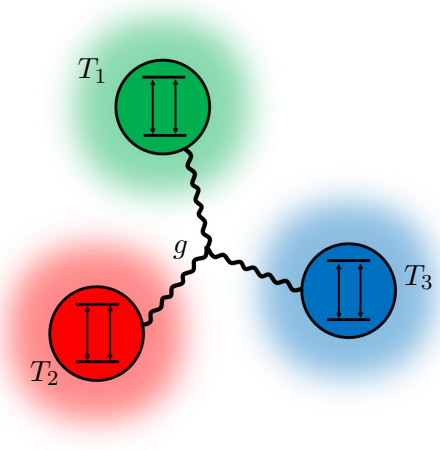

FIGURE 2.5 – Schematic representation of the three-body self-contained quantum thermal machine. Three interacting quantum systems are coupled to three independent thermal reservoirs at different inverse temperatures, β_1, β_2 and β_2. The three bodies are enabled to exchange energy through a resonant interaction Hamiltonian by means of the transition between the two degenerate states $|0\rangle_1 |1\rangle_2 |0\rangle_3$ and $|1\rangle_1 |0\rangle_2 |1\rangle_3$.

Two degenerate states, $|0\rangle_1 |1\rangle_2 |0\rangle_3$ and $|1\rangle_1 |0\rangle_2 |1\rangle_3$, emerge from this energy conservation process, so that transitions between the two levels can be induced without external input :

$$|1\rangle_1 |0\rangle_2 |1\rangle_3 \longleftrightarrow |0\rangle_1 |1\rangle_2 |0\rangle_3 . \tag{2.82}$$

This transition mechanism effectively suppresses excitation in the first and third bodies to generate excitation in the second one and vice versa. Once again, a more appropriate way to describe this process consists of expressing the interaction Hamiltonian in terms of a virtual qubit

$$H_{int} = g(|0\rangle_V |1\rangle_3 \langle 1|_V \langle 0|_3 + |1\rangle_V |0\rangle_3 \langle 0|_V \langle 1|_3), \tag{2.83}$$

describing the interaction between the third system and the virtual qubit on the transitions

$$|0\rangle_V |1\rangle_3 \longleftrightarrow |1\rangle_V |0\rangle_3 . \tag{2.84}$$

With this in mind, the device can operate in two different ways. Firstly, if the virtual temperature is lower than the temperature of the third body $T_3 > T_v$, heat flows from the latter to the virtual qubit, thereby cooling the third system.

2.4 Entropy production

Entropy production stands as a crucial aspect in exploring thermodynamic principles, universally linked to the inherent characteristics of the system's thermodynamic journey. While there's no standardized expression for entropy production in quantum systems, its determination relies closely on the specific conditions of the thermodynamic process and the quantum system in question. Despite this brief overview, understanding the true significance of entropy production remains elusive. The exact definition of this quantity is an ongoing subject of examination and debate in various cases. Currently, the prevailing notion is to perceive entropy production as a key means of guaranteeing the irreversibility of a thermodynamic process.

Let's consider the simplest scenario of an open system $\mathcal{S}$ interacting with a thermal bath $\mathcal{R}$ at an inverse temperature β. Entropy production can be adopted to identify the cohesion of the trajectory followed by the system during the process. In fact, a thermodynamic process is considered irreversible when the entropy production of the system remains positive over time :

$$\dot{\Sigma} := -\frac{d}{dt} S(\rho_{\mathcal{S}}(t) \| \rho_{\mathcal{S}}^{ss}) \geq 0, \tag{2.85}$$

where $S(\rho_{\mathcal{S}}(t) \| \rho_{\mathcal{S}}^{ss})$ is the relative entropy of the total system at time t with respect to its steady state $\rho_{\mathcal{S}}^{ss}$. In particular, for a system evolving according to Markov dynamics,

$$\dot{\rho}_{\mathcal{S}}(t) = \mathcal{E}_t(\rho_{\mathcal{S}}(0)), \tag{2.86}$$

the previous relation is also relevant and can be stated as follows,

$$\begin{aligned} \dot{\Sigma} := -\frac{d}{dt} S(\rho_{\mathcal{S}}(t) \| \rho_{\mathcal{S}}^{ss}) &= -\frac{d}{dt} Tr\left[\rho_{\mathcal{S}}(t) \ln(\rho_{\mathcal{S}}(t)) - \rho_{\mathcal{S}} \ln(\rho_{\mathcal{S}}^{ss})\right] \\ &= -Tr\left[\mathcal{E}_t(\rho_{\mathcal{S}}(0))(\ln(\rho_{\mathcal{S}}(t) - \ln(\rho_{\mathcal{S}}^{ss}))\right] - \frac{d}{dt} Tr\left[\rho_{\mathcal{S}}(t)\right] + Tr\left[\frac{\rho_{\mathcal{S}}(t)\mathcal{E}_{ss}(\rho_{\mathcal{S}}(0))}{\rho_{\mathcal{S}}^{ss}}\right] \\ &= -Tr\left[\mathcal{E}_t(\rho_{\mathcal{S}}(0))(\ln(\rho_{\mathcal{S}}(t)) - \ln(\rho_{\mathcal{S}}^{ss})\right] \geq 0. \end{aligned} \tag{2.87}$$

The inequality (2.87) is commonly known as Spohn's inequality. It is achieved thanks to the trace-preserving of the dynamical maps $\mathcal{E}_t$ and given that the stationary state $\rho_{\mathcal{S}}^{ss}$ satisfies the condition

$$\dot{\rho}_{\mathcal{S}}^{ss} = \mathcal{E}_{ss}(\rho_{\mathcal{S}}(0)) = 0. \tag{2.88}$$

Referring to the general form of the dynamical evolution (1.112), the trace $Tr\left[\mathcal{E}_t(\rho_{\mathcal{S}}(0)) \ln(\rho_{\mathcal{S}}(t))\right]$ can be reduced to

$$Tr\left[\mathcal{E}_t(\rho_{\mathcal{S}}(0)) \ln(\rho_{\mathcal{S}}(t))\right] = Tr\left[\mathcal{L}_{\mathcal{R}}(\rho_{\mathcal{S}}(t)) \ln(\rho_{\mathcal{S}}(t))\right] = -\frac{d}{dt} S(\rho_{\mathcal{S}}(t)). \tag{2.89}$$

For a system coupled to a thermal bath, the steady state is usually a thermal state which can be written in the form of a Gibs state,

$$\rho_S^{ss} = Z^{-1} \exp(-\beta H_S), \tag{2.90}$$

with Z the partition function and β the inverse of the thermal bath temperature. In this case, we have :

$$\begin{aligned} Tr(\mathcal{L}_{\mathcal{R}}(\rho(t)) \ln(\rho_{\mathcal{S}}^{ss})] &= Tr\left[\mathcal{L}_{\mathcal{R}}(\rho_{\mathcal{S}}) \ln \frac{e^{-\beta H_{\mathcal{S}}}}{Z}\right] \\ &= -\beta Tr\left[\mathcal{L}_{\mathcal{R}}(\rho_{\mathcal{S}}) H_{\mathcal{S}}\right]. \end{aligned} \tag{2.91}$$

The following relation can be derived by exporting Eq. (2.85) into the previous expression (2.87)

$$\dot{\Sigma} := \frac{d}{dt} S(t) - \beta \dot{Q}(t) \geq 0. \tag{2.92}$$

Inequality (2.92) provides a new reformulation of the second law of quantum thermodynamics, based on a lower bound on the variation of the system's entropy in a quantum thermodynamic process,

$$\frac{dS(t)}{dt} \geq \beta \dot{Q}(t). \tag{2.93}$$

2.4.1 Entropy in the steady state quantum thermal machine

Referring to the quantum thermal machine models introduced earlier, we assume that the open system $\mathcal{S}$ is coupled to two different thermal baths $\mathcal{R}_h$ and $\mathcal{R}_c$ with their respective inverse temperatures β_h and β_c. The entropy rate $\dot{\Sigma}$ is then given by :

$$\dot{\Sigma} = \frac{d}{dt}S - \beta_c \dot{Q}_c - \beta_h \dot{Q}_h. \tag{2.94}$$

For a sufficiently long period of operation of the machine, a steady state is eventually attained, characterized by the time invariance of the entropy $dS/dt = 0$ and internal $dU/dt = 0$ energy of the system. Consequently, the first term in equation. (2.94) becomes zero, prompting a reformulation of the second law of thermodynamics :

$$\dot{\Sigma} = -\beta_c \dot{Q}_c - \beta_h \dot{Q}_h \geq 0. \tag{2.95}$$

Furthermore, when the work done during operation of the device is equal to zero, entropy production is redefined in accordance with the first law of thermodynamics as follows,

$$\dot{\Sigma} = (\beta_c - \beta_h)\, \dot{Q}_c \geq 0. \tag{2.96}$$

$$\dot{\Sigma} = -(\beta_c - \beta_h)\, \dot{Q}_h \geq 0. \tag{2.97}$$

In essence, this represents the initial Clausius' reformulation of the second law of thermodynamics. When there is a temperature difference between the thermal baths $\beta_c \geq \beta_h$, the positivity of $\dot{\Sigma}$ ensures that $\dot{Q}_c$ is consistently positive while $\dot{Q}_h$ remains negative. Consequently, in the absence of any external input, heat naturally flows from the hotter thermal bath to the colder one.

2.5 Summary

We have formulated the principal thermodynamic parameters characterizing a quantum system's evolution during a thermodynamic operation influenced by thermal reservoirs, from the basic concepts of open quantum system theory. Assuming a weak coupling between the elements of the device, we have established the expression of certain thermodynamic quantities such as heat and work. This description is strongly based on Lindblad's master equation and the principles of the laws of quantum thermodynamics, giving access to distinct representations.

We have conducted a comprehensive analysis of various quantum thermal machines where the variation in the device's internal energy are prominently driven by a temperature difference among the thermal baths. We elucidated the diverse configurations these machines can adopt. Moving from single-body to multi-body machines, we delineated a spectrum of discrete yet interconnected operations inherent to all machines. A notable distinction emerges when considering controllable versus autonomous machines, as well as cyclic versus continuous machines. For each device category, we meticulously identified the spectrum of unconfined variations in the system's internal energy engendered by exchanges with thermal baths or an external control protocol. we meticulously identified the types of variations in the system's internal energy engendered by exchanges with thermal baths or an external control protocol.

Exploring thermodynamics at the level of quantum devices presents several potential extensions. Notably, the advancement of configurations for multi-body quantum devices driven by thermal baths presents a promising direction for further investigation. These devices are anticipated to manifest quantum properties that must be considered in their analysis. Within the realm of multi-body thermal machines, the unavoidable emergence of quantum correlations appears to be a central concern. These properties can wield a substantial influence on system

performance, giving rise to both generic and progressive effects. Furthermore, we have introduced the concept of entropy production during a thermodynamic process, highlighting its intrinsic connection with the laws of thermodynamics.

Chapitre 3

Quantum thermal refrigerator

Once the basic concepts of quantum thermodynamics have been reviewed, it is relevant to delve into a description of common quantum refrigerator designs found in the current scientific literature, which will serve as reference models for our research. The quantum refrigerator stands out as the most common thermal machine, featuring a wide range of one or multi-body designs [21, 112]. As mentioned earlier, these machines are essentially characterized by two cost-efficiency factors : cooling power and coefficient of performance. Additionally, quantum thermal refrigerators display diversity in structure and operation. Distinctions, such as the number of components in multi-body devices or the differences between driven and autonomous machines, are notable examples. Despite this diversity, the primary focus has been on identifying appropriate approaches to control the transport and dissipation of heat flow within these devices, with the overarching goal of improving their power and cooling capacity. Achieving this necessitates meticulous control of the various components, underscoring the imperative for integrated control mechanisms.

From an overview perspective, quantum thermal machines offer novel avenues for exploring both quantum phenomena in many-body systems. Moreover, there are correlations among machine components and thermodynamic principles encompassing heat exchange, work production, energy flow, and more. This convergence of quantum mechanics and thermodynamics poses fresh challenges for understanding many-body system physics. Ideally, a comprehensive depiction of a quantum thermal machine should explicitly incorporate the quantum effects of all working system components, external controls and the requisite resources for device preparation and operation. Thus far, numerous studies have concentrated on developing novel models for quantum thermal machines, including quantum batteries, engines, and refrigerators, alongside efforts to enhance their performance. These endeavors encompass various factors such as machine size, subsystem coupling parameters, and the characteristics of thermal reservoirs. Recent progress has facilitated the establishment of a correspondence between quantum effects and thermodynamic performance in quantum thermal machines, paving the way for experimental studies of thermodynamic devices in the near future. This convergence of theoretical advancements and experimental possibilities holds promise for advancing our understanding of both quantum thermodynamics and practical device engineering.

In this chapter, we propose a thermodynamic description of quantum refrigerator models, which are essentially dependent on non-equilibrium thermal reservoirs and system parameters. We highlight the operational characteristics of these machines and discuss their striking thermodynamic consequences. Furthermore, we introduce the concept of a correspondence between quantum properties and the operation of quantum thermal machines, setting the stage for the subsequent chapters where we will delve deeper into this notion.

3.1 Quantum Otto refrigerator

In the quantum rendition of an Otto cycle, the working system is composed of quantum systems performing operations on the different strokes of the cycle and, of course, subject to the laws of quantum mechanics. In each stroke, the working system undergoes a dynamic evolution over a specific period, during which thermodynamic operations, such as work production or heat transfer, take place. Notably, the Otto quantum cycle is also distinguished from the classical cycle by its isochoric processes, which do not necessarily require complete thermalization. Current investigations continue to explore such instances, employing a limited set of elements as the working system, subject to various external agents acting as control mechanisms [138, 139].

The dynamics of the working system during each stroke is characterized by a quantum dissipator, which accounts for the impact of the external agent in adiabatic processes or the heat exchange with hot and cold reservoirs in isochoric processes. In adiabatic processes, where the system is decoupled from any thermal bath, its evolution follows unitary dynamics, as described by the Liouville-von Neumann equation :

$$\dot{\rho}(t) = -i\left[H_{\mathcal{S}}, \rho(t)\right], \tag{3.1}$$

where $H_{\mathcal{S}}$ and ρ are respectively the Hamiltonian and the density operator of the working system. In the dynamics of hot and cold isochoric processes, the working system becomes an open quantum system that is explicitly influenced by the thermal baths. Its state is then a solution to the master equation :

$$\dot{\rho} = -i\left[H_{\mathcal{S}}, \rho(t)\right] + \mathcal{L}_{\mathcal{R}}(\rho(t)), \tag{3.2}$$

where $\mathcal{L}_{\mathcal{R}}(.)$ represents the dissipative term responsible for driving the working system. It's important to note that under standard operating conditions, thermalization during these isochoric processes is not necessarily complete, as only a finite amount of time is allocated for these processes. Recent advancements have underscored that incomplete or partial thermalization can be advantageous in achieving better performance in cyclic quantum heat devices.

3.1.1 Otto quantum refrigerator based on anisotropic spin-1/2 Heisenberg XYZ chains

Let us consider a model of the Otto quantum refrigerator based on anisotropic spin-1/2 Heisenberg XYZ chains subject to external homogeneous and inhomogeneous magnetic fields with a Dzyaloshinskii-Moriya (DM) interaction [140]. In our approach, we consider a z-axis distribution for both magnetic fields and the DM interaction. The Heisenberg model serves as a fundamental example for exploring the thermodynamic aspects of discrete quantum machines. For convenience, the system is assumed to be influenced by a constant magnetic field acting as an external control agent. The Hamiltonian governing the system is given by :

$$H = \frac{1}{2}\left[J_x\sigma_1^x\sigma_2^x + J_y\sigma_1^y\sigma_2^y + J_z\sigma_1^z\sigma_2^z + (B_z + b_z)\sigma_1^z + (B_z - b_z)\sigma_2^z + D_z(\sigma_1^x\sigma_2^y - \sigma_1^y\sigma_2^x)\right]. \tag{3.3}$$

Here J_x, J_y and J_z are the coupling constants along the x, y, and z-axis respectively, B_z (b_z) represents the homogeneous (inhomogeneous) magnetic fields, D_z is the component of the DM interaction along the z-axis, and $\sigma_i (i = x, y, z)$ are the Pauli matrices,

$$\sigma_x = \begin{pmatrix} 0 & 1 \\ 1 & 0 \end{pmatrix}, \quad \sigma_y = \begin{pmatrix} 0 & -i \\ i & 0 \end{pmatrix}, \quad \sigma_y = \begin{pmatrix} 1 & 0 \\ 0 & -1 \end{pmatrix}. \tag{3.4}$$

Without loss of generality, we consider the standard basis of the four-level composite system $\{|00\rangle, |01\rangle, |10\rangle, |11\rangle\}$ with $|0\rangle$ and $|1\rangle$ being the fundamental and excited states of each two-level

particle. The four energy eigenvalues of the Hamiltonian are derived from Eq.(3.3) as :

$$E_{1,2} = \frac{J_z}{2} \mp \mu \quad , \quad E_{3,4} = \frac{J_z}{2} \mp \nu, \tag{3.5}$$

with $J_{\mp} = (J_x \mp J_y)/2$. The eigenvectors on the standard basis of the four-level composite system $\{|00\rangle, |01\rangle, |10\rangle, |11\rangle\}$ are given by

$$\begin{aligned} |\psi_{1,2}\rangle &= \frac{1}{\sqrt{1 + \frac{(B_z \mp \mu)^2}{J_-^2}}} \left(\frac{B_z \mp \mu}{J_-} |00\rangle + |11\rangle \right), \\ |\psi_{3,4}\rangle &= \frac{1}{\sqrt{1 + \frac{(b_z \mp \nu)^2}{J_+^2 + D_z^2}}} \left(\frac{b_z \mp \nu}{J_+ - iD_z} |01\rangle + |10\rangle \right), \end{aligned} \tag{3.6}$$

where $J\mp = (J_x \mp J_y)/2$, $\mu = \sqrt{B_z^2 + J_-^2}$ and $\nu = \sqrt{b_z^2 + J_+^2 + D_z^2}$. Assumptions include all coupling constants being positive in the antiferromagnetic case, and the condition $J_x > J_y$ is satisfied, ensuring J_- remains positive. Furthermore, to observe the impact of the coupling constants on the system operation, two cases are investigated : $J_\mu(\mu = x, y, z) > 1$ for strong interactions and $J_\mu(\mu = x, y, z) \leq 1$ for weak interactions.

When the working system reaches thermal equilibrium with its environment at the inverse temperature β, its state is characterized by the density operator $\rho_{\mathcal{S}}$ diagonal in the basis provided by the set of eigenvectors $\{|\psi_i\rangle\}_i$,

$$\rho_{\mathcal{S}} = \sum_i p_i |\psi_i\rangle \langle\psi_i| , \tag{3.7}$$

where $p_i = e^{\frac{\beta E_i}{k_B}}/Z$ is the probability of occupation of each state $|\psi_i\rangle$, β is the inverse temperature, k_B is the Boltzmann's constant and Z is the partition function of the system. For simplicity, we reconsider the expression for the density operator $\rho_{\mathcal{S}}$ in the standard basis, taking the form :

$$\rho_{\mathcal{S}} = \frac{1}{Z} \begin{pmatrix} a & 0 & 0 & b \\ 0 & e & f & 0 \\ 0 & f^* & h & 0 \\ b & 0 & 0 & d \end{pmatrix}. \tag{3.8}$$

The different components of the density matrix in equation.(3.8) are expressed as :

$$\begin{aligned} a &= \left[\cosh(\beta\mu) - \frac{B_z}{\mu} \sinh(\beta\mu) \right] e^{-\frac{\beta J_z}{2}}, \\ b &= -\frac{J_-}{\mu} \sinh(\beta\mu) e^{-\frac{\beta J_z}{2}}, \\ d &= \left[\cosh(\beta\mu) + \frac{B_z}{\mu} \sinh(\beta\mu) \right] e^{-\frac{\beta J_z}{2}}, \\ e &= \left[\cosh(\beta\nu) - \frac{b_z}{\nu} \sinh(\beta\nu) \right] e^{\frac{\beta J_z}{2}}, \\ f &= -\frac{J_+ + iD_z}{\nu} \sinh(\beta\nu) e^{\frac{\beta J_z}{2}}, \\ h &= \left[\cosh(\beta\nu) + \frac{b_z}{\nu} \sinh(\beta\nu) \right] e^{\frac{\beta J_z}{2}}. \end{aligned} \tag{3.9}$$

where we assume $k_B = 1$. The partition function Z is given by :

$$Z = 2e^{-\frac{\beta J_z}{2}} \cosh(\beta\mu) + 2e^{\frac{\beta J_z}{2}} \cosh(\beta\nu). \tag{3.10}$$

It's noteworthy that the density matrix $\rho_{\mathcal{S}}$ exhibits only non-zero elements in an "X" formation, along the main diagonal and anti-diagonal, referred to as an X-matrix.

Such a simple setup allows us to clearly appreciate the dependence of the working system's evolution on its parameters. The behavior of the system's components (energy levels and states) is intricately tied to the influence of the magnetic field and the interaction constants of the device. In the absence of a magnetic field ($B_z = 0$), the system's eigenstates reduce to the well-known Bell states, highlighting the profound influence of external factors on the quantum behavior of the system. This observation underscores the versatility of the model in capturing and elucidating various quantum phenomena in the context of thermodynamic processes.

3.1.2 Complete thermalisation

In a complete thermalization cycle, the working system is driven to a thermal state at the end of the two thermalization processes, as illustrated in Fig.3.1. At this stage, the coherence induced during the two unitary evolutions is completely dissipated and the state of the system returns to a diagonal representation on the system basis. In fact, the non-commutativity of the Hamiltonian operator at different instants of the adiabatic processes $\left[H(t), H^{(}t^{'})\right] \neq 0$ allows for the generation of coherence during the unitary evolution without altering the populations of the energetic eigenstates, according to the quantum adiabatic theorem. This coherence is then completely dissipated or not in the thermalization processes, depending on the period of interaction between the system and the thermal bath.

Assuming adequate interaction between the system and the thermal environment in order for the working system to reach an equilibrium thermal state at the end of both thermalization processes. The system's final state can be characterized by a density operator in the Gibs state form, which is diagonal in terms of the energy states :

$$\rho^{th} = \frac{e^{-\beta H}}{Z} = \sum_{i=1}^{4} p_i \left|\psi_i\right\rangle \left\langle\psi_i\right|, \tag{3.11}$$

where

$$p_i = \frac{e^{\beta E_i/k_B}}{Z}, \tag{3.12}$$

is the probability of occupation in each state $|\psi_i\rangle$, β is the inverse temperature of the thermal bath, k_B is Boltzmann's constant, and $Z = Tr\left[e^{-\beta H}\right]$ is the partition function of the system. However, the long interaction criterion is not an absolute requirement. It is possible to interrupt the interaction between the system and the thermal baths after a short period of time, resulting in a final state that retains some coherence.

One may wonder about the state of the model used here at the start of the cycle. Indeed, the dynamics of the system and the variation of its internal energy are dependent on the initial state, for systems governed by equations of motion with determined variables. The choice of initial state is therefore decisive in modeling the operation of the device. Here, we consider that at the beginning of the cycle, the working system is in thermal equilibrium with the reservoir at the inverse hot temperature β_1

$$\rho_0^{th} = \frac{e^{-\beta_1 H_1}}{Z_1} = \sum_{i=1}^{4} p_{i,1} \left|\psi_{i,1}\right\rangle \left\langle\psi_{i,1}\right|, \tag{3.13}$$

with $\beta_1 = 1/k_B T_1$ is the inverse temperature of the hot bath and Z_1 is the partition function.

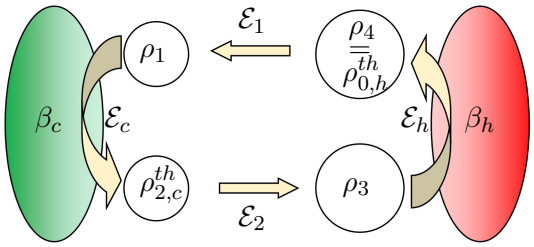

FIGURE 3.1 – Schematic representation of the complete thermalization of Otto's quantum refrigerator. The device consists of a working system interacting in four strokes with two thermal baths placed at two different inverse temperatures β_c and β_h. At the end of the second stroke, which illustrates complete thermalization, the system reaches a thermal state $\rho_{2,c}^{th}$ with the cold bath.

First step : The first stroke is an isentropic compression, with the working substance detached from the hot reservoir to the cold bath. During this step, the energy gaps of the system are compressed from $E_{i,1}$ to $E_{i,2}$. This operation can be described by means of a unitary operator $\mathcal{U}_1$, and the state of the working substance at the end of the stroke simply reads

$$\rho_1 = \mathcal{U}_1 \rho_0^{th} \mathcal{U}_1^\dagger, \tag{3.14}$$

where $\mathcal{U}_1$ satisfies the equation :

$$i\hbar \frac{d}{dt}\mathcal{U}_1 = H_1 \mathcal{U}_1. \tag{3.15}$$

In this step, there is no heat exchange with the reservoirs, while the external drive performs a quantity of work,

$$\begin{aligned} W_1 &= Tr\left[\rho_1 H_2\right] - Tr\left[\rho_0 H_1\right] \\ &= Tr\left[\rho_0 (\mathcal{U}_1^\dagger H_2 \mathcal{U}_1 - H_1)\right]. \end{aligned} \tag{3.16}$$

Second step : The second stroke is an isochoric process in which the Hamiltonian of the working system is kept fixed at H_2. In this step, the working system is put into contact with the cold reservoir at β_2, until reaching an equilibrium thermal state

$$\rho_2^{th} = \frac{e^{-\beta_2 H_2}}{Z_2} = \sum_{i=1}^{4} p_{i,2} \left|\psi_{i,2}\right\rangle \left\langle\psi_{i,2}\right| \tag{3.17}$$

with $\beta_2 = 1/k_B T_2$ and Z_2 the partition function. In this stroke, all the energy changes in the working system are due to the absorption of heat from the cold bath

$$Q_2 = Tr\left[(\rho_{2,2}^{th} - \rho_1) H_2\right]. \tag{3.18}$$

Third step : The third stroke corresponds to an isentropic expansion, where the working substance is again detached from the cold reservoirs to the hot reservoirs. During this

process, the energy gaps of the system are expensed back from $E_{i,2}$ to $E_{i,1}$. This operation can be described by means of a unitary operator $\mathcal{U}_2$, and the state of the working substance at the end of the stroke simply reads

$$\rho_3 = \mathcal{U}_2 \rho_2^{th} \mathcal{U}_2^\dagger, \tag{3.19}$$

where $\mathcal{U}_2$ satisfies the equation :

$$i\hbar \frac{d}{dt}\mathcal{U}_2 = H_2 \mathcal{U}_2. \tag{3.20}$$

In a similar way to the first step, the work required to complete the process is given by

$$\begin{aligned} W_2 &= Tr\left[\rho_3 H_1\right] - Tr\left[\rho_2^{th} H_2\right] \\ &= Tr\left[\rho_2^{th}(\mathcal{U}_2^\dagger H_1 \mathcal{U}_2 - H_2)\right]. \end{aligned} \tag{3.21}$$

*Fourth step :*Finally, the cycle is closed with the fourth stroke, which corresponds to the second isochoric process that takes place at the fixed position of the external control agent. This process allows the system to expand upon contact with the thermal reservoir at the inverse temperature β_1 and return to its initial state

$$\rho_4 = \rho_0^{th}. \tag{3.22}$$

The heat extracted from the system to the hot bath during this last stroke is expressed by

$$Q_1 = Tr\left[(\rho_0^{th} - \rho_3)H_1\right]. \tag{3.23}$$

α) Analytical study

Now we can explore the analytical expressions for the thermodynamic quantities from the information provided in the description so far. Using the previously defined expressions and the form of the Hamiltonian operator, we derive the expressions for the quantities of heat exchanged between the working system and the thermal baths. In the absence of any additional interaction, the heat exchanged with the cold bath is delivered by

$$\begin{aligned} Q_2 = &- J_z\left[\frac{1}{Z_1}e^{-\beta_1 J_z/2}\cosh(\beta_1\mu_1) - \frac{1}{Z_2}e^{-\beta_2 J_z/2}\cosh(\beta_2\mu_2)\right] \\ &+ 2\mu_2\left[\frac{1}{Z_1}e^{-\beta_1 J_z/2}\sinh(\beta_1\mu_1) - \frac{1}{Z_2}e^{-\beta_2 J_z/2}\sinh(\beta_2\mu_2)\right] \\ &+ J_z\left[\frac{1}{Z_1}e^{\beta_1 J_z/2}\cosh(\beta_1\nu_1) - \frac{1}{Z_2}e^{\beta_2 J_z/2}\cosh(\beta_2\nu_2)\right] \\ &+ 2\nu_2\left[\frac{1}{Z_1}e^{\beta_1 J_z/2}\sinh(\beta_1\mu_1) - \frac{1}{Z_2}e^{\beta_2 J_z/2}\sinh(\beta_2\mu_2)\right], \end{aligned} \tag{3.24}$$

where the factors in square brackets correspond to the difference in the population of the system state from the post-thermalization state to the pre-thermalization state with the cold bath.

Similarly, the amount of heat exchanged with the hot bath is such that

$$\begin{aligned} Q_1 =& J_z \left[\frac{1}{Z_1} e^{-\beta_1 J_z/2} \cosh(\beta_1 \mu_1) - \frac{1}{Z_2} e^{-\beta_2 J_z/2} \cosh(\beta_2 \mu_2) \right] \\ & - 2\mu_1 \left[\frac{1}{Z_1} e^{-\beta_1 J_z/2} \sinh(\beta_1 \mu_1) - \frac{1}{Z_2} e^{-\beta_2 J_z/2} \sinh(\beta_2 \mu_2) \right] \\ & - J_z \left[\frac{1}{Z_1} e^{\beta_1 J_z/2} \cosh(\beta_1 \nu_1) - \frac{1}{Z_2} e^{\beta_2 J_z/2} \cosh(\beta_2 \nu_2) \right] \\ & - 2\nu_1 \left[\frac{1}{Z_1} e^{\beta_1 J_z/2} \sinh(\beta_1 \mu_1) - \frac{1}{Z_2} e^{\beta_2 J_z/2} \sinh(\beta_2 \mu_2) \right], \end{aligned} \tag{3.25}$$

where

$$Z_\mu = 2e^{-\frac{\beta_\mu J_{z,\mu}}{2}} \cosh(\beta_\mu \sqrt{B_{z,\mu}^2 + J_{-,\mu}^2}) + 2e^{\frac{\beta_\mu J_{z,\mu}}{2}} \cosh(\beta_\mu J_{+,\mu}), \mu = c, h, \tag{3.26}$$

is the partition function of the system, when it is in thermal equilibrium with a bath at inverse temperature β_μ ($\mu = c, h$). Thus, the description of the energy conversion into work and heat in a cyclic process leads us to deduce the work performed throughout the operation as

$$\begin{aligned} W =& 2(\sqrt{B_{z,c}^2 + J_{-,c}^2} - \sqrt{B_{z,h}^2 + J_{-,h}^2}) \left[\frac{1}{Z_1} e^{-\beta_c \frac{J_z}{2}} \sinh(\beta_c \sqrt{B_{z,c}^2 + J_{-,c}^2}) - \frac{1}{Z_2} e^{-\beta_h \frac{J_z}{2}} \sinh(\beta_h \sqrt{B_{z,h}^2 + J_{-,h}^2}) \right] \\ & + 2(J_{+,c} - J_{+,h}) \left[\frac{1}{Z_c} e^{\beta_c J_{z,c}/2} \sinh(\beta_c J_{+,c}) - \frac{1}{Z_h} e^{\beta_h J_{z,h}/2} \sinh(\beta_h J_{+,h}) \right]. \end{aligned} \tag{3.27}$$

where

$$Z_{(1,2)} = 2e^{-\frac{\beta_{(1,2)} J_z}{2}} \cosh(\beta_{(1,2)} \mu_{(1,2)}) + 2e^{\frac{\beta_{(1,2)} J_z}{2}} \cosh(\beta_{(1,2)} \nu_{(1,2)}), \tag{3.28}$$

with inverse temperatures $\beta = 1/T$. From the first law of thermodynamics, we can deduce the total work performed on the two adiabatic processes,

$$\begin{aligned} W =& 2(\mu_1 - \mu_2) \left[\frac{1}{Z_1} e^{-\beta_1 J_z/2} \sinh(\beta_1 \mu_1) - \frac{1}{Z_2} e^{-\beta_2 J_z/2} \sinh(\beta_2 \mu_2) \right] \\ & + 2(\nu_1 - \nu_2) \left[\frac{1}{Z_1} e^{\beta_1 J_z/2} \sinh(\beta_1 \mu_1) - \frac{1}{Z_2} e^{\beta_2 J_z/2} \sinh(\beta_2 \mu_2) \right]. \end{aligned} \tag{3.29}$$

The coefficient of performance (COP) of the quantum refrigerator is defined as the quotient between the heat absorbed from the cold bath and the work performed along the cycle.

The system's performance in its cooling mode is conditioned by two critical factors : positive work $W > 0$ and cooling power $Q_2 > 0$. The expressions we just defined clearly show that different aspects influence these factors. The work done throughout the cycle is mainly governed by the system parameters, the thermal bath temperatures, and the external magnetic field. It should be noted that the system operates with almost zero work for constant magnetic fields and coupling constants. Prior research has delved into several strategies aimed at optimizing the efficiency of an Otto quantum refrigerator. These strategies include adjusting the degree of interaction among the constituent components of the working system and exploring correlations between these components. This avenue of investigation will undergo more comprehensive scrutiny in subsequent chapters.

β)Effect of homogeneous magnetic field B

On the basis of these analytical expressions, we have investigated the variations in thermodynamic quantities generated during the system's operating process and efficiency. We analyzed

the machine's sensitivity to all the parameters acting during its operation and assessed the extent to which this enables us to control the refrigerator's output. In our analysis, we delve into the general context defined by equation (3.3), considering all system parameters with non-zero values. Our primary objective is to gain a nuanced understanding of the absorbed heat Q_2 and the coefficient of performance (COP) ε under various values of the magnetic fields.

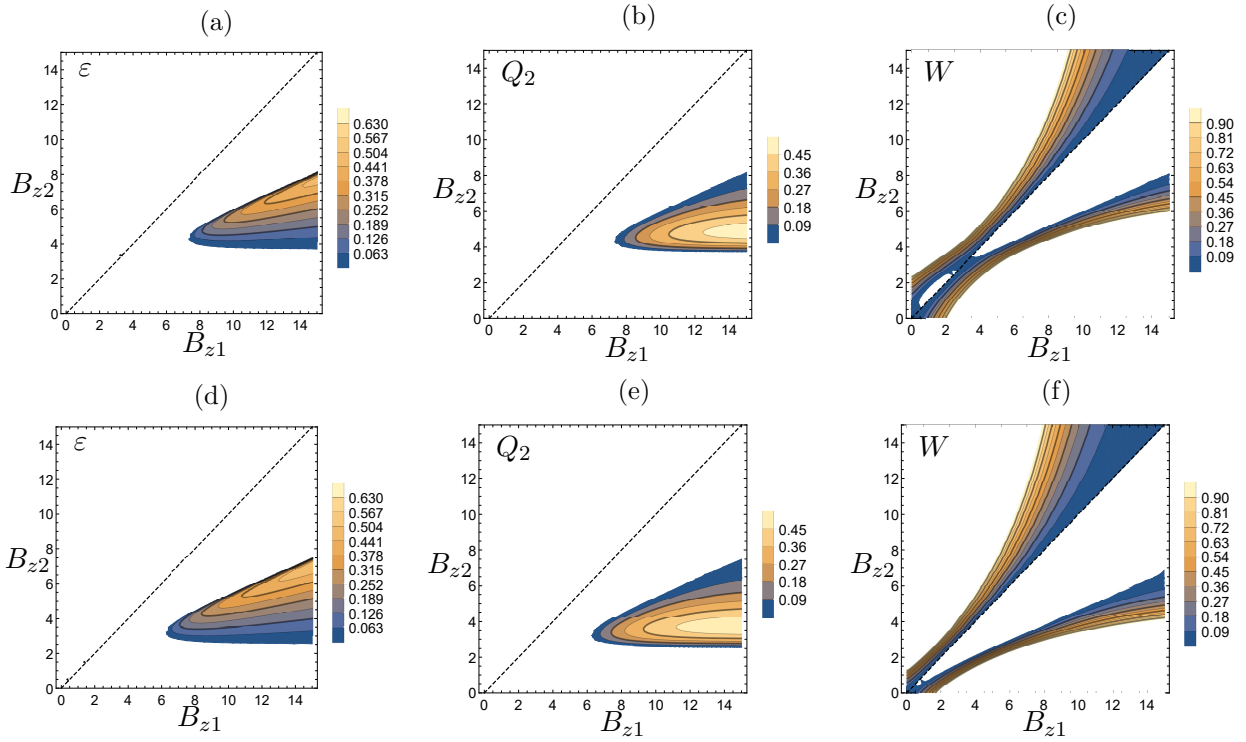

FIGURE 3.2 – The variations in the coefficient of performance (COP) ε, absorbed heat Q_2 and work W are depicted in the first line for the case of strong interaction ($J_x = 2.0$, $J_y = 1.8$, $J_z = 1.6$) and in the second line for weak interaction ($J_x = 0.9$, $J_y = 0.7$, $J_z = 0.5$). The remaining parameters are fixed as follows : $D_z = 1.9$, $b_z = 0.5$, $T_1 = 2.2$, and $T_2 = 0.9$.

In figure. 3.2, where both the inhomogeneous magnetic field and the DM interaction remain constant throughout the cycle, we plot the isolines of Q_2, ε and W, which provide valuable insights into the range of system operation in the cooling regime. It is evident that although there are traces of positive work applied to the system in the two regions ($B_{z_1} < B_{z_2}$ and $B_{z_1} > B_{z_2}$), the isolines for the absorbed heat Q_2 and the COP ε are restricted to the region where $B_{z1} > B_{z2}$. Note that the isolines for both the COP ε and the amount of heat Q_2 do not follow open trajectories, suggesting a non-monotonic evolution. This implies that even within the well-defined productivity region of the machine, achieving better performance depends on a judicious choice of magnetic field values. It is also apparent that variations in the coupling constants do not have a significant effect on the performance of the device. For both weak and strong interaction models, the maximum of Q_2 is capped at $Q_{2\max} \approx 0.45$, while the maximum of ε remains close to $\varepsilon_{\max} \approx 0.63$.

γ) Effect of DM interaction

We then look at the effects of strong DM interactions on the thermodynamic performance of the system. For this purpose, we set the inhomogeneous magnetic field to a constant value $b_z = 3$ and analyze the system's behavior while varying the DM interactions across different values of the homogeneous magnetic fields, considering two sets of coupling constants. The results depicted

in figure. 3.3 unmistakably indicate that the system operates within the cooling regime when $D_{z1} > D_{z2}$. The heat absorption from the cold bath Q_2 is only realized when $D_{z1} > D_{z2}$, specifically when D_{z1} is twice as large as D_{z2}. Furthermore, the TQ isolines are depicted as open lines, illustrating a monotonic increase in COP and Q_2 as we hold D_{z1} fixed and increase D_{z2}. Additionally, we note that the model with weak coupling constants yields superior results in terms of the absorbed heat, $Q_{2\,\max} = 0.22$ (figure.3.3b), compared to $Q_{2\,\max} = 0.045$ for the model with higher coupling constants (figure.3.3c).

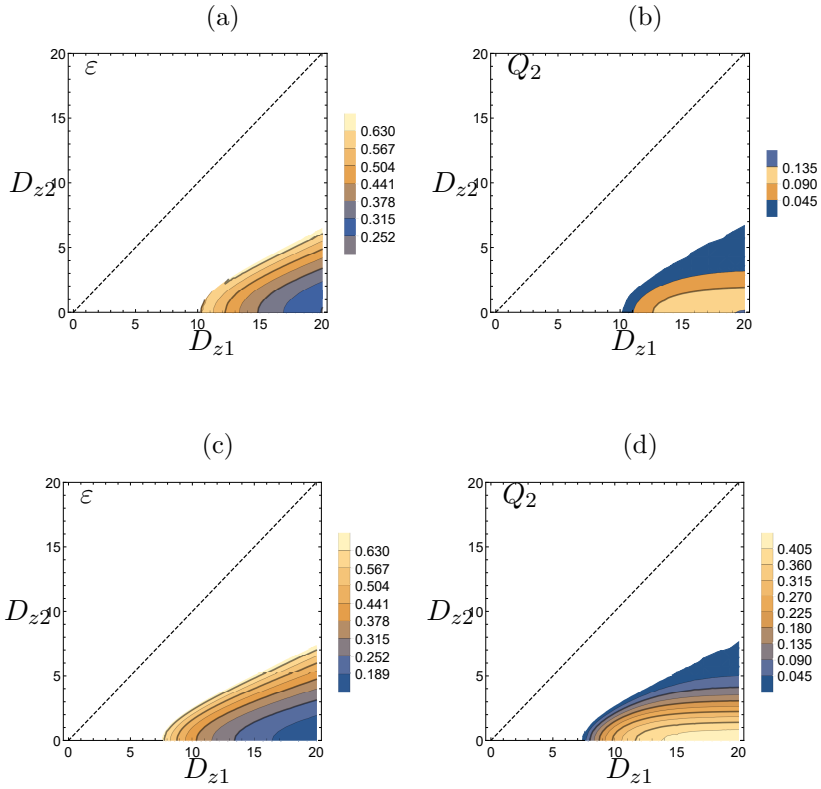

FIGURE 3.3 – Variation of the Variation of the COP ε and the heat flux Q_2, as a function of D_{z1} and D_{z2} with a strong interaction ($J_x = 2.$, $J_y = 1.8$, $J_z = 1.6$) first line and weak interaction ($J_x = 0.9$, $J_y = 0.7$, $J_z = 0.5$) second line($b_z = 3$, $B_{z1} = 3.5$, $B_{z2} = 1.5$, $T_1 = 2.2$ and $T_2 = 0.9$).

3.1.3 Non-complete thermalisation

Up to this point, our discussions have centered around steady-state thermal conditions. However, there exists a class of processes occurring beyond thermal steady states, making them amenable to the theory of open quantum systems dynamical evolution. The formalism of thermal machines, thus, encounters the constraint of time, which means that the formalism must be carefully developed over the whole period of operation. This evolution introduces a dynamic aspect to the analysis, allowing for the consideration of transient effects and time-dependent phenomena.

In our previous analysis of quantum Otto refrigerators, we assumed complete thermalization during the second stroke, ensuring that the working system reaches thermal equilibrium at the end of this stage. This requires the condition $\tau_c \gg \tau_r$ to be satisfied, where τ_c and τ_r represent the thermalization time and relaxation time, respectively, of the working substance interacting with the cold reservoir. During complete thermalization, any coherence established in the first stroke is removed by dissipation effects caused by the thermal bath. It reduces the system's state to a diagonal shape in its energy basis.

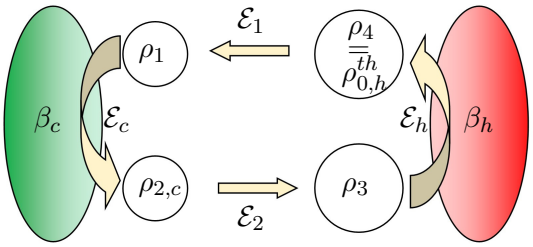

FIGURE 3.4 – Schematic representation of the complete thermalization of Otto's quantum refrigerator. The device consists of a working system interacting in four strokes with two thermal baths placed at two different inverse temperatures, β_c and β_h. At the end of the second stroke, which illustrates incomplete thermalization, state $\rho_{2,c}(t) \neq \rho_{2,c}^{th}$ is not necessarily a thermal state.

Another scenario arises when considering incomplete thermalization during the second stage (Fig.3.4), where a portion of the coherence generated in the first stage is conserved [141, 142]. Incomplete thermalization occurs when the working system interacts with the cold bath for a short time, leaving a thermalization time of the order of the thermal relaxation time $\tau_c \leq \tau_r$. At the end of this stage, the state of the working system differs from the thermal Gibbs state :

$$\mathcal{E}_c \rho_1 \mathcal{E}_c^\dagger = \rho_{2,c}(t) \neq \rho_{2,c}^{th}, \tag{3.30}$$

with $\mathcal{E}_c$ the dissipative operator generating the dynamics induced by the cold bath. It follows that some of the coherence induced in the first stroke can be transferred dynamically to the third stroke. In this way, the thermodynamic behavior of the device becomes dependent on the dynamics of the system's evolution $\rho_{2,c}(t)$, and the time allocated to the different strokes. Specifically, a careful optimization of the thermalization step duration provides a situation where the performance of quantum thermal machines could be controlled. This phenomenon results in part from interference between the residual coherence of the second stage and the coherence generated in the third stage, which in turn can affect the performance of the machine. Recent studies have taken advantage of these observations to improve the performance of certain machines, such as the work performed and the efficiency of Ottot quantum engines. Furthermore, incomplete Otto thermal refrigerators have been proposed thanks to the study of memory effects on the thermodynamic performance of the device and have provided promising results.

3.2 Multi-body continuous quantum refrigerator

Continuous Thermal refrigerators with a sequence of interacting systems are the fundamental prototype of non cyclical systems. In their basic design, each element of the chain is coupled to a thermal bath and, eventually, the heat transfer between the machine components can be driven by a control agent. This configuration is advantageous in terms of detecting heat flows associated with the unit's operation and, as far as possible, the work cost involved in completing the system's operation. Furthermore, they are useful tools for studying a variety of exciting quantum phenomena in the evolution of many-body systems in dissipative baths, including decoherence and quantum correlations.

Many-body quantum thermal machines are good at modeling information flow between reservoirs with non-equilibrium thermal properties. In the context of heat transport, interacting systems are connected to thermal baths at different temperatures. This results in fluctuating

heat flow, which is impacted by device features such as size, coupling constants, and even the degree of connection between device components. Our study will focus on the special case of linear systems driven by their boundary thermal baths. This will be based on an overview of the thermodynamic behavior of the two-qubit thermal refrigerator, which is the most classical form of many-body thermal device. We will describe the thermodynamic phenomena, such as the heat flows involved in the operation of the machine, based on the structure of the components that transport energy, while ensuring compliance with certain crucial aspects, such as the laws of thermodynamics.

Consider a generic system $\mathcal{S}$ coupled to two heat baths at their boundary under different temperatures characterised respectively by the inverse temperatures $\beta_c(cold)$ and $\beta_h(hot)$. The Hamiltonian of the total machine is then described by

$$H = H_{\mathcal{S}} + H_{\mathcal{R}_c} + H_{\mathcal{R}_h} + H_{\mathcal{S}\mathcal{R}_c} + H_{\mathcal{S}\mathcal{R}_h}, \tag{3.31}$$

where $H_{\mathcal{S}}$ is the Hamiltonian of the internal system, $H_{\mathcal{R}_c}$ and $H_{\mathcal{R}_h}$ are the Hamiltonians of the boundary thermal baths labeled cold and hot baths, respectively. $H_{\mathcal{S}\mathcal{R}_\mu}$ represents the Hamiltonian of the interaction between the internal system and a bath $\mathcal{R}_\mu$. So as to model the behavior of non-equilibrium systems even more realistically, we introduce the perspective of considering that the coupling between the elements of the system is weak. In addition, we assume that each transition between the boundary elements is locally and weakly coupled to its respective bath, characterized by a short bath correlation time $\tau_{\mathcal{R}}$ much smaller than the characteristic time scale of the system. Thus, the correlation functions of each bath decay rapidly and memory effects in the reduced dynamics of the system can be neglected. This allows the system dynamics to be described by the standard Markov master equation.(1.112),

$$\dot{\rho}_S(t) = -i\left[H_S, \rho_S(t)\right] + \mathcal{L}_c(\rho_S(t)) + \mathcal{L}_h(\rho_S(t)) \tag{3.32}$$

where $\mathcal{L}_\mu(.)$ is the dissipator atrribute to the thermal baths $\mathcal{R}_\mu$.

3.2.1 Heat current for multi-body systems driven by boundary thermal baths

A further consideration of the system evolution described above can be achieved by granting each thermal bath the ability to interact or not with the system for well-defined periods, through a control protocol. A more illustrative example is the repeated interaction model, where the reservoirs comprise an infinite set of identical systems, and each copy interacts with the system for a set period. The components of the reservoir can be independent, meaning that the state of the system during a period of interaction depends solely on its previous state and the dynamics induced by the copy with which it interacts. Alternatively, they may be correlated, influencing the system's dynamics through correlation effects. While the second case has been widely studied and has shown significant interest in the control and operation of quantum thermal machines, we consider that the reservoir components are not correlated. In this context, the interaction between the system and the reservoir takes the form

$$H_{\mathcal{S}\mathcal{R}_\mu} = k_\mu(t) V_{\mathcal{S}\mathcal{R}_\mu} \tag{3.33}$$

$k_\mu(t)$ is a connection and interruption protocol between the system and the reservoir. For the current set-up, the interaction between the working system and the different reservoirs clearly appears to be time-dependent. Instead of the previous approach using the time-invariant Hamiltonian, this can be used to establish a strongly time-interaction based approach to quantum thermodynamics.

In a slightly different direction, but related to our previous approach, we examine the total system thermodynamic approach. This method allows us to efficiently model quantum thermodynamic networks of finite size. We first need to assess the energy of the total system,

$$U_{tot}(t) = Tr\left[\rho_{tot}(t)H\right], \tag{3.34}$$

with $\rho_{tot}(t)$ the density operator of the total system which evolves under the Liouvil-Von Neumann equation

$$\dot{\rho}_{tot}(t) = -i\left[H, \rho_{tot}(t)\right]. \tag{3.35}$$

Note that in our current examination, we treat the total system as a closed system. From this perspective, the variation in the internal energy of the total system is partitioned into the heat exchanged between the working system and the thermal baths, and the work cost required for dispensing the energy flows. Building upon the earlier definition of work, the work required to operate the device can therefore be given in the sense of the total system state by

$$\begin{aligned} W &= \int_0^t Tr\left[\frac{dH}{dt}\rho_{tot}(t)\right] \\ &= \int_0^t Tr\left[\frac{d}{dt}\left(H_{\mathcal{S}} + H_{\mathcal{SR}}\right)\rho_{tot}(t)\right]. \end{aligned} \tag{3.36}$$

Expression (3.36) is obtained by assuming that the thermal baths are sufficiently large for the Hamiltonian of the environment to be time-invariant. Furthermore, this allows us to physically investigate the work cost defined above as the contribution of two complementary quantities : the first quantity $\int_0^t Tr\left[\frac{d}{dt}\left(H_{\mathcal{S}}\right)\rho_{tot}(t)\right]$ describes the work required to disperse the energy flows among the components of the working system and the second $\int_0^t Tr\left[\frac{d}{dt}\left(H_{\mathcal{SR}}\right)\rho_{tot}(t)\right]$ is the contribution required for the heat exchange between the working system and the thermal baths.

Thanks to the dynamics of the open system, we opt for a reformulation of the quantum work Eq. (3.36) by means of the Liouvil equation $Tr[H\dot{\rho}_{tot}] = 0$,

$$Tr\left[(H_{\mathcal{S}} + H_{\mathcal{SR}}(t))\dot{\rho}_{tot}(t)\right] = -Tr\left[(H_{\mathcal{R}_C} + H_{\mathcal{R}_H}(t))\dot{\rho}_{tot}(t)\right]. \tag{3.37}$$

With the equivalence (3.37), we can illustrate the recovery of the work in the form :

$$\begin{aligned} W &= \int_0^t \frac{d}{dt}Tr\left[(H_{\mathcal{S}} + H_{\mathcal{SR}})\rho_{tot}(t)\right] - Tr\left[(H_{\mathcal{S}} + H_{\mathcal{SR}})\dot{\rho}_{tot}(t)\right] \\ &= \int_0^t \frac{d}{dt}Tr\left[(H_{\mathcal{S}} + H_{\mathcal{SR}}(t))\rho_{tot}(t)\right] - \int_0^t -Tr\left[(H_{\mathcal{R}_C} + H_{\mathcal{R}_H})\dot{\rho}_{tot}(t)\right]. \end{aligned} \tag{3.38}$$

Referring to the expression for the total energy of the system (3.34) and the definition of the variation of the quantity of heat in a system, we show that Eq.(3.38) expresses the first law of thermodynamics in the sense of the total system,

$$\dot{U} = \dot{W}(t) + \dot{Q}(t), \tag{3.39}$$

where $Q = Q_{\mathcal{R}_c} + Q_{\mathcal{R}_h}$ is the variation in average heat at the boundary thermal baths. At the same time, we introduce the expression for the heat change in a thermal bath before and after an interaction,

$$Q_{\mathcal{R}_\mu} = \int_0^t \frac{d}{dt}Tr\left[H_{R_\mu}\dot{\rho}_{tot}(t)\right]. \tag{3.40}$$

This formulation of the second law, adapted to the total system, allows us to conclude that the heat flows in the device can be approximated by the variation of the energy in the thermal baths. Note that, for a resonant coupling between the working system and the thermal baths, the average change in the working system's heat quantity is directly equal to the variation in the thermal baths to which it is coupled.

3.2.2 Two-body

Let's focus here on the case of a two-body linear chain, where our working system comprises two interacting qubits coupled to independent thermal baths. With this setup, we can utilize the earlier formalisms not only to describe the dynamics of the system but also to derive a depiction of the device's thermodynamic properties and traits.

The Hamiltonian of the working system is given in the form :

$$H_S = H_0 + H_I, \tag{3.41}$$

where H_0 is the free hamiltonian of the two systems component and H_I is the interaction part. For the sake of simplicity, we consider the case where the control protocol for the interaction between the working system and the thermal baths takes place during a period τ :

$$H_{SR} = k_c(t)V_{\mathcal{SR}_c} + k_h(t)V_{\mathcal{SR}_h}. \tag{3.42}$$

where $k_\mu(t) \approx \Theta(t)/\sqrt{\tau}$ is a switch on/off protocol between the system and a thermal bath R_μ during a period of interaction τ and $\Theta(t)$ is such that :

$$\Theta(t) = \begin{cases} 1, & \forall t \in [0,\tau] \\ 0, & \forall t \notin [0,\tau] \end{cases}. \tag{3.43}$$

Note that this approach is similar to that introduced in Chapter 1, except that an interaction part with the factor $1/\sqrt{\tau}$ is embedded in the interaction Hamiltonian. This configuration enables the transition to a continuous model in the limit of small τ. Thus, we can write the derivative of the density operator of the system as follows

$$\begin{aligned} \dot{\rho}_{tot}(t) &= \lim_{\tau\to 0} \frac{1}{\tau}\Delta\rho_{tot}(t) \\ &= \lim_{\tau\to 0}\left(-i\left[H,\rho_{tot}\right] - \frac{\tau}{2}\sum_\mu \left[H_{\mathcal{SR}_\mu},\left[H_{\mathcal{SR}_\mu},\rho_{tot}(t)\right]\right]\right), \end{aligned} \tag{3.44}$$

where $\Delta\rho_{tot}(t) = \rho_{tot}(t+\tau) - \rho_{tot}(\tau)$ and $\rho_{tot}(t+\tau)$ is the state of the system after interaction with a thermal bath for a period t. The last equation is an approximation of the second-order master equation in τ where we ignore the second-order and higher-order terms.

From Eq.(3.44), we are now in a position to establish an expression for the thermodynamic quantities. The local heat flux in a thermal bath is defined as the energy produced by the bath during the post- and pre-interaction intervals with the system,

$$\begin{aligned} \dot{Q}_{\mathcal{R}_\mu} &= -\lim_{\tau\to 0}\frac{1}{\tau}Tr\left[H_{\mathcal{R}_\mu}\Delta\rho_{tot}\right] \\ &= \lim_{\tau\to 0}\frac{\tau}{2}k_\mu^2(t)Tr\left[H_{\mathcal{R}_\mu}\left[V_{\mathcal{SR}_\mu},\left[V_{\mathcal{SR}_\mu},\rho_{tot}(t)\right]\right]\right] \\ &= \lim_{\tau\to 0}\frac{\tau}{2}k_\mu^2(t)\langle\left[V_{\mathcal{SR}_\mu},\left[V_{\mathcal{SR}_\mu},H_{\mathcal{R}\mu}\right]\right]\rangle. \end{aligned} \tag{3.45}$$

Note that the latter expression does not systematically and straightforwardly align with the expression $\dot{Q}_\mu = \lim_{\tau\to 0}\tau Tr\left[H_S\mathcal{L}_\mu(\rho(t))\right]$ involving an expectation value of the dissipator $\mathcal{L}_\mu$ applied to the Hamiltonian of the system with $\mathcal{L}_\mu = -\frac{1}{2}k_\mu^2(t)\left[V_{SB_\mu},\left[V_{SB_\mu},V_{SB\mu}\right]\right]$. Unless the interaction between the thermal baths and the system is resonant, additional terms may appear in proportion to the energy difference between the system and the environment. In what follows, we will always consider a situation in which this resonance condition is met, so that $\dot{Q}_\mu = \dot{Q}_{\mathcal{R}_\mu}$.

By defining the rate of change of the internal energy of the system,

$$\dot{U}_{\mathcal{S}} = \lim_{\tau \to 0} \frac{1}{\tau} Tr \left[H_{\mathcal{S}} \Delta \rho_{tot} \right], \tag{3.46}$$

the first law of thermodynamics automatically provides us with a means to express the total power that must be injected or extracted from the working system to operate the device :

$$\begin{aligned} W &= \lim_{\tau \to 0} \frac{1}{\tau} Tr \left[(H_{\mathcal{S}} + H_{\mathcal{R}}) \Delta \rho_{tot} \right] \\ &= -\lim_{\tau \to 0} \frac{1}{\tau} \sum_{\mu = c,h} \frac{k_\mu^2(t)}{2} Tr \left[V_{\mathcal{SR}_\mu}, \left[V_{\mathcal{SR}_\mu}, (H_{\mathcal{S}} + H_{\mathcal{R}}) \right] \right] \rho_{tot}(t) \\ &= -\lim_{\tau \to 0} \frac{k_\mu^2(t)}{2} \sum_{\mu = c,h} Tr \left[V_{\mathcal{SR}_\mu}, \left[V_{\mathcal{SR}_\mu}, H_{\mathcal{S}} + H_{\mathcal{R}_\mu} \right] \right] \rho(t) \\ &\quad -\lim_{\tau \to 0} \frac{k_\mu^2(t)}{2} Tr \left[V_{\mathcal{SR}_\mu}, \left[V_{\mathcal{SR}_\mu}, H_I \right] \right] \rho_{tot}(t). \end{aligned} \tag{3.47}$$

The first term of the work expression in Eq.(3.47) specifies the power required to ensure heat transfer between the system and the thermal baths. It will be practically zero with local conservation of energy, while the second part is attributed to that which ensures exchange between the sub-systems.

3.3 Autonomous quantum refrigerator

Once we have explored our explicit model, it's evident that there are many subtleties associated with the concept of work in quantum thermal systems of finite size. A closer examination of the various modelizations of thermodynamic devices reveals that many of them entail intricate external protocols applied to the systems of interest. Thus, a high degree of control is necessary over the various components of the system to effectively manage the acquisition of energy flows in such a context. Building upon the reflections developed in the previous chapters, our aim now is to investigate more broadly the scenarios in which thermal devices are implemented in a completely closed quantum system.

A finite-size quantum refrigeration system will invariably absorb energy from the cold bath to the hot bath, and this inversion requires additional work to complete the operation. In section 3.2, we tried to tackle this problem with the interesting concept of an additional work input to ensure this operation. In what follows, we will show that a much more elegant and functional solution consists of replacing the work coast with an integrated supplementary system. This technique fulfills a dual function : not only does it supply the machine with additional energy, but it also stabilizes it and maintains its ability to operate autonomously. One explicit method is to adopt Scovil's proposal by substituting the external control agent with a thermal bath, referred to as a working bath, which then becomes an integral component of the device. In this way, each transition between two levels is coupled to a thermal bath, rendering the system independent of any external control.

The operation of the refrigerator follows a simple three-step procedure : first, a quanta of energy E_c is absorbed from the cold bath, taking the system from the state $|0\rangle$ to the state $|1\rangle$; next, a second quanta of energy E_w is absorbed from the working bath, taking the system from the $|1\rangle$ state to the $|2\rangle$ state ; finally, the system returns from state $|2\rangle$ to $|1\rangle$, emitting a quantum of energy E_h into the hot bath. To ensure autonomous operation of the refrigerator, the condition for energy conservation,

$$E_h = E_c + E_w, \tag{3.48}$$

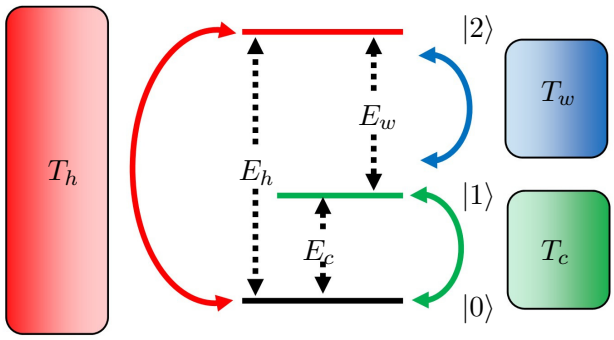

FIGURE 3.5 – Schematic representation of the three-level quantum thermal machine. The working system is a three-level system with energy levels $|0\rangle$, $|1\rangle$ and $|2\rangle$ and populations n_1, n_2 and n_3, respectively. A hot bath with temperature T_h induces transitions between energy levels $|0\rangle$ and $|2\rangle$, while a cold bath with temperature T_c induces transitions between $|0\rangle$ and $|1\rangle$. Work is performed by an external field in resonance with the energy gap $E_w = E_h - E_c$.

must be satisfied.

3.3.1 Dynamique of the system

The total Hamiltonian of the machine is

$$H = H_{\mathcal{S}} + H_{\mathcal{R}} + H_{\mathcal{SR}}, \tag{3.49}$$

where $H_{\mathcal{S}}$ denotes the free Hamiltonian of the system

$$H_{\mathcal{S}} = E_c \left|1\right\rangle \left\langle 1\right| + E_h \left|2\right\rangle \left\langle 2\right|. \tag{3.50}$$

We adopt the notation $E_c = E_1 - E_0$, $E_h = E_2 - E_0$, and $E_w = E_2 - E_1$. The thermal baths $\mathcal{R}_\mu$ is modeled as a family of independent harmonic oscillators,

$$H_{\mathcal{R}_\mu} = \sum_k \Omega_{k,\mu} b_{k,\mu} b_{k,\mu}^\dagger, \tag{3.51}$$

with $b_{k,\mu}(b_{k,\mu}^\dagger)$ the creation (annihilation) operator of mode k with frequency $\Omega_{k,\mu}$, in the bath $\mathcal{R}_\mu = c, h, w$. Each thermal bath is coupled to a specific transition within the system,

$$H_{\mathcal{SR}} = B_c(|0\rangle \langle 1| + |1\rangle \langle 0|) + B_h(|0\rangle \langle 2| + |2\rangle \langle 0|) + B_w(|1\rangle \langle 2| + |2\rangle \langle 1|), \tag{3.52}$$

with

$$B_\mu = \sum_k \lambda_{k,\mu}(b_{k,\mu} + b_{k,\mu}^\dagger), \tag{3.53}$$

are global bath operators. Following the local approach in the weak coupling limit, the dynamics of the reduced density matrix can be derived in the form of a Markovian quantum master equation :

$$\dot{\rho}_{\mathcal{S}} = -\frac{i}{\hbar}\left[H_{\mathcal{S}}, \rho_{\mathcal{S}}(t)\right] + \mathcal{L}_w(\rho_{\mathcal{S}}(t)) + \mathcal{L}_c(\rho(t)) + \mathcal{L}_h(\rho_{\mathcal{S}}(t)) \tag{3.54}$$

The Lindbladian dissipative operators reflect the local effects of thermal baths on each transition of the system to which they are coupled, taking the form :

$$\begin{aligned}
\mathcal{L}_c &= \gamma_{c\downarrow}\Big(\sigma^{01}\rho_{\mathcal{S}}(t)\sigma^{01\dagger} - \frac{1}{2}\{\sigma^{01}\sigma^{01\dagger}, \rho_{\mathcal{S}}(t)\}\Big) + \gamma_{c\uparrow}\Big(\sigma^{01\dagger}\rho_{\mathcal{S}}(t)\sigma^{01} - \frac{1}{2}\{\sigma^{01\dagger}\sigma^{01}, \rho_{\mathcal{S}}(t)\}\Big) \\
\mathcal{L}_h &= \gamma_{h\downarrow}\Big(\sigma^{02}\rho_{\mathcal{S}}(t)\sigma^{02\dagger} - \frac{1}{2}\{\sigma^{02}\sigma^{02\dagger}, \rho_{\mathcal{S}}(t)\}\Big) + \gamma_{h\uparrow}\Big(\sigma^{02\dagger}\rho_{\mathcal{S}}(t)\sigma^{02} - \frac{1}{2}\{\sigma^{02\dagger}\sigma^{02}, \rho_{\mathcal{S}}(t)\}\Big) \\
\mathcal{L}_w &= \gamma_{w\downarrow}\Big(\sigma^{12}\rho_{\mathcal{S}}(t)\sigma^{12\dagger} - \frac{1}{2}\{\sigma^{12}\sigma^{12\dagger}, \rho_{\mathcal{S}}(t)\}\Big) + \gamma_{w\uparrow}\Big(\sigma^{12\dagger}\rho_{\mathcal{S}}(t)\sigma^{12} - \frac{1}{2}\{\sigma^{12\dagger}\sigma^{12\dagger}, \rho_{\mathcal{S}}(t)\}\Big)
\end{aligned} \tag{3.55}$$

3.3.2 Average heat production

From the master equation (3.55), we can deduce the change in the internal energy of the system by :

$$\begin{aligned}
\partial_t\langle H_{\mathcal{S}}\rangle &= Tr(H_{\mathcal{S}}\mathcal{L}_w(\rho_{\mathcal{S}}(t))) + Tr(H_{\mathcal{S}}\mathcal{L}_c(\rho_{\mathcal{S}}(t))) + Tr(H_{\mathcal{S}}\mathcal{L}_h(\rho_{\mathcal{S}}(t))) \\
&= \dot{Q}_w(t) + \dot{Q}_c(t) + \dot{Q}_h(t),
\end{aligned} \tag{3.56}$$

being

$$\dot{Q}_\mu(t) = Tr(H_{\mathcal{S}}\mathcal{L}_\mu(\rho_{\mathcal{S}}(t))), \tag{3.57}$$

the heat exchanged between the thermal bath $\mathcal{R}_\mu$ and the system. In the standard basis, we can express these quantities as :

$$\dot{Q}_c(t) = E_c\left[\gamma_{c\uparrow}(\langle 0|\,\rho_{\mathcal{S}}(t)\,|0\rangle) + \gamma_{c\uparrow}(\langle 1|\,\rho_{\mathcal{S}}(t)\,|1\rangle)\right] \tag{3.58}$$

$$\dot{Q}_w(t) = E_w\left[\gamma_{c\uparrow}(\langle 1|\,\rho_{\mathcal{S}}(t)\,|1\rangle) + \gamma_{c\uparrow}(\langle 2|\,\rho_{\mathcal{S}}(t)\,|2\rangle)\right] \tag{3.59}$$

$$\dot{Q}_h(t) = E_h\left[\gamma_{c\uparrow}(\langle 0|\,\rho_{\mathcal{S}}(t)\,|0\rangle) + \gamma_{c\uparrow}(\langle 2|\,\rho_{\mathcal{S}}(t)\,|2\rangle)\right]. \tag{3.60}$$

In long-term operation, the system reaches a steady-state operation, when ($\dot{\rho} = 0$), the change in internal energy becomes zero, $\partial_t\langle H_S\rangle = 0$, leading to the relation :

$$\dot{Q}_c + \dot{Q}_w + \dot{Q}_h = 0. \tag{3.61}$$

Relation (3.61) represents a form of the first law of thermodynamics for autonomous quantum machines. It does not imply an absence of energy or information flow within the system in a steady state. Rather, it states that the amount of information entering the system equals the amount leaving it, thereby maintaining the system in an invariant state.

For the system to function as a refrigerator, conditions $Q_c \geq 0$, $Q_w > 0$ and $Q_h \leq 0$ must be satisfied, which means that heat circulates through the system from the cold bath to the hot bath accompanied by heat absorbed from the work bath. In the steady-state limit and under the assumption of weak coupling, a necessary condition for meeting these characteristics is :

$$T_W > T_h > T_c. \tag{3.62}$$

By invoking the second law of thermodynamics introduced earlier (2.95), which states that the total rate of heat exchange divided by the respective temperatures of the baths,

$$\sum_{\mu=c,h,w} \dot{Q}_\mu/T_\mu \neq 0, \tag{3.63}$$

we can reformulate the conservation of energy (3.61) as :

$$\dot{Q}_c\left(\frac{1}{T_c} - \frac{1}{T_h}\right) \leq Q_w\left(\frac{1}{T_h} - \frac{1}{T_w}\right). \tag{3.64}$$

Consequently, we can effectively show that the cooling efficiency, which is defined here as the ratio between the cooling power and the heat flow from the hottest reservoir, is bounded by the form :

$$COP = \frac{Q_c}{Q_w} \leq \frac{T_w - T_h}{T_h - T_c}\frac{T_c}{T_h} \simeq \varepsilon_C, \tag{3.65}$$

where ε_C is the Carnot coefficient of performances. In particular, Eq.(3.65) allows us to state a higher bound on the performance of the autonomous quantum refrigerator. However, this approach is limited to the control of a machine's performance as a function of device properties. According to Eqs. (3.65) and (3.58), refrigeration performance can be optimized through the energy differentials E_c, E_w, E_c and the temperatures of the various thermal baths.

3.4 Quantum correlation in thermal machines

So far, we have reported how the models of thermal machines require the involvement of different interacting components, from the working system to the various thermal baths, where dissipation and decoherence processes are more extensive and have a greater impact than in the case of a one-body system [143–146]. This vision of the thermal machine offers a thermodynamic perspective on the quantification of quantum correlations in thermal systems, which proves to be an ideal platform for exploring the close connection between thermodynamic properties and quantum information theory. Two visions emerge : How do quantum properties arise from thermodynamic processes, and how do these properties relate to the parameters of thermodynamic devices ? Do quantum correlations, such as entanglement, offer thermodynamic advantages or obstacles ?

3.4.1 Creation of quantum correlations from a quantum thermal machine

Specific research has been devoted to the generation and control of quantum correlations in thermodynamic processes by means of non-coherent resources. This focus intensifies in non-equilibrium thermal situations where temperature gradients induce energy flows between interacting subsystems. The central element in this framework was long considered to be the work cost required to transfer the flow of energy between the different thermal baths and the components of the working system. Thus, various studies have reported a close correspondence between the work cost and quantum correlation measurable on different thermodynamic device models. A thermodynamic method for quantifying quantum correlations has been developed, exploiting the strong connection between thermodynamic quantities and quantum properties [147, 148]. The key idea in this context is the work cost, defined as the thermodynamic work deficit required to operate a quantum multi-body device in a correlation regime.

Despite this approach, recent studies have highlighted another aspect of quantum correlation. Namely the dependence of quantum correlation on the thermal properties of the machine, such as temperature or degree of energy flow, even with devices that do not require work costs. The generation of steady-state quantum correlations by independent local baths or common baths has been investigated, particularly in the presence of a weak coupling limit. Interestingly, it has been shown that a thermal current is generally required to generate steady-state entanglement between interacting bodies and such entanglement can be effectively controlled by the addition of a common bath. The energy current can therefore be seen as a coherence control resource for interacting qubits coupled to heat baths at different temperatures, and by taking advantage of the temperature gradient, it can be enhanced or suppressed depending on the internal coupling strength between the qubits.

3.4.2 Correlation impact in the thermal machine

Secondly, the effect of quantum correlations in thermodynamic systems has proved extremely valuable for the operation of thermal devices. An in-depth discussion of the involvement of quantum correlations and non-thermal properties in the energy transfer and productivity of quantum thermal machines has been carried out over the years and a great contribution has been made to the impact of quantum effects on the operation of quantum thermal machines in different aspects [149–151]. Despite their richness, the effects of quantum coherence give rise to instances where the thermodynamic performances are either unrelated to the quantum correlations or strongly related to the quantum correlations. In the latter instance, correlation noise in the thermal bath, as well as correlation in the components of the working system, can significantly affect the performance of small quantum thermal machines [152–157].

Among other things, improvements in cooling power or reductions in minimum achievable temperatures in the refrigerator can be achieved in regimes where the machines show correlation compared to the non-correlation regime. This shows the extent to which quantum-regime thermal devices can outperform classical devices, thereby illustrating the value of quantum correlations in such systems. Furthermore, it is worth mentioning the validity of these observations for models with total resonance along all the interaction sites or with partial resonance, with some specific differences, often due to the detuning between the energy gaps of the system components and the interaction constants.

3.5 Summary

We have discussed various models of quantum cooling devices, each evolving according to its intrinsic characteristics under the influence of thermal baths. Due to the diverse nature of these models, different approaches have been employed to analyze the refrigeration behavior of the systems.

For each model, we have delineated the various stages in the dynamics of the working system's evolution, considering the changes in the system's internal energy induced by the dissipative effects of thermal baths and occasionally by a control system. We have explored different methodologies to quantify the required work input necessary to complete the operations of the device, showcasing variations in its expression depending on the specific device under consideration. In the case of a system chain interacting with boundary thermal reservoirs, we have identified two primary contributions to the work cost : the work required for exchanges between the baths and the system, and the work involved in exchanges between different components of the system. Additionally, we examined the case of an autonomous quantum refrigerator, where the device's operation is entirely independent of external input, illustrating a self-contained cooling mechanism.

We then focus on the hypotheses stating the equivalence property between the thermodynamic performance of thermal machines and their quantum properties. This investigation sought to develop two distinct lines of thought, specifically delving into the generation of quantum properties within the evolution of quantum thermal machines. Furthermore, these properties, once generated, can significantly influence the production efficiency of thermal machines. Exploring the implications of these properties for system profitability would be particularly intriguing in this context. Ultimately, our goal is to establish the criteria necessary to ensure that refrigerators operating in the quantum regime achieve enhanced productivity.

Chapitre 4

Coupling of two autonomous quantum refrigerators

Building on the foundations established in the previous chapters, we now turn to the central investigation of this thesis, which revolves around exploring the influence of quantum properties on the behavior of quantum thermal refrigerators. Our investigation unfolds in two interrelated ways : first, understanding how we can ensure the presence of quantum properties in our devices during their operation ; and second, once their presence is established, discerning the influence that the evolution of these properties has on the performance of the machines [158, 159]. This two-pronged approach allows us to understand the interplay between quantum properties and the operational efficiency of quantum refrigerator systems. In the following chapters, we explore the intricate interplay between quantum properties and thermodynamic performance. We focus on unraveling how the presence of these properties can affect crucial aspects of thermal machines, such as cooling power and efficiency.

In this chapter, we focus on examining the steady-state characteristics of the units. Our goal is to compare the thermodynamic performance of each refrigerator to that of an independent unit in a steady state. To do this, we first look at the steady state dynamics of our system. It's important to note that the coherence superpositions of the system states decrease with time due to the decoherence induced by the thermal baths, mainly by dissipative processes. However, it's worth noting that contributions induced by degenerate energy levels can persist [160–166]. Consequently, the steady state of the system can be determined by solving the master equation of the system on the standard basis of the composite system, taking into account its population elements and any residual superpositions that have survived decoherence.

4.1 Three-body model

Consider two autonomous three-body quantum refrigerators, as introduced in Section.2.3.3. When there's no coupling between the two refrigerators, each machine operates by absorbing heat from the cold bath through a resonant three-body interaction :

$$\mathcal{H}_I = g(|1_w 0_h 1_c\rangle \langle 0_w 1_h 0_c| + |0_w 1_h 0_c\rangle \langle 1_w 0_h 1_c|). \tag{4.1}$$

In equation.(4.1), g represents the coupling constant between the components of the machine. The states $|0\rangle \mu$ and $|1\rangle_\mu$ denote the ground state and the excited state of the qubit μ ($\mu = w, h, c$). In this sense, we assume that the virtual qubit comprises the two intermediate states of the cooling machine made by the work and hot qubits : $|0\rangle_v = |1\rangle_h |0\rangle_w$ and $|1\rangle_v = |0\rangle_h |1\rangle_w$ with an energy spacing $E_v = E_h - E_w$ and the inverse of the virtual temperature,

$$\beta_v = \frac{\beta_h E_h - \beta_w E_w}{E_h - E_w}. \tag{4.2}$$

Conservation of energy is achieved through a resonant interaction between the cold qubit and the virtual qubit ($E_v = E_c$). This setup enables the cooling of the cold qubit to a local effective temperatue β_c^* by adjusting the virtual temperature of the machine to a temperature less than β_c ($\beta_v > \beta_c$).

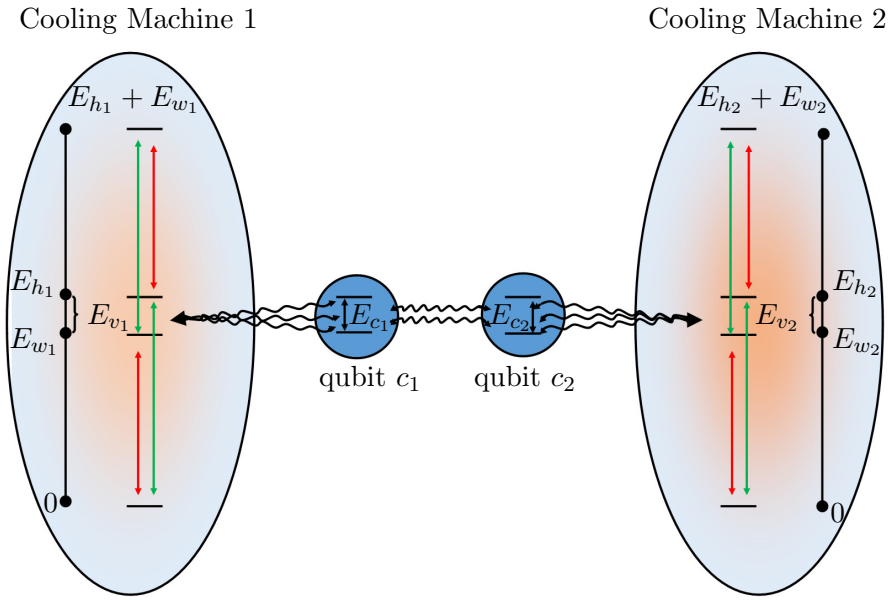

FIGURE 4.1 – An illustration of the energy levels of the composite system. The left and right sections of the figure depict the energy levels of the two cooling machines, while the center focuses on the energy levels of the two objects to be cooled. Dotted arrows represent distinct energy spacings corresponding to E_{h_i} and E_{w_i}, while open labels denote those of the virtual qubits E_{v_i}.

Next, we introduce a coupling of the two refrigerators via their objects to be cooled. This interaction can potentially lead to the generation of a thermal current between the two machines through the two coupled qubits, thus inducing correlation production. The free Hamiltonian of the total system is then given by :

$$\mathcal{H}_{\mathcal{S}} = \sum_{i=1}^{2} (\mathcal{H}_{c_i} + \mathcal{H}_{h_i} + \mathcal{H}_{w_i}) + \mathcal{H}_{int}, \tag{4.3}$$

where each refrigerator is denoted by $i = \{1, 2\}$. The Hamiltonian of each unit is such that $\mathcal{H}\mu_i = E\mu_i \left|1\right\rangle \left\langle 1\right| \mu_i$, and $E\mu_i$ represents the energy spacing of each unit μ_i, satisfying the resonance relations $E_{h_i} = E_{c_i} + E_{w_i}$. The interaction Hamiltonian H_{int} is the collection of three resonant interactions :

$$\begin{aligned} \mathcal{H}_{int} \quad = \quad & g_1(\left|1_{w_1}0_{h_1}1_{c_1}\right\rangle \left\langle 0_{w_1}1_{h_1}0_{c_1}\right| + \left|0_{w_1}1_{h_1}0_{c_1}\right\rangle \left\langle 1_{w_1}0_{h_1}1_{c_1}\right|) \\ & + g_2(\left|1_{w_2}0_{h_2}1_{c_2}\right\rangle \left\langle 0_{w_2}1_{h_2}0_{c_2}\right| + \left|0_{w_2}1_{h_2}0_{c_2}\right\rangle \left\langle 1_{w_2}0_{h_2}1_{c_2}\right|) \\ & + g_3(\left|1_{c_1}0_{c_2}\right\rangle \left\langle 0_{c_1}1_{c_2}\right| + \left|0_{c_1}1_{c_2}\right\rangle \left\langle 1_{c_1}0_{c_2}\right|). \end{aligned} \tag{4.4}$$

The first two lines of equation .(4.4) represent a three-body interaction among the units of each machine, characterized by the coupling constants g_1 and g_2. The third line represents a dipole-dipole interaction of strength g_3 between the two interacting qubits. In addition, we assume that the two cold qubits are identical, $E_{c_1} = E_{c_2} = E_0$, which ensures a resonant interaction without the need for an external system for the operation of the machine.

Furthermore, we establish a difference in the energy spacing of the qubits in the two cooling machines, denoted by :

$$E_d = E_{w_2} - E_{w_1} = E_{h_2} - E_{h_1}. \tag{4.5}$$

While an interaction between two identical machines occurs when $E_d = 0$, we consider the case $E_d \neq 0$ in the rest of this contribution. When the two hot baths and the two work baths are at the same temperature ($\beta_{h_1} = \beta_{h_2}$ and $\beta_{w_1} = \beta_{w_2}$), it is easy to verify that virtual energies and virtual temperatures of both machines are such that $E_{v_2} = E_{v_1} = E_v$ and

$$\beta_{v_2} = \beta_{v_1} + (\beta_h - \beta_w)E_d/E_v. \tag{4.6}$$

The thermal baths are modeled as infinite sets of bosonic modes in thermal equilibrium at the inverse temperature $\beta = 1/kT$ given by the Hamiltonian :

$$\mathcal{H}^{\mathcal{R}^I_{\mu_i}} = \sum_k \Omega_{k,\mu_i} b^\dagger_{k,\mu_i} b_{k,\mu_i}. \tag{4.7}$$

Subsequently, we assume that the two objects to be cooled can be coupled to a common bath $\mathcal{R}_{com}$ (see Fig. (4.2b)), with the Hamiltonian

$$\mathcal{H}^{\mathcal{R}_{com}} = \sum_j \Omega_j a^\dagger_j a_j. \tag{4.8}$$

The operators $b^\dagger_{k,\mu_i}$ and b_{k,μ_i} are creation and annihilation operators for a mode k of the reservoir $\mathcal{H}^{\mathcal{R}^I_{\mu_i}}$. Also, the operators $a^\dagger_j$ and a_j are the creation and annihilation operators for a mode j of the common reservoir.

In the scenario of weak coupling between the system qubits and their respective thermal baths, we can describe the interaction Hamiltonian between the system and the environment using the Rotating Wave Approximation (RWA). This approximation yields :

$$\begin{aligned} \mathcal{H}_{\mathcal{S}\mathcal{R}^I_{\mu_i}} &= \sum_k \lambda_{k,\mu_i}(\sigma^+_{\mu_i} b_{k,\mu_i} + \sigma^-_{\mu_i} b^\dagger_{k,\mu_i}), \\ \mathcal{H}_{\mathcal{S}\mathcal{R}_{com}} &= \sum_j (\lambda_{j,c_1}\sigma^+_{c_1} + \lambda_{j,c2}\sigma^+_{c_2})a_j + (\lambda_{j,c1}\sigma_{c_1} + \lambda_{j,c2}\sigma_{c_2})a^\dagger_j. \end{aligned} \tag{4.9}$$

Here λ_{k,μ_i} denotes the coupling strength between a mode k of an independent bath $\mathcal{R}^I_{\mu_i}$ and a qubit μ_i, while λ_{j,c_1} and λ_{j,c_2} are the coupling strengths between a common bath mode j and the cold qubits c_1 and c_2, respectively.

4.1.1 Master equation

We introduce the master equation governing the dynamic evolution of the density matrix $\rho_\mathcal{S}$ of the total system. We assume a weak and local coupling of each thermal bath to its respective subsystem. This ensures that the effects of the reservoir $\mathcal{R}\mu_i$ on the qubit μ_i do not directly impact the other qubits. Additionally, we consider small couplings between the different nodes of the system, denoted by g_i, where $g_i \ll E_{\mu_i}$. Consequently, the couplings between qubits do not significantly affect the relaxation dynamics of the system and we can approximate the system dynamics with a local standard master equation of the following form :

$$\dot{\rho}_\mathcal{S} = -\frac{i}{\hbar}[\mathcal{H}_S, \rho_\mathcal{S}] + \mathcal{L}(\rho_\mathcal{S}), \tag{4.10}$$

where the Lindblad operator $\mathcal{L}(\rho_\mathcal{S})$ accounts for the dissipative part in the system's dynamics. Considering the influence of each thermal reservoir on the system, this operator is defined in the

(a)

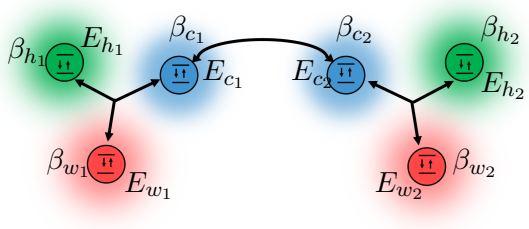

(b)

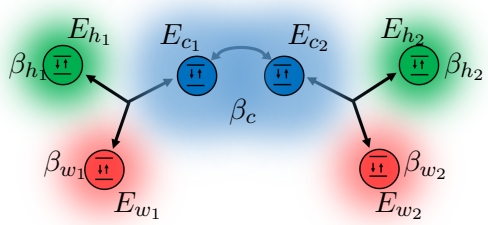

FIGURE 4.2 – Diagram of the interaction between two autonomous quantum refrigerators through their cold qubits. Each refrigerator consists of three qubits - hot, work, and cold - coupled to their respective reservoirs. (a) : The two cold qubits are coupled to two independent baths. (b) : The two cold qubits are coupled to a common bath.

case of independent baths as :

$$\mathcal{L}(\rho_{\mathcal{S}}) = \sum_{\mu=h,c,w} \sum_{i=1}^{2} \mathcal{L}_{\mu_i}(\rho_{\mathcal{S}}), \tag{4.11}$$

with

$$\mathcal{L}_{\mu_i}(\rho_{\mathcal{S}}) = \gamma_{\mu_i\downarrow}(\sigma_{\mu_i}\rho_{\mathcal{S}}\sigma^{\dagger}_{\mu_i} - \frac{1}{2}\{\sigma^{\dagger}_{\mu_i}\sigma_{\mu_i}, \rho_{\mathcal{S}}\}) + \gamma_{\mu_i\uparrow}(\sigma^{\dagger}_{\mu_i}\rho_{\mathcal{S}}\sigma_{\mu_i} - \frac{1}{2}\{\sigma_{\mu_i}\sigma^{\dagger}_{\mu_i}, \rho_{\mathcal{S}}\}). \tag{4.12}$$

In Equation.(4.12), the first and second terms respectively represent the emission and absorption processes of the system due to its interaction with the thermal bath $\mathcal{R}_{\mu_i}$,with damping rates $\gamma_{\mu_i\downarrow} = \gamma_0(\eta_{\mu_i} + 1)$ and $\gamma_{\mu_i\uparrow} = \gamma_0\eta_{\mu_i}$. Here, the mean number of quanta η_{μ_i} in each bath is determined by the Bose-Einstein distribution $\eta_{\mu_i} = (e^{\beta_{\mu_i}E_{\mu_i}} - 1)^{-1}$ and γ_0 represents the spontaneous emission rates.

When the two cold qubits are coupled to a common bath, we derive the expression of the superoperator $\mathcal{L}(\rho_{\mathcal{S}})$ by replacing the dissipative terms of the two cold baths $(\mathcal{L}_{c_1}(\rho_{\mathcal{S}}), \mathcal{L}_{c_2}(\rho_{\mathcal{S}}))$ in the equation (4.11) by $\mathcal{L}_{com}(\rho_{\mathcal{S}}) = \mathcal{L}^1_c(\rho_{\mathcal{S}}) + \mathcal{L}^2_c(\rho_{\mathcal{S}}) + \mathcal{L}^{12}_c(\rho_{\mathcal{S}})$ which represents the effects

due to the interaction between the system and the common bath :

$$\begin{aligned}
\mathcal{L}_c^1(\rho_{\mathcal{S}}) &= \gamma_{c\downarrow}^1(\sigma_{c_1}\rho_{\mathcal{S}}\sigma_{c_1}^\dagger - \frac{1}{2}\{\sigma_{c_1}^\dagger\sigma_{c_1},\rho_{\mathcal{S}}\}) + \gamma_{c\uparrow}^1(\sigma_{c_1}^\dagger\rho_{\mathcal{S}}\sigma_{c_1} - \frac{1}{2}\{\sigma_{c_1}\sigma_{c_1}^\dagger,\rho_{\mathcal{S}}\}),\\
\mathcal{L}_c^2(\rho_{\mathcal{S}}) &= \gamma_{c\downarrow}^2(\sigma_{c_2}\rho_{\mathcal{S}}\sigma_{c_2}^\dagger - \frac{1}{2}\{\sigma_{c_2}^\dagger\sigma_{c_2},\rho_{\mathcal{S}}\}) + \gamma_{c\uparrow}^2(\sigma_{c_2}^\dagger\rho_{\mathcal{S}}\sigma_{c_2} - \frac{1}{2}\{\sigma_{c_2}\sigma_{c_2}^\dagger,\rho_{\mathcal{S}}\}),\\
\mathcal{L}_c^{12}(\rho_{\mathcal{S}}) &= \gamma_{c\downarrow}^{12}(\sigma_{c_1}\rho_{\mathcal{S}}\sigma_{c_2}^\dagger - \frac{1}{2}\{\sigma_{c_1}^\dagger\sigma_{c_2},\rho_{\mathcal{S}}\}) + \gamma_{c\uparrow}^{12}(\sigma_{c_1}^\dagger\rho_{\mathcal{S}}\sigma_{c_2} - \frac{1}{2}\{\sigma_{c_1}\sigma_{c_2}^\dagger,\rho_{\mathcal{S}}\})\\
&\quad +\gamma_{c\downarrow}^{12}(\sigma_{c_2}\rho_{\mathcal{S}}\sigma_{c_1}^\dagger - \frac{1}{2}\{\sigma_{c_2}^\dagger\sigma_{c_1},\rho_{\mathcal{S}}\}) + \gamma_{c\uparrow}^{12}(\sigma_{c_2}^\dagger\rho_{\mathcal{S}}\sigma_{c_1} - \frac{1}{2}\{\sigma_{c_2}\sigma_{c_1}^\dagger,\rho_{\mathcal{S}}\}). \quad (4.13)
\end{aligned}$$

Here, $\mathcal{L}c^1(\rho_{\mathcal{S}}), \mathcal{L}c^2(\rho_{\mathcal{S}})$ represent the individual dissipative effects of the common bath on each cold qubit with rates $\gamma^i c\downarrow$ and $\gamma^i c\uparrow$, where $i = \{1,2\}$. The term $\mathcal{L}c^{12}(\rho_{\mathcal{S}})$ represents an effective effect with rates $\gamma^{12}c\downarrow$ and $\gamma_{c\uparrow}^{12}$. For simplicity, we assume γ_0 to be identical for all emissions throughout this paper.

4.1.2 Thermodynamics quantities

The average heat transferred across the system and each local thermal bath $\mathcal{R}\mu_i$ is given by $\dot{Q}\mu_i = Tr\left[H_{\mathcal{S}}\mathcal{L}\mu_i(\rho)\right]$, where $\mathcal{L}\mu_i$ stands for the dissipation operators introduced in equations (4.13), and $H_{\mathcal{S}}$ is the Hamiltonian of the composite system. Using equation (4.13), we can derive the local average heat exchange between the cold and work reservoirs and the system as follows :

$$\begin{aligned}
\dot{Q}_{w_1} &= E_{w_1}(-\gamma_{w_1\downarrow}\sum_{jklmn}\rho_{1jklmn}^{ss} + \gamma_{w_1\uparrow}\sum_{jklmn}\rho_{0jklmn}^{ss}),\\
\dot{Q}_{w_2} &= E_{w_2}(-\gamma_{w_2\downarrow}\sum_{ijlmn}\rho_{ij1lmn}^{ss} + \gamma_{w_2\uparrow}\sum_{ijlmn}\rho_{ij0lmn}^{ss}),\\
\dot{Q}_{c_1} &= E_0(-\gamma_{c_1\downarrow}\sum_{ijkln}\rho_{ijkl1n}^{ss} + \gamma_{c_1\uparrow}\sum_{ijkln}\rho_{ijkl0n}^{ss}),\\
\dot{Q}_{c_2} &= E_0(-\gamma_{c_2\downarrow}\sum_{ijklm}\rho_{ijklm1}^{ss} + \gamma_{c_2\uparrow}\sum_{ijklm}\rho_{ijklm0}^{ss}), \quad (4.14)
\end{aligned}$$

where the indices i, j, k, l, m, n take values of 0 and 1. If the two cold qubits are coupled to the same bath, the average heat exchange with the common bath is then given by the relation :

$$\begin{aligned}
\dot{Q}_{com} &= E_0\Bigg(-\gamma_{c\downarrow}^1\sum_{ijkln}\rho_{ijkl1n}^{ss} + \gamma_{c\uparrow}^1\sum_{ijkln}\rho_{ijkl0n}^{ss} - \gamma_{c\downarrow}^2\sum_{ijklm}\rho_{ijklm1}^{ss} + \gamma_{c\uparrow}^2\sum_{ijklm}\rho_{ijklm0}^{ss}\\
&\quad +(\gamma_{c\uparrow}^{12} - \gamma_{c\downarrow}^{12})(\sum_{ijkl}\langle ijkl10|\,\rho^{ss}\,|ijkl01\rangle + \sum_{ijkl}\langle ijkl01|\,\rho^{ss}\,|ijkl10\rangle)\Bigg), \quad (4.15)
\end{aligned}$$

which can be written as $\dot{Q}_{com} = \dot{Q}_{c_1} + \dot{Q}_{c_2} + \dot{Q}_{c_{12}}$. Here $\dot{Q}_{c_1}$ and $\dot{Q}_{c_2}$ represent the quantities of heat independently absorbed by each cold qubit from the common reservoir, and $\dot{Q}_{c_{12}}$ is an excessive damping heat flux characteristic of the coupling of the two qubits to the common reservoir. The quantities $\dot{Q}_{c_1}$ and $\dot{Q}_{c_2}$ are the same as those of the separate cold reservoirs, highlighting the enhancement of the cooling power from the common reservoir by the behavior of the effective heat flux $\dot{Q}_{c12}$.

The operation of each refrigerator is evidently influenced by its interaction with the other. Hence, we define the efficiency of each refrigerator as the relative efficiency when the two cold qubits are solely coupled to independent baths, as shown in Fig.(4.2a). Essentially, the relative

efficiency of each refrigerator is determined by the ratio of its cooling power $\dot{Q}_{c_i}$ to the heat flux $\dot{Q}_{w_i}$ of the hottest baths :

$$\eta_i = \frac{\dot{Q}_{c_i}}{\dot{Q}_{w_i}}, \tag{4.16}$$

where $i = \{1, 2\}$ denotes the first and second refrigerator. Alternatively, we introduce a collective efficiency of the global machine for the scenario where the two cold qubits are coupled to a common bath, as illustrated in Fig.(4.2b). It is expressed as the ratio between the cooling power from the common bath and the heat flux of the two hottest baths :

$$\begin{aligned} \eta_{\text{com}} &= \frac{\dot{Q}_{\text{com}}}{\dot{Q}_{w_1} + \dot{Q}_{w_2}} = \frac{\dot{Q}_{c_1} + \dot{Q}_{c_2} + \dot{Q}_{c12}}{\dot{Q}_{w_1} + \dot{Q}_{w_2}} \\ &= \frac{\eta_1 \dot{Q}_{c_1} + \eta_2 \dot{Q}_{c_2}}{\dot{Q}_{w_1} + \dot{Q}_{w_2}} + \frac{\dot{Q}_{c12}}{\dot{Q}_{w_1} + \dot{Q}_{w_2}}. \end{aligned} \tag{4.17}$$

It's important to note that Eq. (4.17) can be simplified to the following form :

$$\eta_{\text{com}} = \tau\eta_1 + (1 - \tau)\eta_2 + \upsilon, \tag{4.18}$$

where $\tau = \dot{Q}w_1/(\dot{Q}w_1 + \dot{Q}w_2) \leq 1$ and $\upsilon = \dot{Q}c_{12}/(\dot{Q}w_1 + \dot{Q}w_2)$. Consequently, we arrive at the following relation :

$$\min(\eta_1, \eta_2) \leq \eta_{\text{com}} \leq \max(\eta_1, \eta_2) + \upsilon, \tag{4.19}$$

highlighting the potential for achieving a collective efficiency greater than $\max \eta_1, \eta_2$ by optimizing the values of τ and ensuring the positivity of the effective efficiency υ.

4.1.3 Steady state entanglement

In addition, we want to study the steady state entanglement in the two cold qubits. This will be crucial for the analysis of the thermodynamic performance of the two refrigerators with respect to their interaction. Starting from the steady state of the total system ρ^{ss} and performing a partial trace over the two refrigerators, we can deduce the steady state density matrix $\rho^{ss}c_1c_2$ of two cold qubits. In the standard basis $|0_{c_1}0_{c_2}\rangle, |0_{c_1}1_{c_2}\rangle, |1_{c_1}0_{c_2}\rangle, |1_{c_1}1_{c_2}\rangle$ the stationary density matrix $\rho^{ss}_{c_1c_2}$ is given in the form :

$$\rho^{ss}_{c_1c_2} = \begin{pmatrix} a & 0 & 0 & 0 \\ 0 & b & c & 0 \\ 0 & d & e & 0 \\ 0 & 0 & 0 & f \end{pmatrix}, \tag{4.20}$$

where the diagonal elements a, b, e, f represent the population of the system, while the off-diagonal elements c, d represent the coherent superposition induced by the inter-qubit interaction [160–162]. Notably, the density matrix $\rho^{ss}_{c_1c_2}$ has a special X-state form. Its concurrence is described by the following relation :

$$\mathcal{C} = 2\max(0, |c| - \sqrt{a * f}), \tag{4.21}$$

where $\mathcal{C} = 0$ implies zero entanglement, while $\mathcal{C} = 1$ denotes maximum entanglement.

4.1.4 Independant baths

Let's consider a scenario where the two cold qubits are coupled to two independent baths, as shown in Figure 4.2a. We study the effect of the cold bath temperature on the operation of the system. The results shown in figure 4.3 indicate that the thermodynamic performance of the two units mirrors that observed in an independent model. Indeed, the cooling capacities of both

refrigerators, as well as their relative efficiencies, show a monotonic increase with temperature T_c. Conversely, as the energy gap E_0 increases, the cooling capacity of the system decreases. These results underscore the inherent relation between the effective temperature of the object to be cooled and its energy gap, a topic that has been extensively discussed in previous literature. In addition, the distribution of performance among the two machines is unequal. We can see from figure 4.3 that the second machine has a higher efficiency compared to the first. This discrepancy suggests that the difference in the energy gaps E_d influences the system performance.

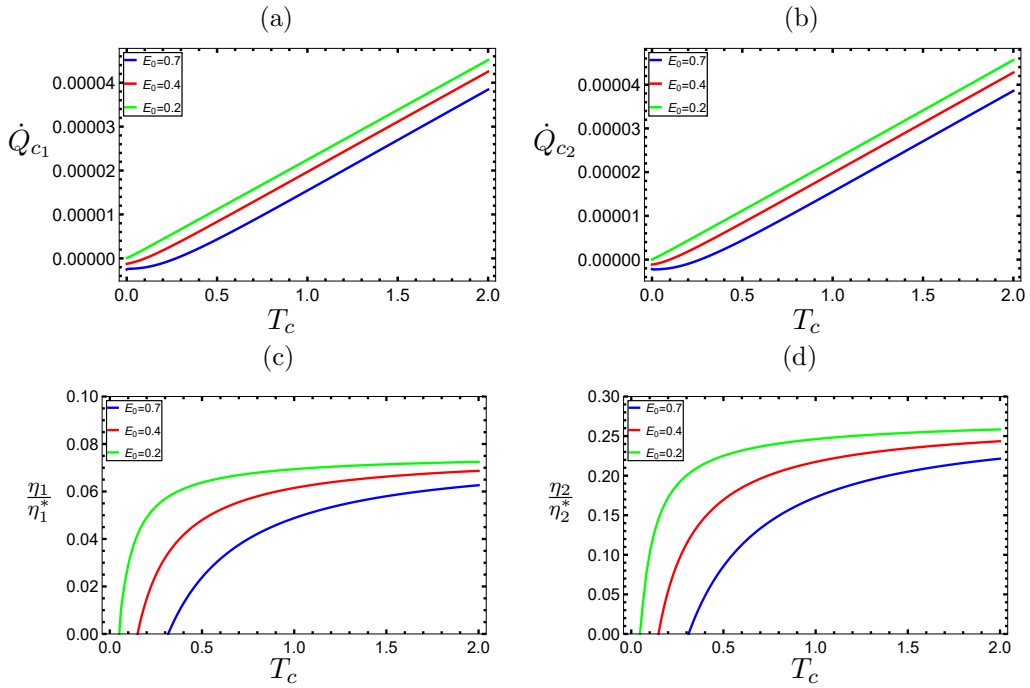

FIGURE 4.3 – Thermodynamic quantities for the case of two independent baths, as a function of the temperature of the cold baths T_c. The first line of Fig.(4.3a-4.3b) shows the ratio $\dot{Q}_{c_1}$, $\dot{Q}_{c_2}$ and the second line of Fig.(4.3c-4.3d), a comparison of the local efficiencies η_1 and η_2 with the Carnot COP of the refrigerators η_i^*. In all plots the other parameters are $\beta_w = 0.02\beta_c, \beta_h = 0.24\beta_c, \gamma_0 = 25 \times 10^{-5}, E_{w_1} = 1., E_d = 0.7, g_1 = g_2 = g_3 = 25 \times 10^{-6}$.

We then analyze in Fig.(4.3) the impact of the difference in energy spacing E_d on the operation of the system. We observe that increasing E_d leads to a reduction in the cooling power of the second refrigerator, while the efficiency shows a monotonic increase with E_d. However, the performance of the first machine does not change significantly. There's a slight enhancement in cooling power and efficiency initially, followed by a decrease for larger values of E_d . It's worth noting that in the absence of coupling, the performance of the first machine should remain unaffected, as any change in E_d would only influence the parameters of the second machine. Therefore, the trends observed in Fig.(4.4) are clear manifestations of the interaction between the two machines. As E_d increases, the discrepancy between the virtual energies of the two machines also increases (see Equation (4.6)), and the dipole-dipole interaction facilitates an energy transfer from the first machine to the second, resulting in alterations in the machines' performance.

4.1.5 Common bath

Next, we explore the scenario where the two cold qubits are connected to a common bath characterized by an inverse temperature β_{com}. This setup is similar to a model with two interacting qubits connected to separate baths with inverse temperatures β_{v_1} and β_{v_2}, which in turn

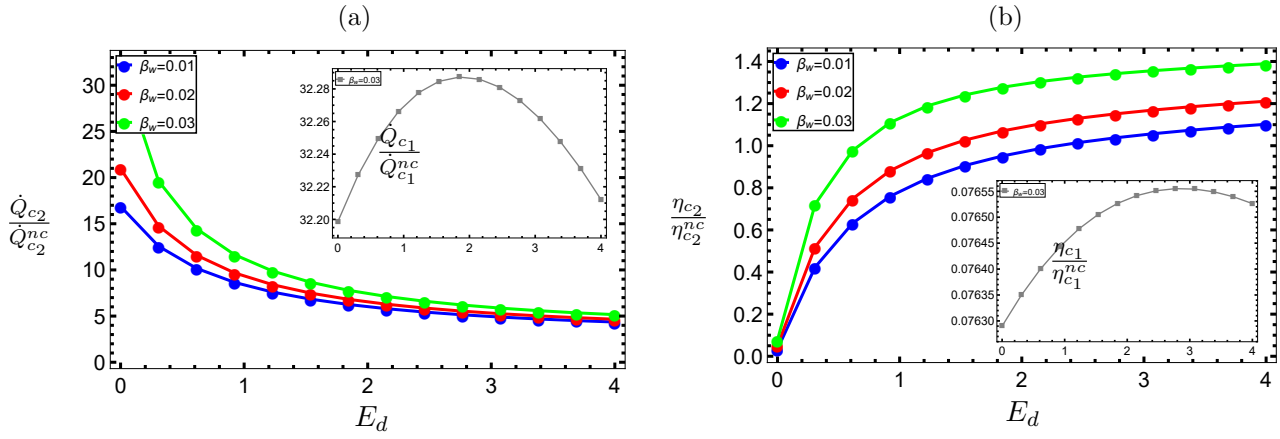

FIGURE 4.4 – A comparison between the system's thermodynamic quantities and those of non-coupled refrigerators with the same parameters, $\dot{Q}_{c_2}/\dot{Q}^{nc}_{c_2}$ and $\eta_{c_2}/\eta^{nc}_{c_2}$, $\dot{Q}_{c_1}/\dot{Q}^{nc}_{c_1}$ and $\eta_{c_2}/\eta^{nc}_{c_2}, \eta_{c_1}/\eta^{nc}_{c_1}$, as a function of E_d for different values of β_w. The other parameters are $\beta_c = 1$, $\beta_h = 0.24\beta_c$, $E_{w_1} = 5.5$, $E_0 = 1$, $\gamma_0 = 25 \times 10^{-5}$, $g_1 = g_2 = g_3 = 25 \times 10^{-6}$.

are connected to a common bath. Three different situations can occur :

When $\beta_{v_1} = \beta_{v_2} = \beta_{\text{com}} = \beta$, there's no observable heat exchange between the common bath and the virtual machines.

In the second scenario, $\beta_{v_1} = \beta_{v_2} \neq \beta_{\text{com}}$, heat transfer is inevitable, and its direction hinges on the temperatures of the various baths.

Finally, when $\beta_{v_1} \neq \beta_{v_2} \neq \beta_{\text{com}}$, besides the heat exchange between the common bath and the virtual machine, there's also an exchange between the two machines.

Starting from the same initial conditions as in the independent case, we investigate how system parameters influence the effective components ($\dot{Q}_{12}$ and ν) of the collective thermodynamic output. It's crucial to note that the results depicted in figures (4.5) don't ensure the positivity of collective performances $(\dot{Q}_{\text{com}}, \eta_{\text{com}})$; rather, they offer a comprehensive view of their trend toward individual performances. Unlike the individual contributions $\dot{Q}_i$, the cooling power $\dot{Q}_{12}$ increases for low temperature values until it reaches a peak before declining for higher T_{com}. Meanwhile, the effective efficiency υ decreases with increasing T_{com}. Moreover, both quantities exhibit an upward trend with increasing E_0. Additionally, we observe that a difference in energy spacing E_d favors an enhancement in the collective system's performance. In Figures (4.5c-4.5d), a monotonic increase in the heat quantity $\dot{Q}_{12}$ and the effective efficiency υ is evident with increasing E_d.

4.1.6 Steady-state entanglement

Utilizing the expression established in Eq. (4.21), we conduct a numerical exploration of the steady-state entanglement of the two cold qubits. The results observed in Fig.(4.6a) depict an increase in entanglement concurrently with E_d and E_0. This trend inversely correlates with the evolution of the cooling performances, which decrease with increasing E_d and E_0. This observation can be justified from two perspectives : Firstly, the increase in the difference between the two virtual temperatures (via E_d) regulates heat transfer between the two machines via the coupled qubit. Secondly, the cold reservoirs act as a heat source on the coupled qubits, affecting their effective temperatures. To elaborate on the latter scenario, we examine in Fig.

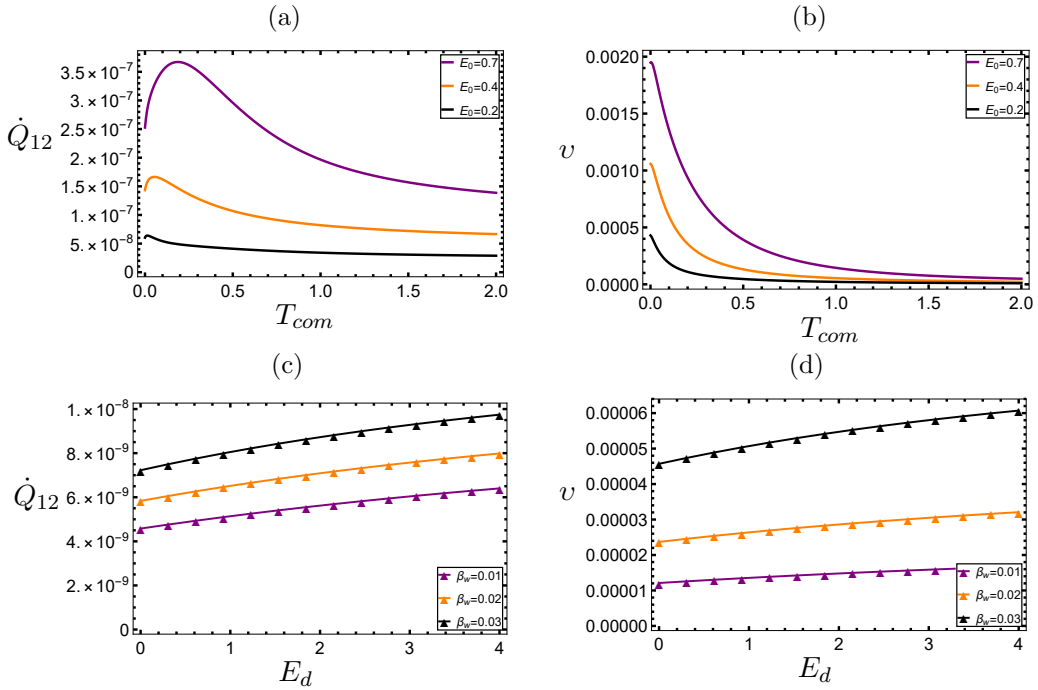

FIGURE 4.5 – Evolution of the effective part $\dot{Q}_{12}$ of the collective cooling power $\dot{Q}_{com}$ and the term υ of the collective efficiency η_{com} as a function of the temperature T_{com} for $\beta_w = 0, 02\beta_{com}$, $\beta_h = 0, 24\beta_{com}$, $E_{w_1} = 1$, $E_d = 0.7$, $\gamma_0 = 25\times10^{-5}$, $g_1 = g_2 = g_3 = 25\times10^{-6}$, on the first line and of the difference in the energy spacing E_d for $\beta_h = 0, 24\beta_{com}$, $E_{w_1} = 5.5$, $E_0 = 1$,$\gamma_0 = 25\times10^{-5}$, $g_1 = g_2 = g_3 = 25\times10^{-6}$ on the second line.

(4.6b) how the temperature $T_c = 1/\beta_c$ of the two cold baths impacts the evolution of steady-state entanglement. Notably, it emerges that large values of temperature T_c deteriorate the generation of thermal entanglement. Specifically, the results in Fig. (4.6b) reveal an entanglement that initially increases with temperature until reaching a maximum value at a critical temperature (threshold temperature). Subsequently, it decreases and eventually disappears for large values of T_c.

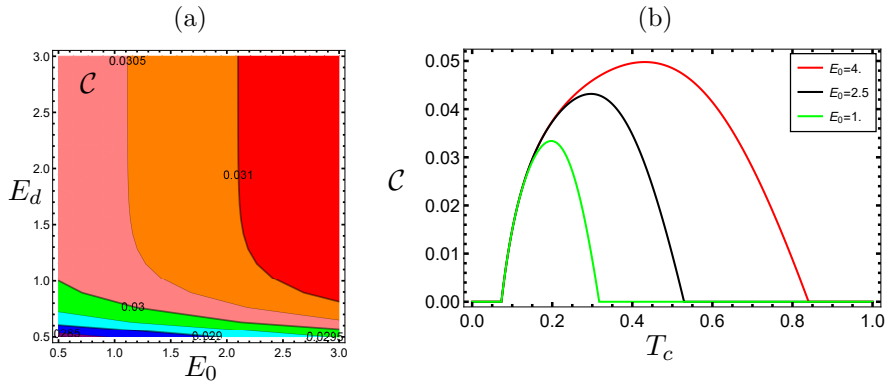

FIGURE 4.6 – Steady state concurrence $\mathcal{C}$, as function of the difference in the energy E_d and energy spacing E_0 (Fig. (4.6a)) with ($\beta_c = 7$,$\beta_w = 0.02\beta_c$, $\beta_h = 0.24\beta_c$, $E_{w_1} = 6$, $\gamma_0 = 12\times10^{-5}$, $g_1 = g_2 = g_3 = 35\times10^{-6}$) and Fig. (4.6b) according to the temperature the two cold baths temperature T_c with the rest of the parameters $E_{w_1} = 6.5$, $\beta_w = 0.02\beta_c$, $\beta_h = 0.24\beta_c$, $E_d = 1$, $\gamma_0 = 10^{-4}$, $g_1 = g_2 = g_3 = 45\times10^{-6}$

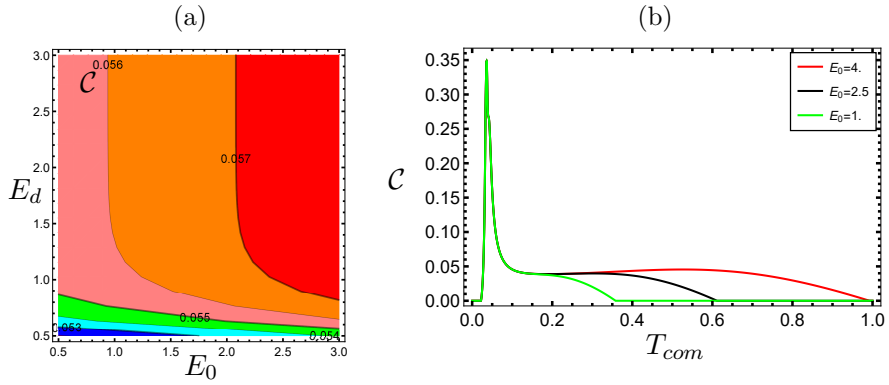

FIGURE 4.7 – Steady state concurrence $\mathcal{C}$, Fig. (4.7a) as function the difference in the energy spacing E_d and energy spacing E_0 with ($\beta_{com} = 7$, $\beta_w = 0.02\beta_{com}$, $\beta_h = 0.24\beta_{com}$, $E_{w_1} = 6$, $\gamma_0 = 12 \times 10^{-5}$, $g_1 = g_2 = g_3 = 35 \times 10^{-6}$) and Fig. (4.7b) as function of the common bath's temperature with the rest of the parameters $E_{w_1} = 6.5$, $\beta_w = 0.02\beta_{com}$, $\beta_h = 0.24\beta_{com}$, $E_d = 1$, $\gamma_0 = 10^{-4}$, $g_1 = g_2 = g_3 = 45 \times 10^{-6}$

Second, we investigate the steady-state entanglement under the scenario of a common thermal bath. While the variation of the entanglement resembles that observed with two independent baths, intriguing results emerge in Fig.(4.7) when we plot the steady-state entanglement $\mathcal{C}$ over the difference between the energy spacing E_d and E_c (Fig.(4.7a)) or over the temperature of the common bath (Fig. (4.7b)). Employing the same system parameters as in the case of two independent baths, we observe an amplification of the entanglement values in both cases studied. This improvement stems from the second role of the common bath : besides the dipole-dipole interaction, the shared bath can act as a physical resource for generating thermal entanglement through its effective influence on the two coupled qubits [167, 168].

4.1.7 Quantum thermodynamic quantities versus entanglement

To deepen our understanding of the inverse correlation between the thermal entanglement of our devices and their cooling ability, we examine the dependence of the thermodynamic properties of the system on the degree of entanglement. Figures (4.8) to (4.9) show the variation of the cooling power and efficiency of the system with respect to the entanglement ($\mathcal{C}$) at different cold bath temperatures.

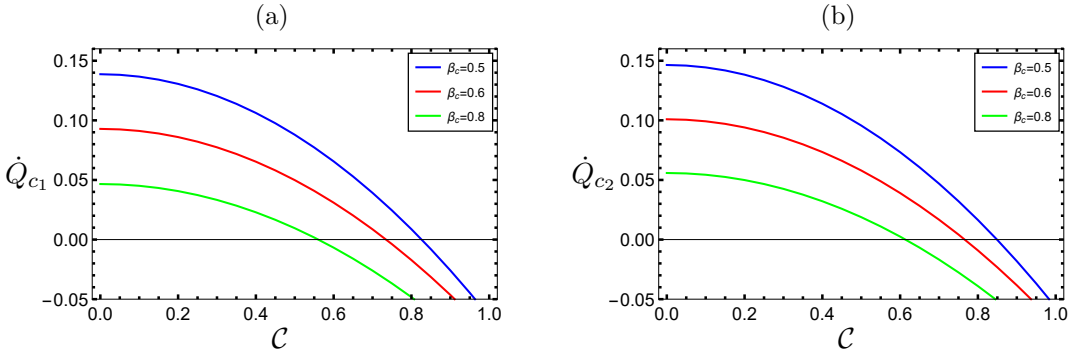

FIGURE 4.8 – Plot of the cooling powers $\dot{Q}_{c_1}$ and $\dot{Q}_{c_2}$ versus the thermal entanglement $\mathcal{C}$ for different values of the inverse temperature β_c. The rest of parameters are : $E_{w_1} = 5$, $\beta_w = 0.02\beta_c$, $\beta_h = 0.24\beta_c$, $E_d = 0.2$, $E_0 = 1.1$, $\gamma_0 = 0.075$, $g_1 = g_2 = g_3 = 0.00025$.

In Figure (4.8) we plot the evolution of the cooling powers $\dot{Q}c_1$ and $\dot{Q}c_2$ with respect to the entanglement $\mathcal{C}$, assuming two independent heat baths and different values of β_c. Since the

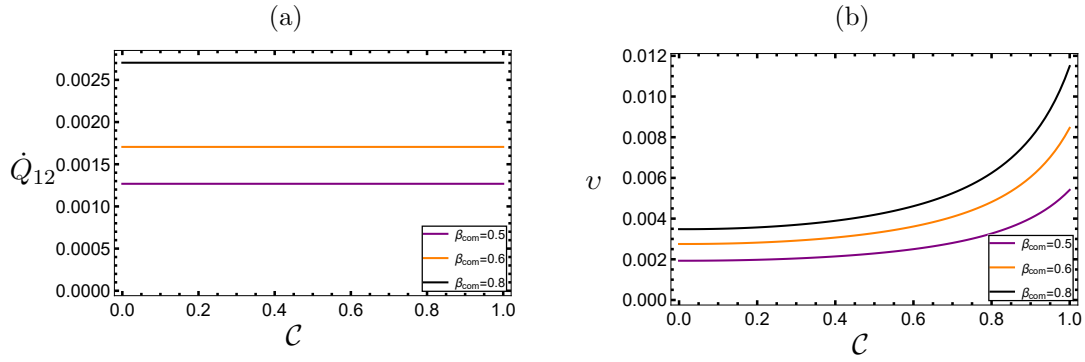

FIGURE 4.9 – Plot of the cooling power $\dot{Q}_{12}$ and effectiveive efficiency υ versus the thermal entanglement $\mathcal{C}$ for different values of β_{com}. The rest of parameters are : $E_{w_1} = 5$, $\beta_w = 0.02\beta_{com}$, $\beta_h = 0.24\beta_{com}$, $E_d = 0.2$, $E_0 = 1.1$, $\gamma_0 = 0.075$, $g_1 = g_2 = g_3 = 0.00025$.

efficiencies closely mirror the trends observed for the heat fluxes, we omit their presentation. From Figure (4.8), we can see a decrease in the cooling power of the coupled devices with increasing entanglement between the qubits. At zero entanglement, $\dot{Q}c_1$ and $\dot{Q}c_2$ peak before decreasing as entanglement increases, eventually reaching zero at high entanglement levels. This behavior suggests that the system transfers heat to the cold reservoirs as the qubits become more entangled.

Conversely, in Figure (4.9), we find that entanglement positively influences the effective performance of the system in the case of a common bath. While the relative cooling power $\dot{Q}_{12}$ remains constant with entanglement, the effective efficiency υ shows a consistent increase with entanglement, peaking at maximum entanglement. In essence, as the cold qubits become more entangled, less heat is absorbed by the working baths. These results suggest that highly entangled qubits facilitate heat transfer between the machines via dipole-dipole interaction, albeit at the expense of cooling efficiency.

4.2 Two-body model

In our previous investigation, we discovered that coupling two distinct refrigerators tends to diminish their cooling efficacy. However, as the configuration shifts towards coupling two identical refrigerators, this reduction gradually improves. To delve deeper into this phenomenon, we turn our attention to a scenario involving two identical autonomous quantum refrigerators. Each device is structured based on the smallest autonomous quantum thermal machine outlined in Section 3.3. When we refer to "identical machines," we specifically mean that the three-level systems and qubits of the two devices share identical distributions of energy level values, while their thermal reservoirs may exhibit different temperature values.

The model's Hamiltonian is composed of three main terms :

$$H = H_{\mathcal{S}} + H_{\mathcal{R}} + H_{\mathcal{SR}}, \tag{4.22}$$

where $H_{\mathcal{S}}$ represents the Hamiltonian of the composite system, encompassing the independent Hamiltonians of the two machines $H_{M_{1(2)}} = E_h \left|2\right\rangle \left\langle 2\right|_{1(2)} + E_c \left|1\right\rangle \left\langle 1\right|_{1(2)}$,as well as the Hamiltonians of the two systems to be cooled $H_{c_{1(2)}} = E_c \left|e\right\rangle \left\langle e\right|_{1(2)}$and the interaction among the system components :

$$\begin{aligned} H_{int} &= g_1 \left(\sigma_1^+ \left|0\right\rangle \left\langle 1\right|_1 + \sigma_1 \left|1\right\rangle \left\langle 0\right|_1\right) \\ &+ g_2 \left(\sigma_2^+ \left|0\right\rangle \left\langle 1\right|_2 + \sigma_2 \left|1\right\rangle \left\langle 0\right|_2\right) \\ &+ \alpha \left(\sigma_1^+ \sigma_2 + \sigma_1 \sigma_2^+\right). \end{aligned} \tag{4.23}$$

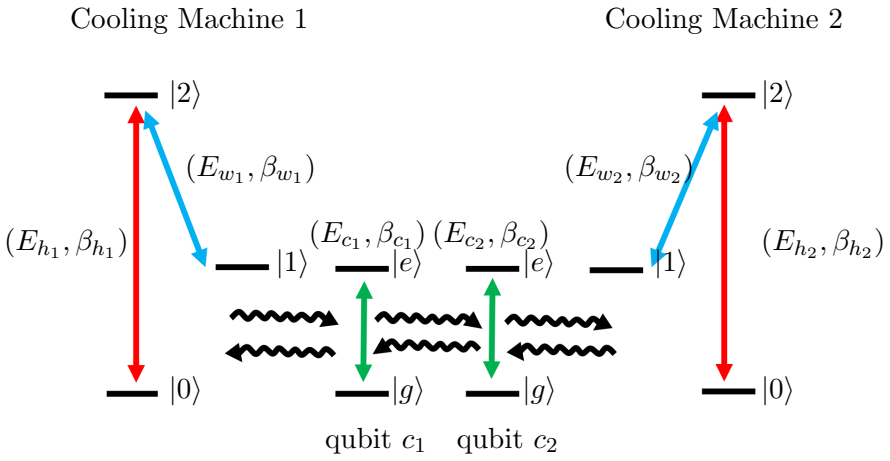

FIGURE 4.10 – Schematic representation illustrating the coupling between two autonomous quantum refrigerators. Each refrigerator consists of a three-level system connected to two reservoirs : the hot bath and the work bath. Additionally, each refrigerator interacts with a qubit, which in turn is coupled to a cold bath. The two machines are connected via a resonant interaction between the two cold qubits, enabling the transfer of energy between the devices.

Here, $\sigma_{1(2)} = |g\rangle\langle e|_{1(2)}$ denotes the lowering operator of the first (second) qubit, $g_{1(2)}$ are the interaction constants between the first (second) cooling machine and its respective system to be cooled, and α signifies the interaction between the two machines via the two cold qubits. Furthermore, each reservoir is modeled as an infinite collection of non-interacting harmonic oscillators, characterized by the Hamiltonian :

$$H_{\mathcal{R}_{\mu_i}} = \sum_k \Omega_{k,\mu_i} b^\dagger_{k,\mu_i} b_{k,\mu_i}, \tag{4.24}$$

where $\mu = \{w, h, c\}$ respectively denote the working, hot, and cold baths coupled to various transitions between a pair of two levels in each refrigerator, and $i = 1, 2$ represents the first or second machine. The bosonic mode operators in Eq.(4.24), are the annihilation and creation operators for a mode k of frequency Ω_k, satisfying the commutation relations $[b_{k,\mu}, b^\dagger_{k',\mu'}] = \delta_{kk'}\delta_{\mu\mu'}$ and $[b_{k,\mu}, b_{k',\mu'}] = 0$. Additionally, we assume weak and local coupling of each transition with its respective bath, characterized by a short bath correlation time τ_{μ_i} much smaller than the system's characteristic time scale. This assumption ensures rapid decay of the correlation function of each bath, allowing us to neglect memory effects in the reduced system dynamics. The system-bath interaction Hamiltonian is then given by :

$$H_{\mathcal{SR}} = \sum_{i=1}^{2} B_{c_i}\left(|e\rangle\langle g|_i + |g\rangle\langle e|_i\right) + B_{h_i}\left(|2\rangle\langle 0|_i + |0\rangle\langle 2|_i\right) + B_{w_i}\left(|2\rangle\langle 1|_i + |1\rangle\langle 2|_i\right), \tag{4.25}$$

with $B_{\mu_i} = \sum_k \lambda_{k,\mu_i}(b_{k,\mu_i} + b^\dagger_{k,\mu_i})$, $\mu = \{w, h, c\}$ $i = 1, 2$ are global operators acting on the Hilbert space of the bath $\mathcal{R}_{\mu_i}$.

4.2.1 Master equation

Starting from our previous assumptions, we derive the master equation governing the dynamics of the system :

$$\dot{\rho} = -i\left[H_{\mathcal{S}}, \rho\right] + \sum_{i=1}^{2} \mathcal{L}_{M_i}(\rho) + \mathcal{L}_{c_i}(\rho), \tag{4.26}$$

where the dissipative operators account for the effects of the cold baths on the system :

$$\mathcal{L}_{c_i}(\rho_m) = \gamma_{i\downarrow}(\sigma_i\rho_m\sigma_i^\dagger - \frac{1}{2}\{\sigma_i^\dagger\sigma_i, \rho_m\}) + \gamma_{i\uparrow}(\sigma_i^\dagger\rho_m\sigma_i - \frac{1}{2}\{\sigma_i\sigma_i^\dagger, \rho_m\}). \tag{4.27}$$

The operators characterizing the dissipative effect of the work and hot baths on the system are given by :

$$\begin{aligned}\mathcal{L}_{M_i}(\rho) &= \mathcal{L}_{h_i}(\rho) + \mathcal{L}_{w_i}(\rho) \\ &= \gamma_{h_i\downarrow}(\sigma_i^{02}\rho\sigma_i^{02\dagger} - \frac{1}{2}\{\sigma_i^{02\dagger}\sigma_i^{02}, \rho\}) + \gamma_{h_i\uparrow}(\sigma_i^{02\dagger}\rho\sigma_i^{02} - \frac{1}{2}\{\sigma_i^{02}\sigma_i^{02\dagger}, \rho\}) \\ &+ \gamma_{w_i\downarrow}(\sigma_i^{12}\rho\sigma_i^{12\dagger} - \frac{1}{2}\{\sigma_i^{12\dagger}\sigma_i^{12}, \rho\}) + \gamma_{h_i\uparrow}(\sigma_i^{12\dagger}\rho\sigma_i^{12} - \frac{1}{2}\{\sigma_i^{12}\sigma_i^{12\dagger}, \rho\}),\end{aligned} \tag{4.28}$$

where $\sigma_i = |g\rangle\langle e|\, i$ is a lowering operator representing a transition between the energy levels of the qubits, $\sigma_i |e\rangle\, i = |g\rangle\, i$. Similarly, we introduce the operators $\sigma i^{02} = |0\rangle\langle 2|\, i$ and $\sigma i^{12} = |1\rangle\langle 2|\, i$, representing transitions between the levels $|0\rangle$ and $|2\rangle$ and between $|1\rangle$ and $|2\rangle$ of each cooling machine, respectively. The rates in Eqs. (4.27) and (4.28) are given by :

$$\begin{aligned}\gamma_{\mu_i\downarrow} &= \gamma_0(\eta th^{\mu_i} + 1), \\ \gamma_{\mu_i\uparrow} &= \gamma_0\eta_{th}^{\mu_i},\end{aligned} \tag{4.29}$$

where $\eta_{th}^{\mu_i} = (e^{\beta_{\mu_i}E_\mu} - 1)^{-1}$ represents the mean number of thermal photons with an inverse temperature β_{μ_i} and energy E_μ, and γ_0 is the spontaneous emission rate.

4.2.2 Evaluating different thermodynamic quantities

Having established the basic notions of the system dynamics, we can now delve into the expressions for the average heat exchanged by the system and the local thermal baths. Building upon the framework established in the previous section, our attention remains on characterizing the heat exchange dynamics between the system, the cold bath, and the working bath to assess the cooling capabilities of the device. The expressions in equations (3.45) and (3.47) enable us to derive the local average heat exchanged between the cold and work baths with the system :

$$\begin{aligned}\dot{Q}_{w_1} &= \sum jklE_{w_1}\left[\gamma_{w_1\uparrow}\langle 1jkl|\,\rho\,|1jkl\rangle - \gamma_{w_1\downarrow}\langle 2jkl|\,\rho\,|2jkl\rangle\right], \\ \dot{Q}_{w_2} &= \sum ijkE_{w_2}\left[\gamma_{w_2\uparrow}\langle ijk1|\,\rho\,|ijk1\rangle - \gamma_{w_2\downarrow}\langle ijk2|\,\rho\,|ijk2\rangle\right], \\ \dot{Q}_{c_1} &= \sum iklE_{c_1}\left[\gamma_{c_1\uparrow}\langle igkl|\,\rho\,|igkl\rangle - \gamma_{c_1\downarrow}\langle iekl|\,\rho\,|iekl\rangle\right], \\ \dot{Q}_{c_2} &= \sum ijlE_{c_2}\left[\gamma_{c_2\uparrow}\langle ijgl|\,\rho\,|ijgl\rangle - \gamma_{c_2\downarrow}\langle ijel|\,\rho\,|ijel\rangle\right],\end{aligned} \tag{4.30}$$

Here, $|ijkl\rangle \in \mathcal{H}_{M_1}\otimes\mathcal{H}_{c_1}\otimes\mathcal{H}_{c_2}\otimes\mathcal{H}_{M_2}$ belongs to the composite system's Hilbert space, where i and l take values in $\{0,1,2\}$, and j and k take values in $\{e,g\}$. The relative efficiency of each machine is quantified by the ratio between the cooling power $\dot{Q}_{c_i}$ and the average heat $\dot{Q}_{w_i}$ absorbed from the work bath $\mathcal{R}_{w_i}$:

$$\eta_i = \frac{\dot{Q}_{c_i}}{\dot{Q}_{w_i}}. \tag{4.31}$$

Furthermore, in the weak coupling limit at all interaction sites $g_i, \alpha \ll E_{\mu_i}$ and with a small value of the emission rate γ_0, the expressions in equation. (4.30) are derived, neglecting terms $Tr\left[H_{int}\mathcal{L}_{\mu_i}\right] \approx g_i\gamma_0(\alpha\gamma_0)$, which represent relatively minor contributions to the heat fluxes and can be disregarded in numerical calculations.

4.2.3 Quantum Discord

Without the dipole-dipole interaction between the two qubits, each machine would operate independently. In addition, even when the two machines are coupled, the temperature difference between them might not be substantial enough to facilitate significant amount of heat flow, hindering the generation of notable thermal entanglement. This suggests that the two devices operate close to an independent model regime and therefore cannot be entangled. Nonetheless, despite their separation, they can exhibit correlations. It therefore makes sense to use the quantum discord measure, which captures quantum correlations even in the case of separate systems.

To quantify the degree of correlation between the two quantum refrigerators, understanding the dynamics of the composite system comprising the two cold qubits is crucial. This composite system is influenced by interactions with both cooling machines and cold baths. The density matrix derived from equation (4.26) encapsulates information about the total system composed of the qubits and the cooling machines. By performing a partial trace over the cooling machines, we obtain the density matrix $\rho_{c_1c_2}$ of the two cold qubits, presented in a specific X-matrix form :

$$\rho_{c_1c_2} = \begin{pmatrix} a & 0 & 0 & 0 \\ 0 & b & c & 0 \\ 0 & d & \mathsf{h} & 0 \\ 0 & 0 & 0 & f \end{pmatrix}. \tag{4.32}$$

The elements on the diagonal a, b, h, f represent the population of the composite system and those on the off-diagonal c, d are the coherent elements. In the following analysis, we employ the quantum discord, as defined in Equation. (1.57), as a measure of correlation between the two machines :

$$\mathcal{Q}(\rho) = \mathcal{I}(\rho) - \mathcal{C}(\rho). \tag{4.33}$$

While this approximation is conceptually clear, its practical calculation has proven challenging due to the necessity of optimizing all possible measurements on a qubit, as demonstrated in Equation (1.56). Nevertheless, specific methodologies have been developed for determining it, particularly in cases where the system's state conforms to the X-matrix form.

4.2.4 Results and discussions

We start our analysis with the first scenario, wherein all parameters and temperatures of the two machines are identical. Our aim is to scrutinize how the performance of the refrigerators ($\dot{Q}_{c_i}$, η_i) deviate from those of a non-coupled model, contingent upon the ratio between the interaction constants $g = g_1 = g_2$ and the interaction among the machines α. It becomes apparent that as the interaction constants (g_1, g_2) approach zero, the machines experience a reduction in their cooling power (as illustrated in Figure 4.11). This decline in performance for the coupled machines is notably swift compared to the independent models, $\dot{Q}_{c_i}/\dot{Q}^*_{c_i} \leq 1$ and $\eta_i/\eta^*_i \leq 1$. This trend is particularly pronounced in the region where the interaction between the two refrigerators exceeds that of the cold qubits with the cooling machines ($g < \alpha$). However, as the interaction constant g increases, the thermodynamic quantities exhibit improvement until they eventually reach a regime akin to that of independent machines.

Secondly, we investigate a scenario where the two qubits are coupled to reservoirs at different temperatures. Figure (4.12) illustrates the thermodynamic performance of the two refrigerators concerning the ratio between the two cold temperatures. We maintain the temperature of the cold bath $\mathcal{R}_{c_2}$ constant and analyze how the ratio β_{c_2}/β_{c_1} influences the thermodynamic performances. To ensure that the conditions $\beta_{c_i} > \beta_{h_i} > \beta_{w_i}$ are satisfied, we vary β_{c_2}/β_{c_1} within the range $[0.5, 1.6]$. The results depicted in Figure (4.12) reveal a form of thermodynamic performance transfer between the two refrigerators. Specifically, when $\beta_{c_2} \leq \beta_{c_1}$, the first machine

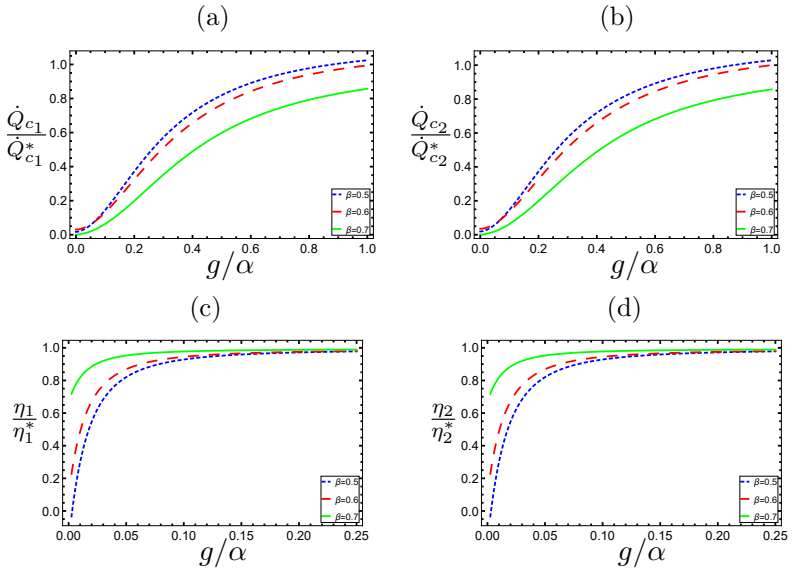

FIGURE 4.11 – Thermodynamic quantities in comparison to those of an independent refrigerator under identical parameters. The top row of plots shows the ratios of the relative cooling powers $\dot{Q}_{c_2}/\dot{Q}^*_{c_2}$ and $\dot{Q}_{c_1}/\dot{Q}^*_{c_1}$, respectively, with respect to the independent models, plotted against the ratio of interaction constants g/α, where $g = g_1 = g_2$. The bottom row presents a comparison of the coefficient of performance. The rest of parameters are fixed as $\beta_{c_i} = 0.6$, $\beta_{h_i} = 0.1$, $\beta_{w_i} = 0.04$, $\gamma_0 = 0.25 \times 10^{-5}$, $E_{c_i} = 7$, $E_{w_i} = 16$, and $\alpha = 0.045$

operates less efficiently than an independent machine, while the second machine benefits from an improved regime. As we increase the ratio β_{c_2}/β_{c_1}, we observe an enhancement in the performance of the first machine at the expense of a decline in the performance of the second one. These outcomes can be attributed to two primary factors : firstly, the impact of the increase in the cold bath temperature on the cooling window, which influences the cooling performance ; and secondly, the contribution of correlation between the two machines to the enhancement of the relative thermodynamic performance of both systems.

4.2.5 Quantum discord

Finally, we delve into the analysis of quantum correlation between the refrigerators in the two examined scenarios, employing the discord measure. We explore this correlation regarding the ratio of the interaction constants g/α and the temperatures of the cold baths. Figure (4.13a) depicts a subtle presence of correlation, which tends towards minimal values as the interaction constant g between the components of each refrigerator approaches that of the interaction between the machines, α. This observation supports our earlier prediction that, in this regime, the device's operation converges towards that of a model featuring two uncoupled refrigerators.

Moreover, when the temperatures of the two cold reservoirs differ, we observe a weaker yet significant presence of correlation, diminishing as the temperatures of the thermal baths increase. Notably, in both studied cases, the quantum correlation between the machines evolves alongside the cooling powers $\dot{Q}_i$, $i = 1, 2$, in response to variations in the temperatures of the cold baths. Specifically, an increase in cold temperature leads to enhanced correlation when the cold baths of the two systems are at the same temperature, whereas this correlation decreases when the cold baths have different temperatures.

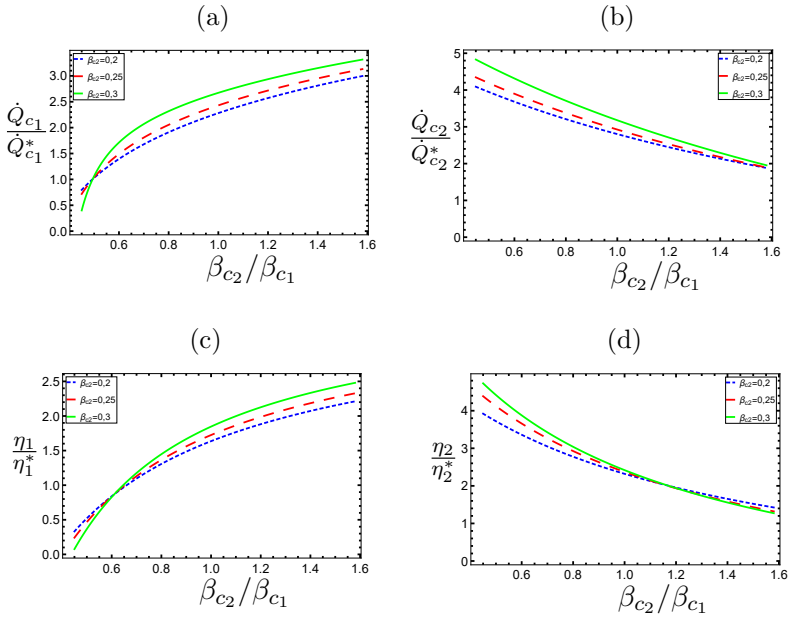

FIGURE 4.12 – Comparison of the thermodynamic quantities with those of an independent refrigerator under identical parameters. The top row shows the ratio of the relative cooling powers $\dot{Q}c_1$ and $\dot{Q}c_2$ to those of the independent models $\dot{Q}c_1{}^*$ and $\dot{Q}c_2{}^*$, respectively, as a function of the ratio of cold temperatures β_{c_2}/β_{c_1}. The bottom row shows a comparison of the power coefficient. The other parameters are set as follows : $\beta_{c_2} = 0.2$, $\beta_{h_i} = 0.1$, $\beta_{w_i} = 0.03$, $\gamma_0 = 0.27 \times 10^{-5}$, $E_{c_i} = 1$, $E_{w_i} = 8.5$, $\alpha = 0.045 \times 10^{-3}$, $g_i = 0.15$.

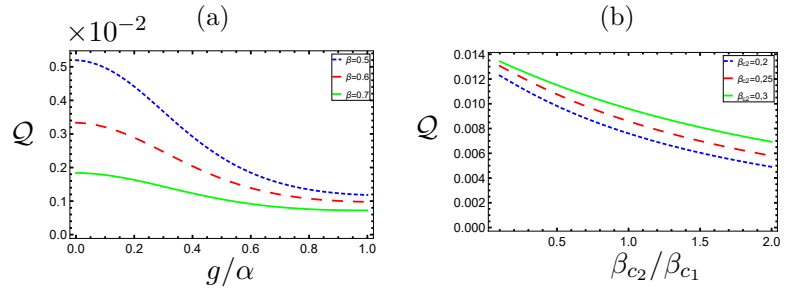

FIGURE 4.13 – Plot of the quantum discord in the two studied cases. In figure. (4.13a), we consider the first case where all parameters of the two refrigerators are equal and in figure. (4.13b), when the two cold baths are at different temperatures. The rest of the parameters are identical to those considered in the study of thermodynamic quantities in both cases (Figure. (4.11) and Figure. (4.12)).

4.3 Summary

We've explored the coupling of two autonomous quantum refrigerators based on conventional refrigerator models. This coupling involves a weak, resonant interaction via the two cold qubits of each machine. We investigated two scenarios : one where the two machines have identical parameters and another where they differ across a range of parameters. Our analysis focused on two specific cases : when the cold qubits are coupled to a common reservoir and when each qubit is coupled to an independent reservoir. We studied the thermodynamic performance of the system and the correlation induced by the interaction of the two devices when the system reaches its steady state, considering various parameters.

Our findings reveal that coupling two non-identical devices with different energy spacings

diminishes the relative cooling power of the coupled refrigerators, despite a potential enhancement in efficiency. Conversely, a substantial enhancement in cooling power is observed when moving towards a configuration with two identical refrigerators. This contrasts with the effective performance of the system in the case of a common bath, where improvement occurs with an increase in the difference in energy spacing E_d between the two machines. Additionally, in both studied cases, augmenting the energy spacing difference E_d enhances the entanglement of the two cold qubits. However, such correlation does not favor the individual cooling powers of the system when independent baths are considered.

Furthermore, for two machines with the same parameters, a strong coupling between the devices compared to that of the elements of each machine leads to a weak generation of quantum correlation between the refrigerators and a degradation of the thermodynamic performance of each machine. Conversely, increasing the coupling constants between the elements of each machine improves the relative thermodynamic performance of the machines at the cost of a deterioration in the quantum correlation between them. Notably, when the two qubits are coupled to cold reservoirs of different temperatures, the performance of the machines can be enhanced compared to that of an independent machine, while the correlation maintains the same order of variation with the cooling power in this scenario.

Chapitre 5

Non-Markovian Effects on Quantum Refrigerator Performances

We have studied various quantum refrigerators in depth, with the specific aim of identifying how the system parameters and quantum properties of the devices can be exploited to improve their cooling capabilities. Our aim is to contribute to improving the cooling performance of quantum refrigerators by addressing more general aspects. By focusing on the relevant parameters and quantum correlations inherent in the working system, we have carried out numerous analyses to determine the essential aspects of device operation and clarify ways of making devices more or less productive. However, one element that remains to be considered is the effects induced by the interaction between the working system and the thermal baths.

With the above motivation, we are interested in studying a particular quantum refrigerator approach consisting of a working medium and two hierarchical environments as thermal baths. Each environment consists of a Markovian thermal bath weakly coupled to an auxiliary qubit. We explore the close links between the theory of dynamics induced by the interaction between the working medium and the reservoirs, and the resulting thermodynamic limitations of the device. In addition to the quantities of work and heat generated in the evolution of the system, we are interested in their behavior in the different regimes that can occur in the dynamics of the device, and in exploring the difference in quality between these two dynamics.

5.1 Continuous quantum refrigerator with hierarchical environment

Let's consider a system $\mathcal{S}_0$ coupled to a hierarchical environment consisting of an auxiliary system $\mathcal{S}_1$, weakly connected to a thermal bath $\mathcal{R}$ via a coupling strength g, as illustrated in Figure (5.1). Subsequently, the system $\mathcal{S}_0$ interacts with the overall environment through an interaction with $\mathcal{S}_1$, characterized by a coupling constant κ. In this setup, the composite reservoir can induce non-Markovian dynamics for the system $\mathcal{S}_0$, as we will explore later. On the other hand, assuming weak coupling between $\mathcal{S}_1$ and $\mathcal{R}$, we can model $\mathcal{S}_0$ and $\mathcal{S}_1$ as a composite open quantum system $\mathcal{S} = \mathcal{S}_0 \otimes \mathcal{S}_1$ subject to Markovian dynamics due to the dissipations induced by the reservoir $\mathcal{R}$. The Hamiltonian of the composite system S is expressed as :

$$H_{\mathcal{S}} = H_{\mathcal{S}_0} + H_{\mathcal{S}_1} + H_I, \tag{5.1}$$

where $H_{\mathcal{S}_i}$ represents the free Hamiltonian of the subsystem $\mathcal{S}_i$ for $i = 0, 1$, and H_I describes the interaction between the subsystems $\mathcal{S}_0$ and $\mathcal{S}_1$. Additionally, $H_{\mathcal{R}}$ is the free Hamiltonian of the Markovian thermal bath, and $H_{\mathcal{SR}}$ denotes the interaction between the system and the thermal bath.

5.1.1 System-bath interaction

In our primary approach, we consider the thermal reservoir $\mathcal{R}$ as a large collection of identical, non-interacting ancillas. Furthermore, we adopt the repeated interaction model to describe the interaction between the system and the bath elements [169–175]. This model entails sequential and unitary interactions of the system with each unit of the thermal bath over specific time intervals. The interaction Hamiltonian $H_{\mathcal{SR}}$ is then expressed as follows :

$$H_{\mathcal{SR}} = \sum_k \frac{g_k}{\sqrt{\tau}}(B_k^\dagger A + B_k A^\dagger) = \frac{1}{\sqrt{\tau}} V_{\mathcal{SR}}, \tag{5.2}$$

where g_k is the interaction constant between the system and each bath element, A and B_k are operators in the Hilbert space of the system S_1 and ancillas, respectively. Finally, τ is the period of interaction between the system and an ancilla. In the remainder of this work, we shall consider the case where A and B_k are the eigenoperators of the system $\mathcal{S}_1$ and the thermal bath element $\mathcal{R}_k$, respectively.

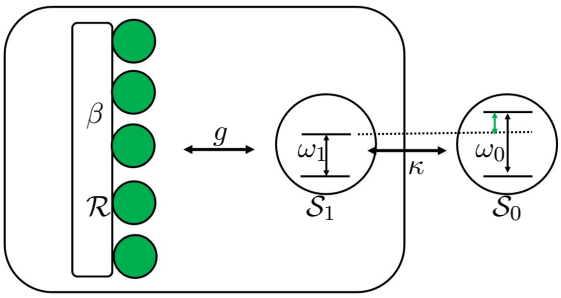

FIGURE 5.1 – Illustration of the open quantum system coupled to an engineered environment. The auxiliary system $\mathcal{S}_1$ is coupled to the Markovian thermal bath $\mathcal{R}$, which together form the engineered environment and in turn $\mathcal{S}_0$ interacts with the whole environment via a direct interaction with S_1.

Based on the previous assumptions, a single collision during the time τ transforms the system from the state $\rho_{\mathcal{S}}$ to $\rho'_{\mathcal{S}}$ as follows :

$$\rho'_{\mathcal{S}} = Tr_{\mathcal{R}}(\rho_{\mathcal{SR}}) = Tr_{\mathcal{R}}(U_{\mathcal{SR}}\rho_{\mathcal{SR}}U_{\mathcal{SR}}^\dagger), \tag{5.3}$$

where $\rho_{\mathcal{SR}}$ represents the system-reservoir state and $U_{\mathcal{SR}} = \exp(-iH_{Tot}\tau)$ denotes the unitary time evolution operator. Furthermore, we assume a small period of interaction for each collision, so that the unitary evolution operator $U_{\mathcal{SR}}$ can be approximated to second order as,

$$U_{\mathcal{SR}} = \mathbb{1} - iH_{Tot}\tau - \frac{\tau^2}{2}V_{\mathcal{SR}}^2, \tag{5.4}$$

where $\mathbb{1}$ is the identity operator. This approximation allows us to construct a continuous limit of the master equation governing the dynamics of the S system. By substituting $U_{\mathcal{SR}}$ from equation.(5.4) into equation.(5.3) and taking the continuous limit $\tau \to 0$, equation.(5.3) yields a quantum master equation for the system S in the form :

$$\dot{\rho}_{\mathcal{S}} = -i\left[H_{\mathcal{S}}, \rho_{\mathcal{S}}\right] + \mathcal{L}(\rho_{\mathcal{S}}), \tag{5.5}$$

with the dissipator $\mathcal{L}$ given by,

$$\mathcal{L}(\rho_{\mathcal{S}}) = \sum_k g_k^2 \langle B_k B_k^\dagger \rangle_{\rho_{\mathcal{R}}} \left(A \rho_{\mathcal{S}} A^\dagger - \frac{1}{2}\{A^\dagger A, \rho_{\mathcal{S}}\} \right) + g_k^2 \langle B_k^\dagger B_k \rangle \left(A^\dagger \rho_{\mathcal{S}} A - \frac{1}{2}\{A A^\dagger, \rho_{\mathcal{S}}\} \right), \quad (5.6)$$

where $\langle . \rangle_{\rho_{\mathcal{R}}}$ is the average over the state $\rho_{\mathcal{R}}$ of the Markovian bath $\mathcal{R}$.

5.1.2 Non-Markovian dynamics of the system $\mathcal{S}_0$

Below, we present a numerical analysis of the non-Markovian behavior affecting the dynamics of the subsystem S_0, involving resonant couplings between S_0-S_1 and S_1-$\mathcal{R}$. We emphasize that the consideration of a coupling without resonance between S_0 and S_1 does not show a considerable impact on the degree of non-Markovianity on the dynamics of $\mathcal{S}_0$. We set the state of the thermal bath to be a Gibbs state at the inverse temperature β and the auxiliary system is initially in thermal equilibrium with the bath, i.e., $\rho_{\mathcal{R}} = e^{-\beta H_{\mathcal{R}}}/Z_{\mathcal{R}}$ and $\rho_{S_1} = e^{-\beta H_{S_1}}/Z_{S_1}$. Moreover, we have chosen the pair of pure, orthogonal states $|0\rangle$ and $|1\rangle$ as the initial states of the S_0 system intended to satisfy the maximization of σ in equation (5.7).

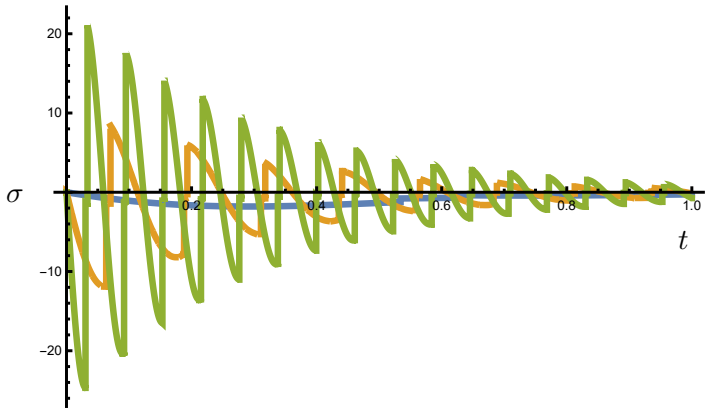

FIGURE 5.2 – Evolution of the time derivative of the trace distance between the initial states $|0\rangle$ and $|1\rangle$ of the subsystem S_0, for different values of the ratio κ/g : $\kappa/g = 1$ (blue solid line), $\kappa/g = 5$ (orange line) and $\kappa/g = 10$ (green lines). The rest of the parameters are $\omega_0 = \omega_1 = \Omega_{\mathcal{R}} = 3.2$, $g = 0.8\omega_0$, $T = 6.5\omega_0$.

In Fig.(5.2), we plot the time evolution of the trace distance derivative

$$\sigma(t, \rho_1(0), \rho_2(0)) = \frac{d}{dt} D(\rho_1(t), \rho_2(t)), \quad (5.7)$$

for different values of the ratio κ/g. Our results provide valuable constraints on the correspondence between various values of the interaction constants and the underlying dynamics of the primary system. Notably, we observe that the derivative of the trace distance remains negative when $\kappa = g$, indicating a Markovian nature in the dynamics of S_0. However, for higher ratios of κ/g, such as $\kappa = 5g$ and $\kappa = 10g$, it becomes apparent that σ exhibits positive values during certain time intervals, signaling non-Markovian dynamics in S_0. In addition, we observe a decrease in the amplitude of the derivative of the trace distance over time within the non-Markovian regime, which typically indicates a decrease in the flow of information from the environment into the system.

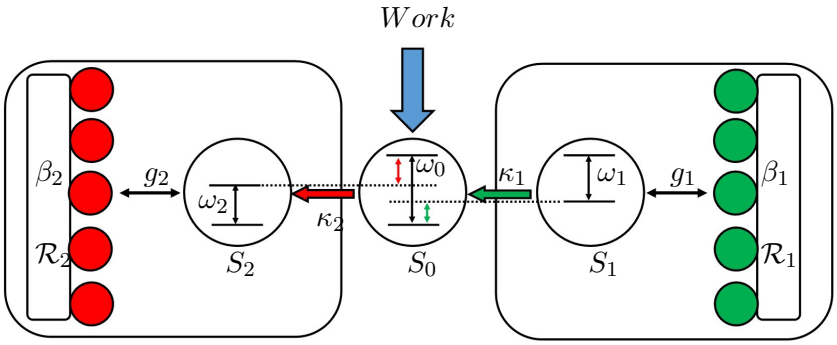

FIGURE 5.3 – A schematic representation of our proposed continuous quantum thermal refrigerator. A working system S_0 is coupled to a pair of engineered environments. Each environment consists of an auxiliary system S_j interacting with a Markovian thermal bath $\mathcal{R}_j$ at inverse temperature β_j, $j = 1, 2$.

5.1.3 Description of the proposed model

Let us introduce our proposed device, which is depicted in figure.5.3 a continuous quantum thermal machine comprised of a qubit S_0 coupled to two engineered environments at different temperatures. Each environment is made up of an auxiliary subsystem S_j that is weakly coupled to a Markovian thermal reservoir R_j at an inverse temperature $\beta_j, j = 1, 2$. For simplicity, we will call the first and second environments cold and hot environments respectively, meaning $\beta_1 > \beta_2$. The Hamiltonian of the qubit S_0 is written as

$$H_{\mathcal{S}_0} = \omega_0 \sigma_0^\dagger \sigma_0, \tag{5.8}$$

where ω_0 is the frequency of S_0 and $\sigma_0 = |0\rangle\langle 1|_{S_0}$. In addition, we assume that each reservoir is composed of an auxiliary qubit S_j weakly coupled to a Markovian thermal reservoir $\mathcal{R}_j$ which is made up of a collection of qubits. For convenience of notation, we will refer to the bath $\mathcal{R}_1$ as the cold bath and the bath $\mathcal{R}_2$ as the hot one. The Hamiltonians of the auxiliary and Markovian thermal baths read

$$H_{\mathcal{S}_j} = \omega_j \sigma_j^\dagger \sigma_j \quad , \quad H_{\mathcal{R}_j} = \sum_j \Omega_j \sigma_{\mathcal{R}_j}^\dagger \sigma_{\mathcal{R}_j}, \tag{5.9}$$

where ω_j and Ω_j are the frequency of the qubit S_j and thermal baths $\mathcal{R}_j$, $\sigma_j = |0\rangle\langle 1|_{S_j}$ and $\sigma_{\mathcal{R}_j} = |0\rangle\langle 1|_{\mathcal{R}_j}$ $(j = 1, 2)$. Furthermore, we look at the case of resonance coupling between subsystems S_j and their relative thermal baths R_j, i.e., $\omega_j = \Omega_j$. The interaction Hamiltonian between the subsystem S_0 and the auxiliary qubits is given as

$$H_I = \sum_{j=1}^{2} \kappa_j (\sigma_0 \sigma_j^\dagger + \sigma_0^\dagger \sigma_j), \tag{5.10}$$

with κ_j $(j = 1, 2)$ denoting the interaction constants between S_0 and S_j. The form of Eq.(5.10) shows that the system S_0 interacts on both sides with S_1 and S_2 without any direct interaction between S_1 and S_2. Moreover, the local interaction for each qubit S_j and the corresponding Markovian bath $\mathcal{R}_j$ is expressed as

$$H_{\mathcal{S}_j \mathcal{R}_j} = \sum_j \frac{g_j}{\sqrt{\tau}} (\sigma_j \sigma_{\mathcal{R}_j}^\dagger + \sigma_j^\dagger \sigma_{\mathcal{R}_j}), \tag{5.11}$$

g_j is the local system-bath coupling constant.

Following these previous considerations, the master equation governing the dynamics of the system S can be modeled in the form :

$$\dot{\rho}_S = -i\,[H_S, \rho_S] + \sum_{j=1}^{2} \mathcal{L}_j(\rho_S). \tag{5.12}$$

The first term in equation.(5.12) represents the unitary evolution of the system, which can be varied by inserting a control parameter in the Hamiltonian of the total system

$$H_{\mathcal{S}} = H_{\mathcal{S}_0} + \sum_{j=1}^{2} H_{\mathcal{S}_j} + H_{\mathcal{S}_0\mathcal{S}_j} \tag{5.13}$$

while the second part represents the dissipation effects of the thermal reservoirs :

$$\mathcal{L}_j(\rho_S) = g_j^2 \langle \sigma^\dagger_{\mathcal{R}_j} \sigma_{\mathcal{R}_j} \rangle \Big(\sigma_j^\dagger \rho_S \sigma_j - \frac{1}{2}\{\sigma_j \sigma_j^\dagger\} \Big) + g_j^2 \langle \sigma_{\mathcal{R}_j} \sigma^\dagger_{\mathcal{R}_j} \rangle \Big(\sigma_j \rho_S \sigma_j^\dagger - \frac{1}{2}\{\sigma_j^\dagger \sigma_j, \rho_S\} \Big), \tag{5.14}$$

where $\langle \sigma^\dagger_{\mathcal{R}_j} \sigma_{\mathcal{R}_j} \rangle$ denotes the average with respect to the bath state $\rho_{\mathcal{R}}$. Without loss of generality, we assume that the ancillas are prepared in a thermal state at inverse temperature β_j,

$$\rho_{\mathcal{R}_j} = \frac{e^{-\beta_j H_{\mathcal{R}_j}}}{Z_j}, \quad \text{with } Z_j = Tr\left(e^{-\beta_j H_{\mathcal{R}_j}} \right). \tag{5.15}$$

5.1.4 Quantitative thermodynamic quantities

We determine the quantities of heat resulting from the interaction between the working system and the hierarchical reservoirs, along the work cost to complete the operation of the device. By applying equation. (3.45)-(3.47), we can derive the expression for the average heat exchanged with a bath $\mathcal{R}_j$ as :

$$\dot{Q}_j = g_j^2 \omega_j \Big(\langle \sigma^\dagger_{\mathcal{R}_j} \sigma_{\mathcal{R}_j} \rangle - \Big(\langle \sigma^\dagger_{\mathcal{R}_j} \sigma_{\mathcal{R}_j} \rangle + \langle \sigma_{\mathcal{R}_j} \sigma^\dagger_{\mathcal{R}_j} \rangle \Big) \langle \sigma_j^\dagger \sigma_j \rangle \Big), \tag{5.16}$$

while, the total work performed takes the following form

$$\dot{W} = -\frac{1}{2} \sum_{i=1}^{2} g_i^2 k_i \left((\langle \sigma^\dagger_{\mathcal{R}_i} \sigma_{\mathcal{R}_i} \rangle + \langle \sigma_{\mathcal{R}_i} \sigma^\dagger_{\mathcal{R}_i} \rangle)(\sigma_0^\dagger \sigma_i + \sigma_0 \sigma_i^\dagger) \right). \tag{5.17}$$

Remarkably, the average heat and the work performed throughout the system operation satisfy the first law of thermodynamics,

$$\dot{U}_{\mathcal{S}} = \dot{W} + \sum_{i=1}^{2} \dot{Q}_i, \tag{5.18}$$

where $U_S = Tr\,(H_S \rho_S)$ refers to the variation of the internal energy. Finally, the efficiency of refrigeration is defined here as the ratio of the cooling power from the cold bath over the work input to the system. On standard devices, it satisfies the following expression,

$$\eta = \frac{Q_1}{W} \leq \eta_C, \tag{5.19}$$

η_C denotes the Carnot coefficient of performance.

5.1.5 Evaluation of different thermodynamic quantities

Now, we can assess the thermodynamic performance of the device under the parameters where the dynamics of S_0 exhibits either Markovian or non-Markovian behavior. The results depicted in Fig. (5.4) illustrate the impact of the non-Markovian regime on the refrigerator's performance under the condition of the non-fully resonant model. It's evident that the thermodynamic quantities of the system display oscillatory behavior for large values of k_j, such as $k_j = 10g_j$ and $k_j = 25g_j$. Particularly, the amplitudes and frequencies of these oscillations increase with the constants k_j and decrease with time, except for the efficiency η, whose oscillation amplitude increases with time. Furthermore, we observe that the non-Markovianity of S_0 enhances the cooling power $\dot{Q}_1$ and efficiency η over prolonged operation periods, whereas the work $\dot{W}$ and heat flux from the hot bath $\dot{Q}_2$ eventually converge with those of the Markovian regime. As the device's operational duration increases, the disparity between the cooling power and efficiency of the Markovian and non-Markovian regimes widens, while the work and heat flux from the hot bath of both regimes tend to converge. This outcome is significant, as it indicates that the non-Markovian regime potentially allows for improved refrigerator performance in terms of $\dot{Q}_1$ and η compared to the Markovian regime, while maintaining consistent input $\dot{W}$ and $\dot{Q}_2$.

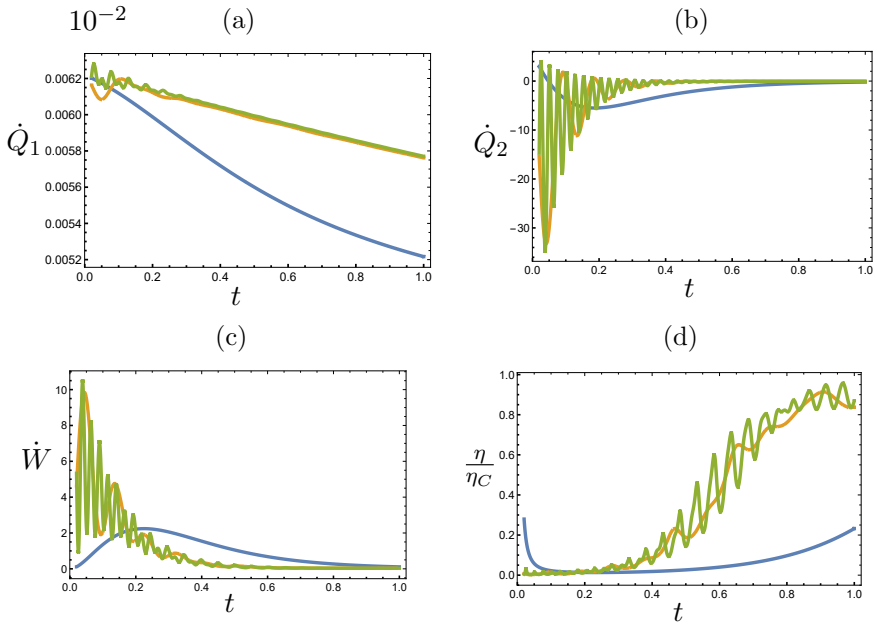

FIGURE 5.4 – Thermodynamic quantities with different values of k_j/g_j : $k_j/g_j = 1$ (blue solid line), $k_j/g_j = 5$ (orange line) and $k_j/g_j = 10$ (green lines). The rest of the parameters are : $\omega_0 = 3$, $g_j = 0.8\omega_j$, $\omega_1 = 0.4$, $\omega_2 = 5.5$, $T_1 = 0.89\omega_1$, $T_2 = 5.77\omega_2$. The initial state of the system is fixed at $|1\rangle$.

Finally, when the device operates in a configuration with full resonance at all coupling sites, no work is required for the system's operation. In this case, the change in the internal energy of the system is solely due to the heat flow from the reservoirs. Fig. (5.5) illustrates the heat current flowing through the system in a resonant configuration, given by

$$J = \dot{Q}_2 - \dot{Q}_1. \tag{5.20}$$

In both invested cases, we obtain the same qualitative behavior as previously. The thermal current exhibits oscillatory behavior whose amplitude and frequency increase with the ratio k/g and decrease with time. Additionally, we notice the enhancement of the thermal current in the non-Markovian regime.

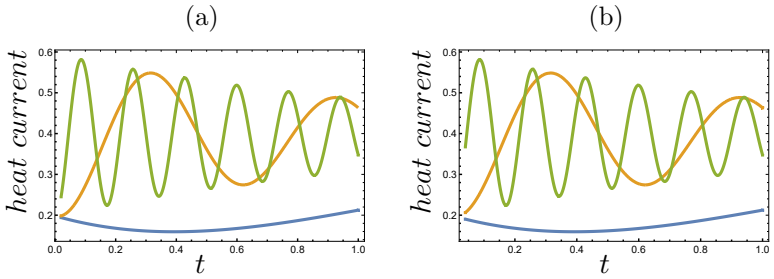

FIGURE 5.5 – Heat current with different values of k_j/g_j : $k_j/g_j = 1$ (blue solid line), $k_j/g_j = 5$ (orange line) and $k_j/g_j = 10$ (green lines). The rest of the parameters are $\omega_0 = \omega_1 = \omega_2 = 1.3$, $g_j = 0.8\omega_j$, $T_1 = 0.5\omega_1$, and $T_2 = 2.5\omega_2$. On the first and second lines, we have taken the initial state of the system S_0 to be equal to $|1\rangle$ and $|0\rangle$, respectively.

5.2 Quantum Otto refrigerator with hierarchical reservoirs

We will now extend the previous discussion to the case of the Otto quantum refrigerator [176]. In this context, we consider an Otto quantum refrigerator model consisting of a qubit system $\mathcal{S}0$ as the working system, characterized by the free Hamiltonian :

$$H_{\mathcal{S}_0} = \omega_{\mathcal{S}_0}\sigma^+_{\mathcal{S}_0}\sigma^-_{\mathcal{S}_0}, \tag{5.21}$$

where $\omega_{\mathcal{S}_0}$ is the frequency associated with $\mathcal{S}_0$, $\sigma^+_{\mathcal{S}0} = (\sigma^-_{\mathcal{S}_0})^\dagger = |e\rangle\langle g|$ denote the raising and lowering operators, respectively, with $|e\rangle$ and $|g\rangle$ representing the excited and ground states of the qubit $\mathcal{S}_0$. Additionally, both the system $\mathcal{S}_1$ and the reservoir $\mathcal{R}$ are modeled as qubits with the free Hamiltonians :

$$H_{\mathcal{S}_1} = \omega_{\mathcal{S}_1}\sigma^+_{\mathcal{S}_1}\sigma^-_{\mathcal{S}_1} \quad , \quad H_{\mathcal{R}} = \omega_{\mathcal{R}}\sigma^+_{\mathcal{R}}\sigma^-_{\mathcal{R}}. \tag{5.22}$$

The interaction between the two systems $\mathcal{S}_0$ and $\mathcal{S}_1$, as well as between $\mathcal{S}_1$ and the thermal bath $\mathcal{R}$, is governed by the XX interaction :

$$H_{\mathcal{S}_0-\mathcal{S}_1} = \frac{\kappa}{2}(\sigma^x_{\mathcal{S}_0}\sigma^x_{\mathcal{S}_1} + \sigma^y_{\mathcal{S}_0}\sigma^y_{\mathcal{S}_1}) \quad \text{and} \quad H_{\mathcal{S}_1-\mathcal{R}} = \frac{g}{2}(\sigma^x_{\mathcal{S}_1}\sigma^x_{\mathcal{R}} + \sigma^y_{\mathcal{S}_1}\sigma^y_{\mathcal{R}}), \tag{5.23}$$

where κ and g are interaction constants. From these interactions, we derive the master equation for the dynamics of the composite system $\mathcal{S} = \mathcal{S}_0 \otimes \mathcal{S}_1$, which can be stated as

$$\frac{d\rho_{\mathcal{S}}(t)}{dt} = -i[H_{\mathcal{S}}, \rho_{\mathcal{S}}(t)] + \mathcal{L}(\rho_{\mathcal{S}}(t)), \tag{5.24}$$

where $H_{\mathcal{S}} = H_{\mathcal{S}_0} + H_{\mathcal{S}_1} + H_{\mathcal{S}_0-\mathcal{S}_1}$ is the Hamiltonian of the total system, and $\mathcal{L}$ is the dissipator operator that accounts for the effects of the reservoir $\mathcal{R}$ on the system :

$$\mathcal{L}(\rho_{\mathcal{S}}) = \gamma\langle\sigma^+_{\mathcal{R}}\sigma^-_{\mathcal{R}}\rangle\left(\sigma^+_{\mathcal{S}_1}\rho_{\mathcal{S}}\sigma^-_{\mathcal{S}_1} - \frac{1}{2}\{\sigma^-_{\mathcal{S}_1}\sigma^+_{\mathcal{S}_1}, \rho_{\mathcal{S}}\}\right) + \gamma\langle\sigma^-_{\mathcal{R}}\sigma^+_{\mathcal{R}}\rangle\left(\sigma^-_{\mathcal{S}_1}\rho_{\mathcal{S}}\sigma^+_{\mathcal{S}_1} - \frac{1}{2}\{\sigma^+_{\mathcal{S}_1}\sigma^-_{\mathcal{S}_1}, \rho_{\mathcal{S}}\}\right), \tag{5.25}$$

where $\gamma = 2\pi g^2$ represents the decoherence parameter.

5.2.1 Proposed Model

In this section, we outline the framework of our model, focusing on an Otto quantum refrigerator composed of a qubit serving as the working system coupled to two engineered reservoirs.

Each reservoir is composed of a composite system $\mathcal{S}_i$-$\mathcal{R}_i$, where $\mathcal{R}_i$ represents a thermal bath, and $\mathcal{S}_i$ represents an auxiliary system, as shown in Figure 5.6. We assume that each auxiliary system $\mathcal{S}_i$ is initially in thermal equilibrium with its respective thermal bath. Subsequently, the working system initiates the cycle in a state of thermal equilibrium with the hot reservoir :

$$\rho_{\mathcal{S}}^{h}(\tau_0) = \frac{e^{-\beta_h H_0}}{Z_0^h} \quad , \quad \beta_h = \frac{1}{k_\beta T_h} \quad , \quad Z_0^h = Tr[e^{-\beta_h H_0}], \tag{5.26}$$

where β_h denotes the inverse hot temperature, $H_0 = \hbar\omega_0\sigma_+\sigma$ is the initial Hamiltonian of the system S_0 and Z_0 defines the corresponding partition function.

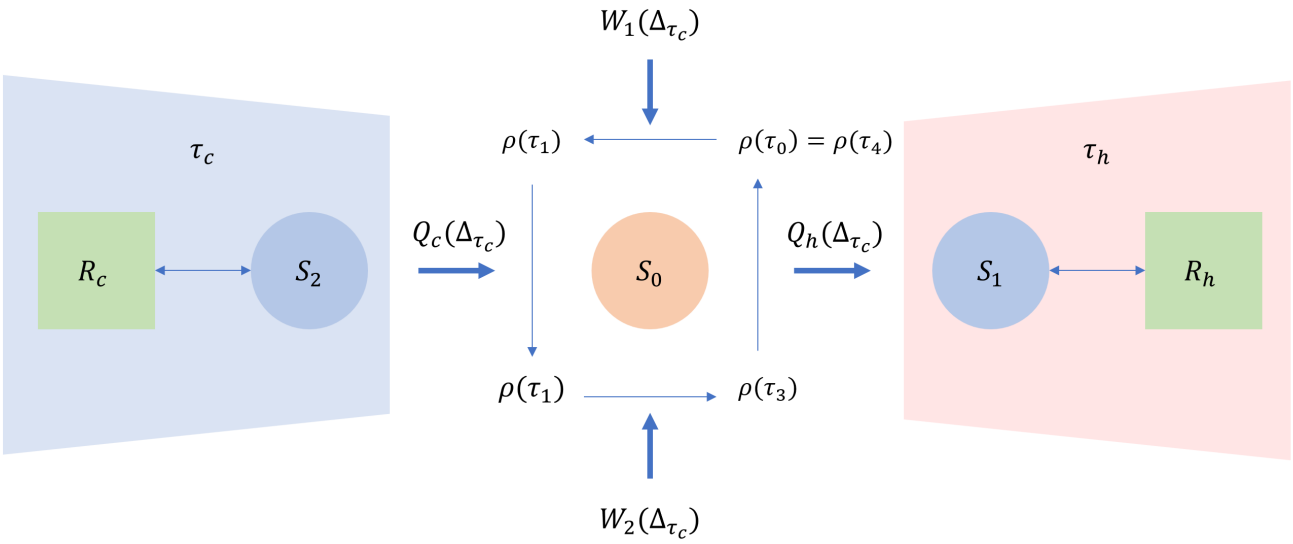

FIGURE 5.6 – Schematic diagram illustrating the Otto refrigerator, comprising four strokes with hot and cold reservoirs labeled as $\mathcal{S}_1$-$\mathcal{R}_h$ and $\mathcal{S}_2$-$\mathcal{R}_c$, respectively.

The cycle starts with an initial stroke, during which the working system undergoes a reduction in energy gap through a compression operation. This operation is governed by the driven Hamiltonian :

$$H(t) = \omega(t)\sigma_+\sigma, \tag{5.27}$$

where $\omega(t)$ represents a linear transformation of the working system frequency over the duration of the operation, given by $\omega(t) = (1 - \frac{t}{\tau_1})\omega_0 + (\frac{t}{\tau_1})\omega_{\tau_1}$. Here, ω_0 and ω_{τ_1} denote the initial and final frequencies of the refrigerant $\mathcal{S}0$, satisfying $\omega 0 > \omega_{\tau_1}$. During this stroke, the working substance is isolated from the hot reservoir, resulting in no energy exchange with the reservoirs. As a consequence, a quantity of work

$$\langle W_1 \rangle = U_{\tau_1} - U_0 = Tr\left[\rho_{\mathcal{S}}(\tau_1)H^C\right] - Tr\left[\rho_{\mathcal{S}}^{h}(\tau_0)H_0\right] \tag{5.28}$$

is performed. At the end of this stroke, the state of the working system is transformed to :

$$\rho(\tau_1) = \mathcal{U}(\tau_1, 0)\rho_{\mathcal{S}}^{h}(\tau_0)\mathcal{U}^{\dagger}(\tau_1, 0), \tag{5.29}$$

where $\mathcal{U}(\tau_1, 0) = \mathcal{T}_e e^{-\frac{i}{\hbar}\int_0^t dt' H^C(t')}$ denotes the time-evolution operator for a duration $t \in [0, \tau_1]$, with $\mathcal{T}_e$ representing the time-ordering operator, and $\rho^h(0)$.

In the second stroke, the working system interacts with the cold engineered reservoir. Throughout this interaction period $t \in [\tau_1, \tau_2]$, the refrigerant Hamiltonian remains fixed at $H^C(t) =$

$\omega_{\tau_1}\sigma_+\sigma$. It's important to note that, traditionally, this thermalization process is assumed to be complete, leading the system to reach a thermal equilibrium state by the end of the stroke. However, we deviate from this convention and opt for incomplete (or partial) thermalization, a strategy that has demonstrated cost-effectiveness in achieving enhanced performance in quantum thermal machines.

At the end of this step, the heat exchange between the working system and the cold reservoir is given by $\langle Q_S^c \rangle = U_{\tau_2} - U_{\tau_1}$. It's worth noting that this quantity doesn't solely represent the energy absorbed from the cold thermal bath, as a portion of it may be consumed in the interaction between the total system and the Markovian reservoir. Thus, the heat flux from the cold bath is expressed as :

$$-\langle Q_R^c \rangle = \langle Q_S^c \rangle + \langle \Delta Q_{SR}^c \rangle, \tag{5.30}$$

where $\Delta Q_{SR}^c = Tr\left[\rho_{\mathcal{S}}(\tau_2) H_{\mathcal{S}_0-\mathcal{S}_1}\right] - Tr\left[\rho_{\mathcal{S}}(\tau_1) H_{\mathcal{S}_0-\mathcal{S}_1}\right]$ represents the mean interaction energy.

In the third stroke, the system undergoes an adiabatic expansion after being decoupled from the structured cold reservoir. During this process, the frequency is increased from ω_{τ_1} to its initial value ω_0 using the corresponding driving Hamiltonian :

$$H^{Ex}(t^{'}) = H^C(\tau_1 + \tau_2 - t^{'}), \tag{5.31}$$

where $t^{'} \in [\tau_2, \tau_3]$. The work performed on the system during this stroke is given by :

$$\langle W_2 \rangle = U_{\tau_3} - U_{\tau_2} = Tr\left[\rho_{\mathcal{S}}(\tau_3) H^{Ex}\right] - Tr\left[\rho_{\mathcal{S}}(\tau_2) H_{\mathcal{S}_0-\mathcal{S}_1}\right]. \tag{5.32}$$

Similar to the first stroke, the system's state evolves under a unitary dynamic :

$$\rho(\tau_3) = \mathcal{V}(\tau_3, \tau_2)\rho_{\mathcal{S}}(\tau_2)\mathcal{V}(\tau_3, \tau_2)^\dagger \quad , \text{ with} \quad \mathcal{V}(\tau_3, \tau_2) = \mathcal{T}e^{-\frac{i}{\hbar}\int_{\tau_2}^{\tau_3} dt H^{Ex}(t)}. \tag{5.33}$$

We assume that the duration of the third stroke is the same as for the first one, $\tau_3 - \tau_2 = \pi_1$, so that $H^{Ex}(\tau_3) = H^C(0)$.

Finally, the fourth stroke involves the hot reservoir completely thermalizing the single qubit $\mathcal{S}_0$ at the inverse temperature β_h. During the time $[\tau_3, \tau_4]$, the system interacts with the hot reservoir until it reaches thermal equilibrium. This requires that the interaction period Δ_{τ_h} verifies the condition $\Delta_{\tau_h} = \tau_4 - \tau_3 \gg \tau_h^{Re}$, where τ_h^{Re} represents the relaxation time of the Markovian hot reservoir. The Hamiltonian for the fourth stroke remains unchanged at $H^{Ex}(\tau_4) = \omega_0\sigma_+\sigma$. Furthermore, we define the duration of the whole cycle as the sum of the periods of each stroke :

$$\tau_{cycle} = \tau_4 = 2\tau_1 + \Delta_{\tau_c} + \Delta_{\tau_h}. \tag{5.34}$$

5.2.2 Work Evaluation

Following the preceding groundwork, we establish the expressions for the device's thermodynamic quantities and explore their behavior concerning the interaction period, $\Delta_{\tau_c} = \tau_2 - \tau_1$, between the working system and the cold reservoir. The total work $\langle W \rangle = \langle W_1 \rangle + \langle W_2 \rangle$ performed during the two driven processes can be expressed as :

$$\begin{aligned}
\langle W(\Delta_{\tau_c}) \rangle &= U_{\tau_1} - U_{\tau_0} + U_{\tau_3} - U_{\tau_2} \\
&= Tr\left[\rho_{\mathcal{S}}(\tau_1) H^C\right] - Tr\left[\rho_{\mathcal{S}}^h(0) H_0\right] + Tr\left[\rho_{\mathcal{S}}(\tau_3) H^{Ex}\right] - Tr\left[\rho_{\mathcal{S}}(\tau_2) H_{\mathcal{S}_0-\mathcal{S}_1}\right] \\
&= \frac{1}{2}(\omega_0 - \omega_{\tau_1})\Big(\rho_{\mathcal{S}}^{11}(\Delta_{\tau_c}) + \rho_{\mathcal{S}}^{22}(\Delta_{\tau_c}) - \rho_{\mathcal{S}}^{33}(\Delta_{\tau_c}) - \rho_{\mathcal{S}}^{44}(\Delta_{\tau_c}) + \tanh\big(\frac{\omega_0}{2T_h}\big)\Big)
\end{aligned} \tag{5.35}$$

where $\rho_{\mathcal{S}}^{ii}(\Delta_{\tau_c})$ $(i = 1, 2, 3, 4)$ are the diagonal elements of the reduced density matrix $\rho_{\mathcal{S}}(\Delta_{\tau_c})$ obtained from equation (5.24).

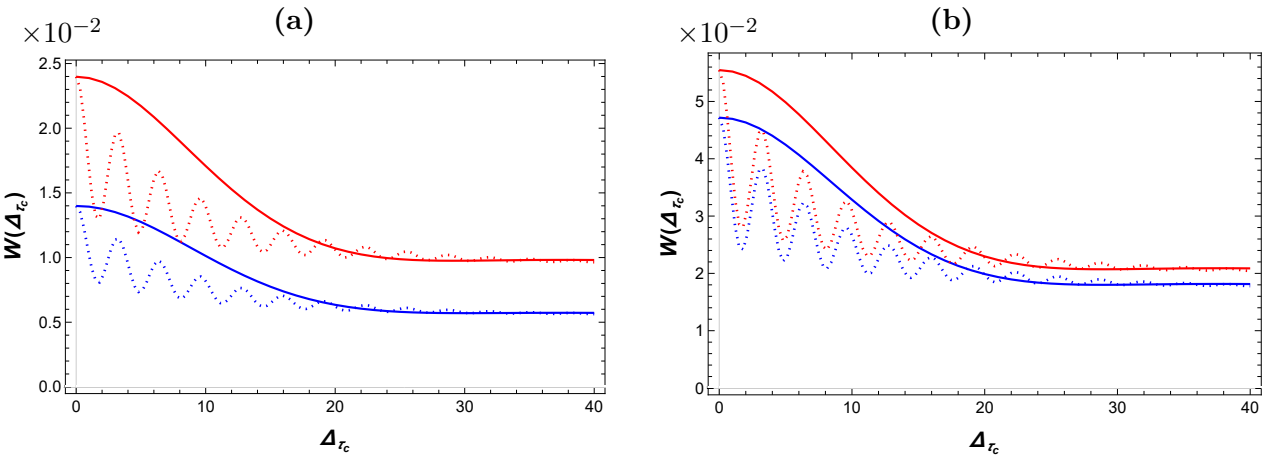

FIGURE 5.7 – Dynamics of work versus Δ_{τ_c} where, $\gamma = 0.22$, $T_h = 10\omega_0$ and $T_c = 3\omega_0$, $\omega = 0.02$, $\kappa = 0.1$ (solid curves) and $\kappa = 0.99$ (dotted curves). Besides, (a) $\omega_0 = 0.3$ (blue) and $\omega_0 = 0.5$ (red), (b) $\omega_0 = 1.2$ (blue) and $\omega_0 = 1.5$ (red).

Figure (5.7) illustrates the evolution of the total work for various values of the initial frequency ω_0 of the refrigerant $\mathcal{S}0$. The continuous lines, corresponding to a fixed weak coupling ($\kappa = 0.1$) between the refrigerant S_0 and the auxiliary system S_1, indicate that the amount of work is initially maximized and decreases with an increase in $\Delta\tau_c$ until reaching a minimum value without vanishing. In contrast, the dotted lines in Figure (5.7) represent the work dynamics as the coupling coefficient κ is increased from 0.1 to 0.99. As previously mentioned, due to this strong coupling, the dynamics of the system S_0 with respect to the engineered reservoir is non-Markovian. It is observable that in this scenario, the work dynamics initially exhibit oscillatory behavior, which converges to Markovian behavior for large values of the interaction time $\Delta\tau_c$. Additionally, it is noteworthy that the performed work improves as the initial frequency of the working system $\omega 0$ progressively increases (indicated by the red solid lines).

5.2.3 Heat Evaluation

We now turn to the cooling power $-\langle Q_R^c(\Delta_{\tau_c})\rangle/\tau_{cycle}$, which refers to the ratio between the heat flow from the cold bath over the cycle duration :

$$\frac{-\langle Q_R^c(\Delta_{\tau_c})\rangle}{\tau_{cycle}} = \frac{\Big(-\rho_{\mathcal{S}}^{23}(\Delta_{\tau_c}) - \rho_{\mathcal{S}}^{32}(\Delta_{\tau_c}) + \frac{1}{2}\omega_{\tau_1}\big(-\rho_{\mathcal{S}}^{11}(\Delta_{\tau_c}) - \rho_{\mathcal{S}}^{22}(\Delta_{\tau_c}) + \rho_{\mathcal{S}}^{33}(\Delta_{\tau_c}) + \rho_{\mathcal{S}}^{44}(\Delta_{\tau_c}) + \tanh\big(\frac{\omega_0}{2T_h}\big)\big)\Big)}{\tau_{cycle}}. \tag{5.36}$$

In Figure (5.8) we plot the dynamics of the cooling power calculated in equation (5.36) for two different choices of κ. When small values of the coupling between the system S_0 and S_1 are taken into account (solid curves), the amount of heat is initially reduced to zero and progressively increases with Δ_{τ_c}, reaching a maximum limit around $\Delta_{\tau_c} = 10$, before sharply decreasing for large values of Δ_{τ_c}. Additionally, we examine the scenario with a high value for the coupling strength κ (dashed curves). The results are comparable to those observed in the evolution of work Figure.5.7. Oscillatory behavior gradually decreases for large values of Δ_{τ_c}, giving way to a continuous evolution for even larger values of Δ_{τ_c}. Furthermore, it's evident that by considering large values of the initial frequency of S_0, we can achieve better results in terms of heat amplitude.

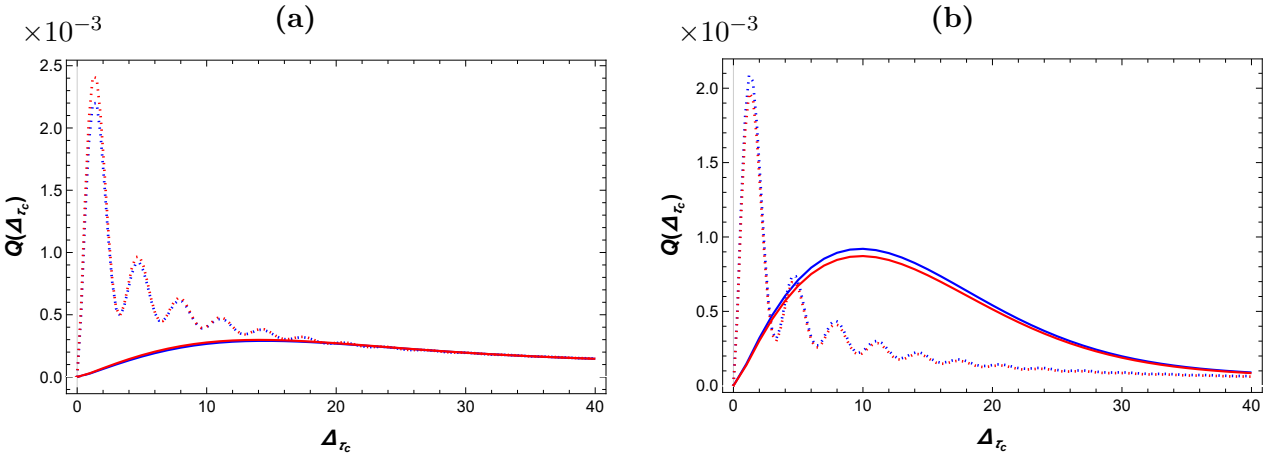

FIGURE 5.8 – Dynamics the amount of heat versus Δ_{τ_c} where, $\gamma = 0.22$, $T_h = 10\omega_0$ and $T_c = 3\omega_0$, $\omega = 0.02$, $\kappa = 0.1$ (solid curves) and $\kappa = 0.99$ (dotted curves). Besides, (a) $\omega_0 = 0.3$ (blue) and $\omega_0 = 0.5$ (red), (b) $\omega_0 = 1.2$ (blue) and $\omega_0 = 1.5$ (red).

.

5.2.4 Efficiency

Finally, it is also insightful to examine the coefficient of performance (COP) of the refrigerator, defined as the ratio between the cooling power and the work performed during the cycle. In a standard configuration, it is set as follows :

$$COP(\Delta_{\tau_c}) = \frac{-\langle Q_R^c(\Delta_{\tau_c})\rangle}{\langle W(\Delta_{\tau_c})\rangle} \leq \eta_r, \tag{5.37}$$

where $\eta_r = T_c/(T_h - T_c)$ is the Carnot coefficient of performance. From the expressions in equations Eq.(5.35) and Eq.(5.36), the coefficient of performance is given by :

$$COP(\Delta_{\tau_c}) = \frac{\Big(-\rho_S^{23}(\Delta_{\tau_c}) - \rho_S^{32}(\Delta_{\tau_c}) + \frac{1}{2}\omega_{\tau_1}\big(-\rho_S^{11}(\Delta_{\tau_c}) - \rho_S^{22}(\Delta_{\tau_c}) + \rho_S^{33}(\Delta_{\tau_c}) + \rho_S^{44}(\Delta_{\tau_c}) + \tanh\left(\frac{\omega_0}{2T_h}\right)\big)\Big)}{\frac{1}{2}(\omega_0 - \omega\tau_1)\Big(\rho_S^{11}(\Delta_{\tau_c}) + \rho_S^{22}(\Delta_{\tau_c}) - \rho_S^{33}(\Delta_{\tau_c}) - \rho_S^{44}(\Delta_{\tau_c}) + \tanh\left(\frac{\omega_0}{2T_h}\right)\Big)}, \tag{5.38}$$

wich encapsulates how effectively the refrigerator converts work input into useful cooling, considering both the heat exchange with the cold reservoir and the work exerted on the system.

In this section, we focus on the coefficient of performance, denoted as $COP(\Delta_{\tau_c})$, as calculated in Eq.(5.38), and examine its behavior as a function of Δ_{τ_c} considering both small and large values of κ simultaneously. Across both coupling choices, we consistently observe a decrease in system efficiency as the frequency of the working system S_0 is increased. Specifically, for both weak and strong coupling scenarios, the COP exhibits higher amplitudes for lower frequencies (blue lines) compared to higher frequencies (red lines). Furthermore, our results underscore the significance of the non-Markovian regime in influencing the device's performance. It's evident that, for identical parameter selections, system efficiency is notably enhanced in the non-Markovian regime compared to the Markovian one. Throughout the entire interaction duration and under the same parameter settings, the dotted lines consistently surpass the solid lines and eventually converge over prolonged interaction periods. This observation underscores the sustained advantage of the non-Markovian regime in optimizing system efficiency.

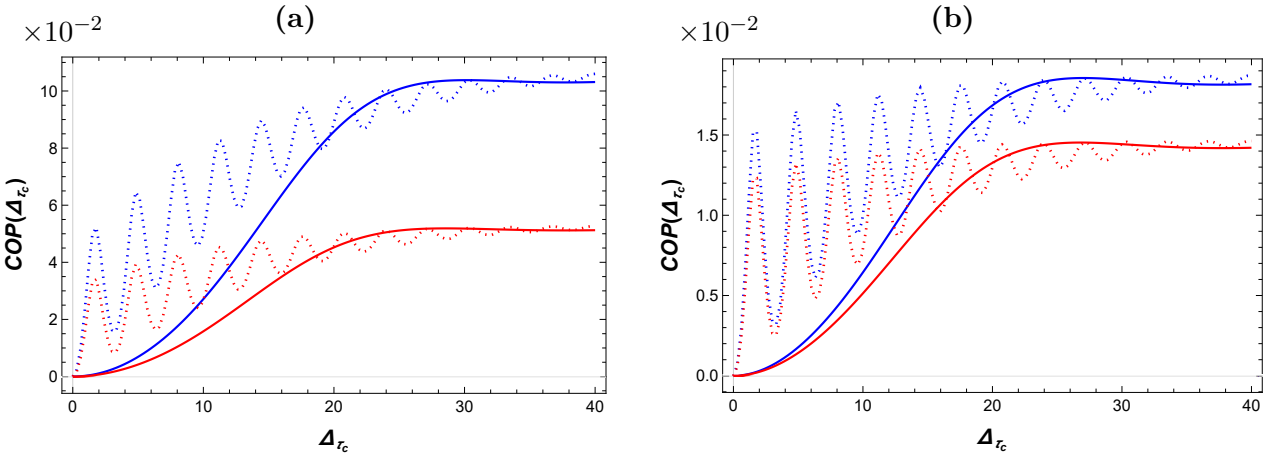

FIGURE 5.9 – Dynamics of the coefficient of performance versus Δ_{τ_c} where, $\gamma = 0.22$, $T_h = 10\omega_0$ and $T_c = 3\omega_0$, $\omega = 0.02$, $\kappa = 0.1$ (solid curves) and $\kappa = 0.99$ (dotted curves). Besides, (a) $\omega_0 = 0.3$ (blue) and $\omega_0 = 0.5$ (red), (b) $\omega_0 = 1.2$ (blue) and $\omega_0 = 1.5$ (red).

5.3 Summary

We have studied a set of quantum refrigerators based on a working system interacting with two engineering environments at different temperatures. We formulated an approximation method to address the master equation governing the evolution of the principal system, and from this, derived a measure to quantify the degree of non-Markovian behavior in its dynamics, with the ratio of interaction constants k/g serving as the principal parameter. Subsequently, we explored the thermal machine framework and investigated the expressions for the thermodynamic quantities involved in the device's operation.

Our numerical analysis reveals a distinct transition in the system's dynamics as the ratio k/g increases, shifting from Markovian to non-Markovian behavior. We then investigated the thermodynamic properties of the device in both regimes. Remarkably, we observed that the non-Markovian regime offers enhancements in the device's cooling performance. Both the cooling power and efficiency exhibit improvements compared to the Markovian regime. Similarly, when considering resonant coupling, the non-Markovian regime demonstrates higher heat fluxes compared to the Markovian regime. Notably, we observed that the non-Markovian characteristics of the system's thermodynamic quantities tend to converge toward Markovian behavior over prolonged operational periods.

The results observed in this chapter are relevant and may be useful in the configuration of quantum thermodynamic devices driven by their bath at the edge. They suggest a particular assignment of coupling constants that leads to improved device performance. It is therefore necessary to study what happens when the number of qubits in the chain is increased.

General Conclusion

In this thesis, we studied the interplay between quantum effects and the thermodynamic properties of quantum thermal refrigerators. In the first approach, we proposed coupled quantum refrigerators and tried to elucidate how intrinsic parameters and quantum correlations influence the thermodynamic performance of the devices. In a second approach, we considered a machine model based on hierarchical environments, which allowed us to establish different regimes in their dynamic evolution. We then turned our attention to the idea of delimiting the regions where the dynamics are Markovian or non-Markovian and subsequently outlined the potential for enhancing machine performance based on the operational regime.

In Chapter 4, we focused on the coupling of two refrigerators via their cold qubits. We showed that coupling two non-identical refrigerators with different energy spacings at the cooling machine components generally reduces the relative cooling capacities of the refrigerators, provided all components are coupled to independent baths. The situation is somewhat different when a common bath is inserted between the qubits to be cooled. We have shown that effective system performance increases with the difference in energy spacing E_d between the two machines. Furthermore, we have shown that even under these two conditions, it is still possible to improve the performance of one of the refrigeratores at the cost of reducing the capacity of the other. This observation suggests the possibility of controlling one machine by another through capacity conversion. Furthermore, we have seen that at the limit of two machines sharing the same parameters, it is possible to configure both machines to operate at the same productivity rate as the independent machines, or even at a more efficient rate. This configuration hinges on the manipulation of coupling constants, which play a pivotal role in setting the machines to either under- or over-productive regimes.

We then sought to analyze our devices in terms of the quantum correlations induced by the interaction between the refrigerators. Our primary objective was to ascertain the degree of correlation between the two machines under steady-state conditions and the interplay with machine productivity. Remarkably, our findings were consistent across both scenarios. We observed that, in general, quantum correlations exhibited no significant correspondence with the productivity of the two refrigerators. Interestingly, our results showed that, with few exceptions, highly correlated machines tend to operate in an underproductive regime, with a decrease in performance associated with an increase in their quantum correlation. However, a peculiar trend emerged when considering the scenario of two objects to be cooled coupled to a common bath. In this instance, we noted that the collective power of the machines evolved in tandem with the correlations. This phenomenon is consistent with previous observations in current research, which posit collective effects in a common bath as an essential resource for the generation of entanglement.

Finally, in Chapter 5, we introduced a device comprising a hierarchical reservoir consisting of a thermal bath and an auxiliary system. Our primary aim was to investigate the degree of non-Markovianity inherent in the dynamics of the working system induced by its interaction with the reservoirs. Initially, we conducted an analysis of the master equation governing the dynamics

of the working system, thereby deriving an expression for the degree of non-Markovianity in its dynamics. Subsequently, we delved into an examination of machine productivity across regions characterized by either Markovian or non-Markovian system dynamics. Our findings unveiled a consistent trend : in scenarios characterized by weak interactions between the working system and the reservoirs, the system dynamics predominantly displayed Markovian behavior. However, as the strength of interaction intensified, a transition to a non-Markovian regime ensued. In this sense, we have shown that operating the device in the non-Markovian regime can improve cooling performance compared to the Markovian regime. Specifically, we observed improvements in cooling performance and device efficiency in the non-Markovian regime, highlighting the potential benefits of non-Markovian dynamics in optimizing device operation.

Based on the results of this thesis, we propose an avenue for improving the performance of quantum refrigerators that exploits quantum aspects in transient or steady-state regimes. We believe this approach holds great promise for the experimental design of quantum refrigerators, especially with respect to the network aspect of quantum systems. In this respect, future efforts must be devoted to increasing the size of the proposed devices in order to verify how device scaling affects the performance of the corresponding thermal refrigerators. Such research could unlock new advances in quantum refrigerator design, potentially leading to quantum refrigerator breakthroughs.

Bibliographie

[1] M. A. Nielsen and I. L. Chuang, Quantum Computation and Quantum Information (Cambridge University Press, Cambridge,UK, 2000).

[2] Steane, A. Quantum Computing. Rep. Prog. Phys. 61, 117–173 (1998).

[3] K. J. Åström and R. M. Murray. Feedback systems - An Introduction for Scientists and Engineers. (Princton University Press, 2008).

[4] M.Hirvensalo. Quantum computing (Springer Science Business Media 2003).

[5] Auffèves, A. Quantum technologies need a Quantum Energy Initiative. PRX Quantum 3, 020101 (2022).

[6] Sagawa, T. Ueda, M. Minimal Energy Cost for Thermodynamic Information Processing : Measurement and Information Erasure. Phys. Rev. Lett. 102, 250602 (2009).

[7] Puebla, J., Kim, J., Kondou, K. Otani, Y. Spintronic devices for energy-efficient data storage and energy harvesting. Commun Mater 1, 24 (2020).

[8] Alicki, R. Kosloff, R. Introduction to Quantum Thermodynamics : History and Prospects. (Springer International Publishing, 2018).

[9] J. Gemmer, M. Michel, and G. Mahler, Quantum Thermodynamics (Springer, Berlin, 2009)

[10] Vinjanampathy, S. Anders, J. Quantum thermodynamics. Contemporary Physics 57, 545–579 (2016).

[11] Deffner, S. Campbell, S. Quantum Thermodynamics : An introduction to the thermodynamics of quantum information. Preprint at http ://arxiv.org/abs/1907.01596 (2019).

[12] F. Binder, L. A. Correa, C. Gogolin, J. Anders, and G. Adesso. Thermodynamics in the Quantum Regime : Fundamental Aspects and New Directions. vol. 195 (Springer International Publishing, Cham, 2018).

[13] Uzdin, R., Levy, A. Kosloff, R. Equivalence of Quantum Heat Machines, and Quantum-Thermodynamic Signatures. (2015).

[14] Koski, J. V., Maisi, V. F., Pekola, J. P. Averin, D. V. Experimental realization of a Szilard engine with a single electron. Proc. Natl. Acad. Sci. U.S.A. 111, 13786–13789 (2014).

[15] Bub, J. Maxwell's demon and the thermodynamics of computation. Preprint at http ://arxiv.org/abs/quant-ph/0203017 (2002).

[16] Callen, H. B., Thermodynamics and an introduction to Thermostatistics, John Wiley Sons, Inc. (1985).

[17] Kosloff, R. Rezek, Y. The Quantum Harmonic Otto Cycle. Entropy 19, 136 (2017).

[18] Andresen, B., Berry, R. S., Nitzan, A. Salamon, P. Thermodynamics in finite time. I. The step-Carnot cycle. Phys. Rev. A 15, 2086–2093 (1977).

[19] Gelbwaser-Klimovsky, D. Kurizki, G. Heat-machine control by quantum-state preparation : from quantum engines to refrigerators. Phys. Rev. E 90, 022102 (2014).

[20] González, J., Alonso, D. Palao, J. Performance of Continuous Quantum Thermal Devices Indirectly Connected to Environments. Entropy 18, 166 (2016).

[21] Kosloff, R. Levy, A. Quantum heat engines and refrigerators : Continuous devices. Annu. Rev. Phys. Chem. 65, 365–393 (2014).

[22] Palao, J. P., Kosloff, R. Gordon, J. M. Quantum thermodynamic cooling cycle. Phys. Rev. E 64, 056130 (2001).

[23] Geva, E. Kosloff, R. The quantum heat engine and heat pump : An irreversible thermodynamic analysis of the three-level amplifier. The Journal of Chemical Physics 104, 7681–7699 (1996).

[24] Bhattacharjee, S. Dutta, A. Quantum thermal machines and batteries. Eur. Phys. J. B 94, 239 (2021).

[25] Braun, D. Creation of Entanglement by Interaction with a Common Heat Bath. Phys. Rev. Lett. 89, 277901 (2002).

[26] Plenio, M. B. Huelga, S. F. Entangled light from white noise. Phys. Rev. Lett. 88, 197901 (2002).

[27] Hartmann, L., Dür, W. Briegel, H.-J. Steady state entanglement in open and noisy quantum systems at high temperature. Phys. Rev. A 74, 052304 (2006).

[28] Brunner, N. et al. Entanglement enhances cooling in microscopic quantum fridges. Phys. Rev. E 89, 032115 (2014).

[29] Brask, J. B. Brunner, N. Small quantum absorption refrigerator in the transient regime : time scales, enhanced cooling and entanglement. Phys. Rev. E 92, 062101 (2015).

[30] Goold, J., Huber, M., Riera, A., Rio, L. D. Skrzypczyk, P. The role of quantum information in thermodynamics—a topical review. J. Phys. A : Math. Theor. 49, 143001 (2016).

[31] Manzano, D., Tiersch, M., Asadian, A. Briegel, H. J. Quantum transport efficiency and Fourier's law. Phys. Rev. E 86, 061118 (2012).

[32] Kosloff, R. Quantum Thermodynamics : A Dynamical Viewpoint. Entropy 15, 2100–2128 (2013).

[33] Bennett, C. H. The thermodynamics of computation—a review. Int J Theor Phys 21, 905–940 (1982).

[34] Ptaszynski, K. Esposito, M. Thermodynamics of Quantum Information Flows. Phys. Rev. Lett. 122, 150603 (2019).

[35] H.P. Breuer and F. Petruccione, The theory of open quantum systems (Oxford University Press, UK 2002).

[36] A. G. Redfield. On the theory of relaxation processes. IBM Journal of Research and Development (1957).

[37] Trushechkin, A. S. Volovich, I. V. Perturbative treatment of inter-site couplings in the local description of open quantum networks. EPL 113, 30005 (2016).

[38] Archak Purkayastha, Abhishek Dhar, and Manas Kulkarni. Out-ofequilibrium open quantum systems : A comparison of approximate quantum master equation approaches with exact results. Phys. Rev. A, 93 :062114 (2016).

[39] González, J. O. et al. Testing the validity of the local and global GKLS master equations on an exactly solvable model. Open Syst. Inf. Dyn. 24, 1740010 (2017).

[40] Szczygielski, K. Gelbwaser-Klimovsky, D. Alicki, R. Markovian Master Equation and Thermodynamics of Two-level System in Strong Laser Field. Phys. Rev. E 87, 012120 (2013).

[41] Lidar, D. A. Lecture Notes on the Theory of Open Quantum Systems. Preprint at http ://arxiv.org/abs/1902.00967 (2020).

[42] Cattaneo, M., Giorgi, G. L., Maniscalco, S. Zambrini, R. Local vs global master equation with common and separate baths : superiority of the global approach in partial secular approximation. New J. Phys. 21, 113045 (2019).

[43] Hofer, P. P. et al. Markovian master equations for quantum thermal machines : local vs global approach. New J. Phys. 19, 123037 (2017).

[44] Rivas, Á., Plato, A. D. K., Huelga, S. F. Plenio, M. B. Markovian Master Equations : A Critical Study. New J. Phys. 12, 113032 (2010).

[45] Levy, A. Kosloff, R. On the Local and Global Approaches to Quantum Transport and Violation of the Second-law of Thermodynamics. EPL 107, 20004 (2014).

[46] Trushechkin, A. S. Volovich, I. V. Perturbative treatment of inter-site couplings in the local description of open quantum networks. EPL 113, 30005 (2016).

[47] De Chiara, G. et al. Reconciliation of quantum local master equations with thermodynamics. New J. Phy s. 20, 113024 (2018).

[48] Wolf, M. M., Verstraete, F., Hastings, M. B. Cirac, J. I. Area Laws in Quantum Systems : Mutual Information and Correlations. Phys. Rev. Lett. 100, 070502 (2008).

[49] Seifert, U. Entropy production along a stochastic trajectory and an integral fluctuation theorem. Phys. Rev. Lett. 95, 040602 (2005).

[50] Esposito, M., Lindenberg, K. Broeck, C. V. den. Entropy production as correlation between system and reservoir. New J. Phys. 12, 013013 (2010).

[51] Spohn, H. Entropy production for quantum dynamical semigroups. Journal of Mathematical Physics 19, 1227–1230 (1978).

[52] Landi, G. T. Paternostro, M. Irreversible entropy production, from quantum to classical. Rev. Mod. Phys. 93, 035008 (2021).

[53] Deffner, S. Lutz, E. Nonequilibrium entropy production for open quantum systems. Phys. Rev. Lett. 107, 140404 (2011).

[54] Vedral, V. The Role of Relative Entropy in Quantum Information Theory. Rev. Mod. Phys. 74, 197–234 (2002).

[55] Alfred Wehrl, General properties of entropy Rev. Mod. Phys. 50, 221 (1978).

[56] C. Shannon. A mathematical theory of communication. The Bell system technical journal (1948).

[57] Jaeger, G. Entanglement, Information, and the Interpretation of Quantum Mechanics. (Springer Berlin Heidelberg, Berlin, Heidelberg, 2009).

[58] Hanbury–Brown, R., and R. Q. Twiss, "Correlation between photons in two coherent beams of light," Nature 177, 27 (1956).

[59] Barrett, J. et al. Non-local correlations as an information theoretic resource. Phys. Rev. A 71, 022101 (2005).

[60] Groisman, B., Popescu, S. Winter, A. On the quantum, classical and total amount of correlations in a quantum state. Phys. Rev. A 72, 032317 (2005).

[61] Scully, M. O. Drühl, K. Quantum eraser : A proposed photon correlation experiment concerning observation and 'delayed choice' in quantum mechanics. Phys. Rev. A 25, 2208–2213 (1982).

[62] Masanes, L. Tight Bell inequality for d-outcome measurements correlations. Preprint at http ://arxiv.org/abs/quant-ph/0210073 (2002).

[63] Kastoryano, M. J., Reiter, F. Sørensen, A. S. Dissipative preparation of entanglement in optical cavities. Phys. Rev. Lett. 106, 090502 (2011).

[64] Hill, S. Wootters, W. K. Entanglement of a Pair of Quantum Bits. Phys. Rev. Lett. 78, 5022–5025 (1997).

[65] Bennett, C. H., Popescu, S., Rohrlich, D., Smolin, J. A. Thapliyal, A. V. Exact and asymptotic measures of multipartite pure-state entanglement. Phys. Rev. A 63, 012307 (2000).

[66] Bennett, C. H., DiVincenzo, D. P., Smolin, J. A. Wootters, W. K. Mixed State Entanglement and Quantum Error Correction. Phys. Rev. A 54, 3824–3851 (1996).

[67] Kraus, B. et al. Preparation of Entangled States by Quantum Markov Processes. Phys. Rev. A 78, 042307 (2008).

[68] Buhrman, H., Cleve, R. van Dam, W. Quantum Entanglement and Communication Complexity. SIAM J. Comput. 30, 1829–1841 (2001).

[69] Yu, T. Eberly, J. H. Evolution from Entanglement to Decoherence of Bipartite Mixed 'X' States. arXiv :quantph/0503089 (2007).

[70] Ma, Z.-H. et al. Measure of genuine multipartite entanglement with computable lower bounds. Phys. Rev. A 83, 062325 (2011).

[71] Rafsanjani, S. M. H., Huber, M., Broadbent, C. J. Eberly, J. H. Genuinely Multipartite Concurrence of N-qubit X-matrices. Phys. Rev. A 86, 062303 (2012).

[72] O'Connor, K. M. Wootters, W. K. Entangled Rings. Phys. Rev. A 63, 052302 (2001).

[73] Ollivier, H. Zurek, W. H. Quantum Discord : A Measure of the Quantumness of Correlations. Phys. Rev. Lett. 88, 017901 (2001).

[74] Luo, S. Quantum discord for two-qubit systems. Phys. Rev. A 77, 042303 (2008).

[75] Ali, M., Rau, A. R. P. Alber, G. Quantum discord for two-qubit X-states. Phys. Rev. A 81, 042105 (2010).

[76] Chen, Q., Zhang, C., Yu, S., Yi, X. X. Oh, C. H. Quantum discord of two-qubit X-states. Phys. Rev. A 84, 042313 (2011).

[77] K. Kraus, A. Böhm, J. D. Dollard, and W. H. Wootters, States, effects, and operations : fundamental notions of quantum theory, Lecture notes in physics (Springer, Berlin, Germany, 1983).

[78] Kraus, K., General state changes in quantum theory, Ann. Phys. (N.Y.) 64, 2,311-335 (1971).

[79] D. Chruscinski, A. Rivas, and E. Størmer, "Divisibility and information flow notions of quantum markovianity for noninvertible dynamical maps, Phys. Rev. Lett. 121, 080407 (2018).

[80] Markov, A. A. ; Nagorny, N. M. The Theory of Algorithms (Mathematics and its Applications), Springer : Dordrecht (2010).

[81] Gagniuc, P. A. Markov Chains : From Theory to Implementation and Experimentation ; Wiley, (2017).

[82] Salem, C.-B., Ploetz, E. Lamb, D. C. Probing dynamics in single molecules. in Spectroscopy and Dynamics of Single Molecules 71–115 (Elsevier, 2019).

[83] Breuer, H.-P. Foundations and Measures of Quantum Non-Markovianity. J. Phys. B : At. Mol. Opt. Phys. 45, 154001 (2012).

[84] Breuer, H.-P., Laine, E.-M. Piilo, J. Measure for the Degree of Non-Markovian Behavior of Quantum Processes in Open Systems. Phys. Rev. Lett. 103, 210401 (2009).

[85] Chruściński, D., Kossakowski, A. Rivas, Á. On measures of non-Markovianity : divisibility vs. backflow of information. Phys. Rev. A 83, 052128 (2011).

[86] Wissmann, S., Karlsson, A., Laine, E.-M., Piilo, J. Breuer, H.-P. Optimal state pairs for non-Markovian quantum dynamics. Phys. Rev. A 86, 062108 (2012).

[87] Breuer, H.-P., Laine, E.-M., Piilo, J. Vacchini, B. Non-Markovian dynamics in open quantum systems. Rev. Mod. Phys. 88, 021002 (2016).

[88] H. Spohn and J. L. Lebowitz. Advances in Chemical Physics : For Ilya Prigogine, Volume 38, chapter Irreversible Thermodynamics for Quantum Systems Weakly Coupled to Thermal Reservoirs. (John Wiley and Sons,Inc., Hoboken, NJ, USA, 1978).

[89] Alicki, R. The quantum open system as a model of the heat engine. J. Phys. A : Math. Gen. 12, L103–L107 (1979).

[90] Geva, E. Kosloff, R. A quantum-mechanical heat engine operating in finite time. A model consisting of spin-1/2 systems as the working fluid. The Journal of Chemical Physics 96, 3054–3067 (1992).

[91] Thermodynamics in the Quantum Regime : Fundamental Aspects and New Directions. vol. 195 (Springer International Publishing, Cham, 2018).

[92] Horodecki, M. Oppenheim, J. Fundamental limitations for quantum and nano thermodynamics. Nat Commun 4, 2059 (2013).

[93] Cavina, V., Mari, A. Giovannetti, V. Slow dynamics and thermodynamics of open quantum systems. Phys. Rev. Lett. 119, 050601 (2017).

[94] Seifert, U. Stochastic thermodynamics : Principles and perspectives. Eur. Phys. J. B 64, 423–431 (2008).

[95] Brandão, F. G. S. L., Horodecki, M., Oppenheim, J., Renes, J. M. Spekkens, R. W. The Resource Theory of Quantum States Out of Thermal Equilibrium. Phys. Rev. Lett. 111, 250404 (2013).

[96] Gelbwaser-Klimovsky, D., Niedenzu, W. Kurizki, G. Thermodynamics of quantum systems under dynamical control. in vol. 64 329–407 (2015).

[97] Perarnau-Llobet, M. et al. Extractable Work from Correlations. Phys. Rev. X 5, 041011 (2015).

[98] Dorner, R. et al. Extracting quantum work statistics and fluctuation theorems by single qubit interferometry. Phys. Rev. Lett. 110, 230601 (2013).

[99] Scully, M. O., Zubairy, M. S., Agarwal, G. S. Walther, H. Extracting Work from a Single Heat Bath via Vanishing Quantum Coherence. Science 299, 862–864 (2003).

[100] Abah, O. et al. Single-Ion Heat Engine at Maximum Power. Phys. Rev. Lett. 109, 203006 (2012).

[101] Zhang, K., Bariani, F. Meystre, P. Theory of an optomechanical quantum heat engine. Phys. Rev. A 90, 023819 (2014).

[102] Skrzypczyk, P., Short, A. J. Popescu, S. Work extraction and thermodynamics for individual quantum systems. Nat Commun 5, 4185 (2014).

[103] Masanes, L. Oppenheim, J. A general derivation and quantification of the third law of thermodynamics. Nat Commun 8, 14538 (2017).

[104] Roßnagel, J., Abah, O., Schmidt-Kaler, F., Singer, K. Lutz, E. A nano heat engine beyond the Carnot limit. Phys. Rev. Lett. 112, 030602 (2014).

[105] Campisi, M., Pekola, J. Fazio, R. Nonequilibrium fluctuations in quantum heat engines : theory, example, and possible solid state experiments. New J. Phys. 17, 035012 (2015).

[106] Gemmer, J., Otte, A. Mahler, G. Quantum Approach to a Derivation of the Second Law of Thermodynamics. Phys. Rev. Lett. 86, 1927–1930 (2001).

[107] Lostaglio, M., Korzekwa, K., Jennings, D. Rudolph, T. Quantum Coherence, Time-Translation Symmetry, and Thermodynamics. Phys. Rev. X 5, 021001 (2015).

[108] Niedenzu, W., Mukherjee, V., Ghosh, A., Kofman, A. G. Kurizki, G. Quantum engine efficiency bound beyond the second law of thermodynamics. Nat Commun 9, 165 (2018).

[109] Brandao, F. G. S. L., Horodecki, M., Ng, N. H. Y., Oppenheim, J. Wehner, S. The second laws of quantum thermodynamics. Proc. Natl. Acad. Sci. U.S.A. 112, 3275–3279 (2015).

[110] Brunner, N., Linden, N., Popescu, S. Skrzypczyk, P. Virtual qubits, virtual temperatures, and the foundations of thermodynamics. Phys. Rev. E 85, 051117 (2012).

[111] Kosloff, R. Levy, A. Quantum heat engines and refrigerators : Continuous devices. Annu. Rev. Phys. Chem. 65, 365–393 (2014).

[112] Mitchison, M. T. Quantum thermal absorption machines : refrigerators, engines and clocks. Contemporary Physics 60, 164–187 (2019).

[113] Linden, N., Popescu, S. Skrzypczyk, P. How small can thermal machines be ? The smallest possible refrigerator. Phys. Rev. Lett. 105, 130401 (2010).

[114] Gelbwaser-Klimovsky, D., Alicki, R. Kurizki, G. Minimal universal quantum heat machine. Phys. Rev. E 87, 012140 (2013).

[115] Quan, H. T., Liu, Y., Sun, C. P. Nori, F. Quantum Thermodynamic Cycles and quantum heat engines. Phys. Rev. E 76, 031105 (2007).

[116] Erker, P. et al. Autonomous quantum clocks : does thermodynamics limit our ability to measure time ? Phys. Rev. X 7, 031022 (2017).

[117] Uzdin, R., Levy, A. Kosloff, R. Quantum Equivalence and Quantum Signatures in Heat Engines.

[118] Rezek, Y. Kosloff, R. Irreversible Performance of a Quantum Harmonic Heat Engine. New J. Phys. 8, 83–83 (2006).

[119] Feldmann, T. Kosloff, R. The Quantum Four Stroke Heat Engine : Thermodynamic Observables in a Model with Intrinsic Friction. Phys. Rev. E 68, 016101 (2003).

[120] Scarani, V., Ziman, M., Stelmachovic, P., Gisin, N. Buzek, V. Thermalizing Quantum Machines : Dissipation and Entanglement. Phys. Rev. Lett. 88, 097905 (2002).

[121] R. Clausius, Über die bewegende kraft der wärme und die gesetze, welche sich daraus für die wärmelehre selbst ableiten lassen. Annalen der Physik 155(3), 368–397 (1850)

[122] R. Clausius, Mechanical Theory of Heat (John van Voorst, London, UK, 1867).

[123] S. Carnot, Réflexions sur la puissance motrice du feu et sur les machines propres à développer cette puissance (Bachelier, Paris, 1824).

[124] F. Curzon and B. Ahlborn, Efficiency of a carnot engine at maximum power input, Am. J. Phys. 43, 22–24 (1975).

[125] N.A. Otto, Gas motor engine, Patent No. 365701 Germany (1887).

[126] J. Yvon, in Proceedings of the International Conference on Peaceful Uses of Atomic Energy, (United Nations, Geneva, 1955).

[127] I.I. Novikov, The efficiency of atomic power stations, Atomnaya Energiya 3 (1957).

[128] H. E. D. Scovil and E. O. Schulz-DuBois, Three-Level Masers as Heat Engines, Phys. Rev. Lett. 2, 262 (1959).

[129] Geusic, J. E., Schulz-DuBios, E. O. Scovil, H. E. D. Quantum Equivalent of the Carnot Cycle. Phys. Rev. 156, 343–351 (1967).

[130] Roßnagel, J. et al. A single-atom heat engine. Science 352, 325–329 (2016).

[131] Levy, A., Alicki, R. Kosloff, R. Quantum Refrigerator and the III-law of Thermodynamics. Phys. Rev. E 85, 061126 (2012).

[132] Rezek, Y., Salamon, P., Hoffmann, K. H. Kosloff, R. The Quantum Refrigerator : The quest for absolute zero. Europhys. Lett. 85, 30008 (2009).

[133] Skrzypczyk, P., Brunner, N., Linden, N. Popescu, S. The smallest refrigerators can reach maximal efficiency. J. Phys. A : Math. Theor. 44, 492002 (2011).

[134] Hofer, P. P. et al. Autonomous Quantum Refrigerator in a Circuit-QED Architecture Based on a Josephson Junction. Phys. Rev. B 94, 235420 (2016).

[135] Klatzow, J. et al. Experimental demonstration of quantum effects in the operation of microscopic heat engines. Phys. Rev. Lett. 122, 110601 (2019).

[136] Dorfman, K. E., Voronine, D. V., Mukamel, S. Scully, M. O. Photosynthetic reaction center as a quantum heat engine. Proc. Natl. Acad. Sci. U.S.A. 110, 2746–2751 (2013).

[137] Myers, N. M., Abah, O. Deffner, S. Quantum thermodynamic devices : from theoretical proposals to experimental reality. AVS Quantum Science 4, 027101 (2022).

[138] Deffner, S. Efficiency of harmonic quantum Otto engines at maximal power. Entropy 20, 875 (2018).

[139] Karimi, B. Pekola, J. P. Otto refrigerator based on a superconducting qubit : classical and quantum performance. Phys. Rev. B 94, 184503 (2016).

[140] M.H.B. Chakour, A.E. Allati, Y. Hassouni, Entangled quantum refrigerator based on two anisotropic spin-1/2 Heisenberg XYZ chain with Dzyaloshinskii-Moriya interaction. Eur. Phys. J. D 75, 42 (2021)

[141] Camati, P. A., Santos, J. F. G. Serra, R. M. Coherence effects in the performance of the quantum Otto heat engine. Phys. Rev. A 99, 062103 (2019).

[142] Bäumer, E., Perarnau-Llobet, M., Kammerlander, P., Wilming, H. Renner, R. Imperfect Thermalizations Allow for Optimal Thermodynamic Processes. Quantum 3, 153 (2019).

[143] Mitchison, M. T., Woods, M. P., Prior, J. Huber, M. Coherence-assisted single-shot cooling by quantum absorption refrigerators. New J. Phys. 17, 115013 (2015).

[144] Franco, R. L., Bellomo, B., Maniscalco, S. Compagno, G. Dynamics of quantum correlations in two-qubit systems within non-Markovian environments. Int. J. Mod. Phys. B 27, 1345053 (2013).

[145] Paz, J. P. Zurek, W. H. Environment-Induced Decoherence and the Transition From Quantum to Classical. in vol. 72 533–614 (2001).

[146] Streltsov, A., Adesso, G. Plenio, M. B. Quantum Coherence as a Resource. Rev. Mod. Phys. 89, 041003 (2017).

[147] Bohr Brask, J., Haack, G., Brunner, N. Huber, M. Autonomous quantum thermal machine for generating steady-state entanglement. New J. Phys. 17, 113029 (2015).

[148] Dillenschneider, R. Lutz, E. Energetics of quantum correlations. Europhys. Lett. 88, 50003 (2009).

[149] Huber, M. et al. Thermodynamic cost of creating correlations. New J. Phys. 17, 065008 (2015).

[150] Brunner, N. et al. Entanglement enhances performance in microscopic quantum fridges. Phys. Rev. E 89, 032115 (2014).

[151] Correa, L. A., Palao, J. P., Alonso, D. Adesso, G. Quantum-enhanced absorption refrigerators. Sci Rep 4, 3949 (2014).

[152] Correa, L. A., Palao, J. P., Adesso, G. Alonso, D. Performance bound for quantum absorption refrigerators. Phys. Rev. E 87, 042131 (2013).

[153] Manzano, G., Giorgi, G.-L., Fazio, R. Zambrini, R. Boosting the performance of small autonomous refrigerators via common environmental effects. New J. Phys. 21, 123026 (2019).

[154] Müller, M. P. Correlating Thermal Machines and the Second Law at the Nanoscale. Phys. Rev. X 8, 041051 (2018).

[155] Perarnau-Llobet, M. et al. Extractable Work from Correlations. Phys. Rev. X 5, 041011 (2015).

[156] Alipour, S. et al. Correlations in quantum thermodynamics : Heat, work, and entropy production. Sci Rep 6, 35568 (2016).

[157] Francica, G., Goold, J., Plastina, F. Paternostro, M. Daemonic ergotropy : enhanced work extraction from quantum correlations. npj Quantum Inf 3, 12 (2017).

[158] Abdou Chakour, M. H. B., El Allati, A. Hassouni, Y. Coupling of two autonomous quantum refrigerators : Collective and relative performances. Physics Letters A 451, 128410 (2022).

[159] Abdou Chakour, M. H. B., El Allati, A. Hassouni, Y. On the coupling of three-level quantum refrigerators in the weak coupling limit. J. Phys. B : At. Mol. Opt. Phys. 57, 105001 (2024).

[160] Reina, J. H., Quiroga, L. Johnson, N. F. Decoherence of quantum registers. Phys. Rev. A 65, 032326 (2002).

[161] G.Massimo Palma, Kalle-antti Suominen, Artur EkertArtur Ekert. Quantum computers and dissipation. Proc.R. Soc. Lond. A 452, 567–584 (1996).

[162] Schlosshauer, M. Quantum decoherence. Physics Reports 831, 1–57 (2019).

[163] Schlosshauer, M. A. Decoherence and the Quantum-to-Classical Transition. (Springer,Berlin,London 2007).

[164] Lidar, D. A., Chuang, I. L. Whaley, K. B. Decoherence Free Subspaces for Quantum Computation. Phys. Rev. Lett. 81, 2594–2597 (1998).

[165] Reina, J. H., Quiroga, L. Johnson, N. F. Decoherence of quantum registers. Phys. Rev. A 65, 032326 (2002).

[166] Lidar, D. A. Review of Decoherence Free Subspaces, Noiseless Subsystems, and Dynamical Decoupling. (2014). doi :10.1002/9781118742631.

[167] Kim, M. S., Lee, J., Ahn, D. Knight, P. L. Entanglement induced by a single-mode heat environment. Phys. Rev. A 65, 040101 (2002).

[168] Benatti, F., Floreanini, R. Piani, M. Environment Induced Entanglement in Markovian Dissipative Dynamics. Phys. Rev. Lett. 91, 070402 (2003).

[169] Kretschmer, S., Luoma, K. Strunz, W. T. Collision model for non-Markovian quantum dynamics. Phys. Rev. A 94, 012106 (2016).

[170] Ciccarello, F., Lorenzo, S., Giovannetti, V. Palma, G. M. Quantum collision models : Open system dynamics from repeated interactions. Physics Reports 954, 1–70 (2022).

[171] Ciccarello, F. Collision models in quantum optics. Quantum Measurements and Quantum Metrology 4, (2017).

[172] Ciccarello, F., Palma, G. M. Giovannetti, V. Collision-model-based approach to non-Markovian quantum dynamics. Phys. Rev. A 87, 040103 (2013).

[173] Ziman, M., Stelmachovic, P. Buzek, V. Description of quantum dynamics of open systems based on collision-like models. Preprint at http ://arxiv.org/abs/quant-ph/0410161 (2004).

[174] McCloskey, R. Paternostro, M. Non-Markovianity and System-Environment Correlations in a microscopic collision model. Phys. Rev. A 89, 052120 (2014).

[175] Laine, E.-M., Breuer, H.-P., Piilo, J., Li, C.-F. Guo, G.-C. Nonlocal memory effects in the dynamics of open quantum systems. Preprint at http ://arxiv.org/abs/1111.4481 (2012).

[176] El Allati, A., El Anouz, K., Ben Abdou Chakour, M. H. Al-Kuwari, S. Non-Markovian effects on the performance of a quantum Otto refrigerator. Physics Letters A 496, 129316 (2024).